
Electronic Theses and Dissertations, 2020-

2022

Generative Modeling of Human Behavior: Social Interaction and Networked Coordination in Shared Facilities

Saumya Gupta
University of Central Florida

Find similar works at: <https://stars.library.ucf.edu/etd2020>
University of Central Florida Libraries <http://library.ucf.edu>

This Doctoral Dissertation (Open Access) is brought to you for free and open access by STARS. It has been accepted for inclusion in Electronic Theses and Dissertations, 2020- by an authorized administrator of STARS. For more information, please contact STARS@ucf.edu.

STARS Citation

Gupta, Saumya, "Generative Modeling of Human Behavior: Social Interaction and Networked Coordination in Shared Facilities" (2022). *Electronic Theses and Dissertations, 2020-*. 1381.
<https://stars.library.ucf.edu/etd2020/1381>

**GENERATIVE MODELING OF HUMAN BEHAVIOR: SOCIAL INTERACTION AND
NETWORKED COORDINATION IN SHARED FACILITIES**

By

SAUMYA GUPTA

B.Tech. Uttar Pradesh Technical University, 2009

M.S. University of Nevada Las Vegas, 2016

A dissertation submitted in partial fulfillment of the requirements
for the degree of Doctor of Philosophy
in the Civil, Environmental, and Construction Engineering
in the College of Engineering and Computer Science
at the University of Central Florida
Orlando, Florida

Fall Term
2022

Major Professor: Mohamed H. Zaki

© SAUMYA GUPTA

ABSTRACT

Urbanization is bringing together various modes of transport, and with that, there are challenges to maintaining the safety of all road users, especially vulnerable road users (VRUs). Therefore, there is a need for street designs that encourages cooperation and resource sharing among road users. Shared space is a street design approach that softens the demarcation of vehicles and pedestrian traffic by reducing traffic rules, traffic signals, road markings, and regulations. Understanding the interactions and trajectory formations of various VRUs will facilitate the design of safer shared spaces. It will also lead to many applications, such as implementing reliable ad hoc communication networks. In line with this motivation, this dissertation develops a methodology for generating VRUs' trajectories that accounts for their walking behaviors and social interactions. The performed study leads to three traffic scenarios covering most pedestrian behavior and interactions traffic scenarios - group interactions, fixed obstacle interaction, and moving obstacle interaction. To implement the different scenarios in shared space facilities, we develop a receding horizon optimization-based trajectory planning algorithm capable of modeling pedestrian behavior and interactions. The generated trajectories are validated using two benchmark pedestrian datasets – DUT and TrajNet++. The validation is shown to yield low or near-zero Mean Euclidean Distance and Final Displacement Error values supporting the performance validity of the proposed generative algorithm. We further demonstrate the application of generated trajectories to predict the communication network topology formation, which leads to a stable network formation when integrated within ad hoc protocols.

The developed pedestrian trajectory planning algorithm can be expanded as a simulation framework to provide a more realistic demonstration of how pedestrians use traffic facilities and interact with their environment. Moreover, the model's applicability is not limited to road traffic and shared spaces. It can find broader applications such as the emergency evacuation of buildings, large events, airports, and railway stations.

To The Believers

ACKNOWLEDGMENTS

I express my sincere gratitude to my advisor, Dr. Mohamed H. Zaki, for mentoring me on the upcoming and challenging research area of pedestrian modeling in urban city planning. Many thanks to his guidance, motivation, valuable suggestions, and patience throughout my dissertation. I am highly grateful to Dr. Adan Vela for his expertise, which helped me develop the proposed framework. Whenever I ran into a trouble spot or had a question about my dissertation, Dr. Vela's feedbacks and proposed solutions were precious. I would also like to extend my gratitude to my committee members, Dr. Samiul Hasan, Dr. Zhaomiao Guo, and Dr. Damla Turgut, for being on my committee, giving helpful advice, and showing belief in my research work. I am thankful to my transportation lab members, Mariam, Redwan, and Abid, for their friendship and maintaining a harmonious research atmosphere. I would also like to recognize the efforts of the Department of Civil, Environmental, and Construction Engineering and the University of Central Florida administration in providing a supportive and conducive environment.

I would like to gratefully acknowledge the countless blessings I have received, the best wishes of my family, and the love and unwavering support of my husband, Shaurya, and my daughter, Shanya. Shanya, you are most important to me; thank you for being the loveliest daughter and inspiring me everyday to improve. I thank my father and my dear friends profusely for all their emotional and mental support during the unanticipated COVID times. It has been a challenging journey sailing through unexpected events. Special thanks to my mother, my mausi, and my mother-in-law for how they are, as it has shaped the various aspects of my life and prepared me enough to take responsibility for my life.

TABLE OF CONTENTS

LIST OF FIGURES	x
LIST OF TABLES	xii
CHAPTER 1: INTRODUCTION	1
1.1 Background and Motivation	1
1.2 Goals and Objectives	4
1.3 Contributions	5
1.4 Research Impact	6
1.5 Interdisciplinary Aspects	7
1.6 Dissertation Outline	7
CHAPTER 2: LITERATURE REVIEW	9
2.1 Evolution of Pedestrian Models	9
2.2 Agent-based Models	10
2.3 Summary and Research Gaps	13
CHAPTER 3: PROPOSED FRAMEWORK	15
3.1 Preliminaries	15
3.1.1 Pedestrian Interactions	15

3.1.2	Trajectory Categorization	15
3.1.3	Solution Concepts	17
3.2	Problem Definition	19
3.3	Receding Horizon Control based trajectory planning	22
3.4	Summary	23
CHAPTER 4:	MODELING INTRA-GROUP INTERACTIONS AND STATIONERY	
	OBSTACLE ENCOUNTERS	24
4.1	Trajectory Optimization	24
4.1.1	Decision Variables	24
4.1.2	Dynamic Constraint Equations	26
4.1.3	Obstacle Constraint Equations	27
4.1.4	Private and Common Objective Functions	29
4.1.5	Model Summary	31
4.2	Implementation Details	32
4.3	Calibration and Validation	34
4.3.1	Key Model Parameters	34
4.3.2	Data Description	35
4.3.3	Model Calibration	36
4.3.4	Performance Metrics	36
4.3.5	Validation process	38
4.4	Experimental Results	39
4.4.1	Case Study 1: Two Agents walk together	39

4.4.2	Case Study 2: Three agents walk together	42
4.4.3	Case Study 3: An agent avoids an obstacle	45
4.4.4	Cross-Validation with TrajNet++	47
4.4.5	Baseline Comparison	49
4.5	Summary	50
CHAPTER 5: MODELING INTER-GROUP INTERACTIONS AND MOVING OB-		
STACLE INTERACTIONS		52
5.1	Scenario Selection and Parameter Design	52
5.1.1	Designed Behavioral Parameters	53
5.2	Trajectory Optimization	58
5.2.1	Decision variables	60
5.2.2	Dynamic Constraint	62
5.2.3	Stationary Obstacle Constraint	63
5.2.4	Collision Avoidance Constraint	65
5.2.5	Private and Common Objective Functions	67
5.2.6	Model Summary	68
5.3	Implementation details	70
5.4	Data description	70
5.5	Model Parameters and Calibration	71
5.6	Performance Metrics	72
5.7	Experimental Results	72
5.8	Summary	76

CHAPTER 6: APPLICATIONS IN NETWORKED COORDINATION	77
6.1 Background and Motivation	77
6.2 Challenges Due To Node Mobility	78
6.3 Node Mobility Considerations in The Literature	79
6.4 Mobility Prediction Formulation and Incorporation	82
6.4.1 Formulation for Reactive Protocols	82
6.4.2 Formulation for Proactive Protocols	85
6.5 Case Studies	86
6.5.1 Case Study 1	89
6.5.2 Case Study 2	90
6.6 Summary	97
CHAPTER 7: CONCLUSION	98
7.1 Summary of Work	98
7.2 Unique Features	98
7.3 Application as a Simulation Tool	100
7.4 Limitations and Future Work	100
REFERENCES	102

LIST OF FIGURES

1.1	A Shared Space concept - Woonerf - where the distinction between various modes of transportation is blurred. There is absence of sidewalks, curbs, lanes. Woonerf is a living street with improved safety for VRUs	4
1.2	Research Goals and Objectives	5
3.1	Pedestrian Trajectory Categories	16
3.2	Pedestrian groups walk towards a common way-point while maintaining a desired separation from each other.	20
3.3	Modeling of the trajectory planning and trajectory execution process using a receding horizon control framework.	21
4.1	Data Collection Location	35
4.2	Sample Extracted Trajectories	35
5.1	Line-of-sight Traffic Scenarios and Designed Behavioral Parameters	54
5.2	Field-of-view Traffic Scenarios and Designed Behavioral Parameters	55
5.3	Line-of-sight Collision Avoidance - Individual	74
5.4	Field-of-view Collision Avoidance - Group	74
5.5	Field-of-View Collision Avoidance - Individual	74
5.6	Performance Metrics Average Values of Case Study ‘Line-of-sight Collision Avoidance-Individual’	75

5.7	Performance Metrics Average Values of Case Study ‘Field-of-view Collision Avoidance-Group’	76
6.1	Benefits of mobility prediction in MANET routing.	80
6.2	Mobility Prediction in Reactive protocols	83
6.3	Mobility Prediction in Proactive protocols	87
6.4	Data Collection Location	88
6.5	Sample Extracted Trajectories	88
6.6	Traffic scenario with four pedestrians	89
6.7	Evolution of PLET for $R = 1m$	91
6.8	Evolution of PLET for $R = 2m$	92
6.9	Traffic scenario with six pedestrians	93
6.10	PLET against transmitting range R at $k = 10s$	94
6.11	Network Graph Structure with varying values of transmitting range R at $k = 10s$. For the case study 2, the PLET value between each two nodes is calculated 10s for the prediction window $m = 10s$	95
6.12	Average PLET vs. Transmission Range at $k=10s$	96

LIST OF TABLES

2.1	Major Approaches to Model Pedestrian Walking Behavior and Interactions	12
3.1	Relevant parameters describing the pedestrian simulation model.	22
4.1	Relevant decision variables for the pedestrian trajectory planning optimization model.	26
4.2	Short-hand markers indicating the ranges over which constraints apply.	31
4.3	Model Calibration for Case Study 1	37
4.4	Model Calibration for Case Study 2	37
4.5	Model Calibration for Case Study 3	37
4.6	Case Study 1 Performance metrics average values for DUT dataset	40
4.7	Case Study 1 Sample Results	41
4.8	Table shows detailed performance metric values of Case Study 1. The average value of the Root Mean Square Error (rmse) is between the agents' generated coordinates and ground truth coordinates.	42
4.9	(a) Step Length (b) Step Frequency of Agents 101 and 102	42
4.10	Case Study 2 Performance metrics average values for DUT dataset	43
4.11	Case Study 2 Sample Results	44
4.12	(a) Step Length (b) Step Frequency of Agents 22, 23, and 24	45
4.13	Case Study 3 Performance metrics average values for DUT dataset	46

4.14	Case Study 3: Sample Results	46
4.15	(a) Step Length (b) Step Frequency of an agent avoiding an obstacle	47
4.16	Cross Validation with TrajNet++ (showing Trajectory generation for Case Study 1: Two Agents Walking Together)	48
4.17	Case Study 1 Performance metrics average values in TrajNet++ dataset	48
4.18	Case Study 2 Performance metrics average values in TrajNet++ dataset	49
4.19	Case Study 3 Performance metrics average values in TrajNet++ dataset	49
4.20	Performance Metrics Comparison chart for Different Pedestrian Trajectory Fore- casting Models based on TrajNet++ dataset	50
5.1	Description of Proposed Parameters	56
5.2	Description of used Parameters.	59
5.3	Description of decision variables.	61
5.4	Short-hand markers indicating the ranges over which constraints apply.	70
5.5	Calibrated Model Parameters	72
5.6	Performance Metrics Table for Simulated Traffic scenarios on DUT dataset and TrajNet++ dataset	75

CHAPTER 1

INTRODUCTION

1.1 Background and Motivation

The last few decades have witnessed an unprecedented growth of cities; one recent report [1] indicates that by 2050 70% of the world's population will be living in metropolitan regions. Questions regarding sustainability and evolving community demands have prompted the need for transportation policy and urban planning to transition from a narrow automobile-centric perspective to one that recognizes and accounts for alternative forms of active mobility [2]. thereby supporting the safe and efficient mobility of vulnerable road users (VRUs) [3]. Vulnerable road users (VRUs), namely (but not limited to) pedestrians and cyclists, are active traffic agents who are unprotected by an outside shield [4]. Because they are mostly unprotected, VRUs face the greatest risk to death and serious injury when involved in traffic accidents with motorized vehicles and static fixtures (e.g. curbs, railroad crossings). In the August 2021 research note [5] the National Highway Traffic Safety Administration indicated an increasing trend in VRU fatalities, both in absolute number and proportion, since 2000. Meanwhile, on a per-capita basis and per-vehicle-mile traveled, motor-vehicle deaths have decreased by almost 25% and 30% between 2000 and 2019 [6].

As the increasing trend in VRU fatalities is concerning, urban planners are also motivated to redesign roadways and traffic infrastructure to provide more equitable access to users. Also, there is a recent trend to promote walking, cycling, and more contemporary modes of micro-mobility (e.g., e-bicycles, e-scooters) as commute options in cities. These commute choices benefits from city planning and infrastructure design to adapt to their needs and provide ease of navigation. One of the city design approaches is *shared spaces* or 'woonerf' - a Dutch term meaning living streets. The concepts such as *shared spaces* are gaining attention as a potential solution to urban transportation challenges. As depicted in Figure 1.1, shared spaces provide for VRUs and cars to make

use of a common physical space without the conventional safety systems of traffic lights, curbs, stop signs, and traffic rules [7]. When operating in shared spaces all road-users must remain alert, attentive, communicative, and responsive to each other. Such urban street design concepts aim to promote active mobility, alleviate congestion, and optimize the efficient utilization of intelligent transportation systems [8]. However, with the transformation of city streets into shared spaces, it becomes essential to identify the traffic safety challenges in shared spaces. Urban city planning also aims to incorporate intelligent transportation systems into the city's infrastructure to enable smart mobility that can maximize safety, alleviate congestion, and promote active mobility.

Among all VRUs and active mobility options, pedestrians are the most common and vulnerable. In fact, recent reports state there has been an increase of 53% in pedestrian fatalities during the last ten years [9, 10]. Hence, it becomes imperative to study pedestrian mobility in shared space and identify the pedestrian safety challenges, which primarily depends on the understanding of pedestrian behavior when interacting with and amongst mixed traffic. Moreover, the need for understanding VRUs' behavior and interaction traits are also useful in operating scenarios such as disaster evacuation, traffic emergencies, and at airports and railway stations. A successful design of shared space requires a better understanding of traffic scenarios involving VRUs and more realistic simulation models.

One way to aid in the design of shared space is to use a modeling and simulation framework. A simulation framework utilizing pedestrian behavior and interactions can simulate and analyze (a) smooth and safe navigation of everyday traffic, (b) better crowd management during social events, (c) traffic infrastructure design applicability and reliability, and (d) an efficient evacuation process during disasters. Within the framework, we can better understand pedestrian interactions with each other, but more so pedestrian interactions with other micro-mobility agents.

There are sustained efforts by researchers and traffic agencies to develop realistic and practical pedestrian simulation models [11, 12, 13, 14, 15, 16]. Developing pedestrian simulation models span many approaches, with noteworthy efforts making use of agent-based modeling techniques

[17] and cellular automaton-based techniques [18] [19]. The availability of reliable datasets [20] has also enabled machine learning algorithms to learn and predict pedestrian trajectories [21].

Pedestrians exhibit unique behavioral and interaction rules depending on traffic scenarios such as individual vs. group, dense vs. sparse type of walking environments. Therefore, an efficient and realistic pedestrian trajectory modeling requires (a) an understanding of pedestrians' behavioral and interaction rules and (b) an estimation of the presence of various environmental elements. Various types of pedestrian traffic interactions can be broadly categorized as human-human and human-environment interactions. The human-human interaction involves pedestrians walking in a group, pedestrians with standing or moving pedestrians, pedestrians with the bicyclist, and other means of micro-mobility (such as e-scooter and e-bikes). The human-environment interaction involves pedestrian interaction with stationary obstacles (such as trees and poles) and moving obstacles (such as autonomous vehicles or delivery robots). The traffic modeling design process necessitates a better understanding of pedestrian behavior and interaction rules in the traffic, which means understanding the traffic scenarios of group interaction, fixed obstacle interaction, and moving obstacle interaction. In all types of interactions, the pedestrian's primary objective is prioritize one's safety. These complex pedestrian interaction scenarios and their responses to such interactions make pedestrian trajectory modeling and simulation challenging.

Pedestrian trajectories are the result of a closed-loop decision-making process that accounts for several factors such as physical, mental, psychological, and static and dynamic environmental conditions. Since the last two decades of twentieth century, significant effort has been placed into understanding and modeling pedestrian behaviors [22], [23], movements [24], and trajectories [25]. For an extensive survey focusing on pedestrian motion analysis one can refer to [26, 27, 28, 29]. Effective modeling of pedestrian behaviors and their motions requires large observational data to capture minute intricacies. However, the availability of pedestrian motion data was limited until recently. Recent advances in sensing and communication have led to an increased availability of pedestrian motion data. For instance, computer vision, along with pattern recognition techniques,

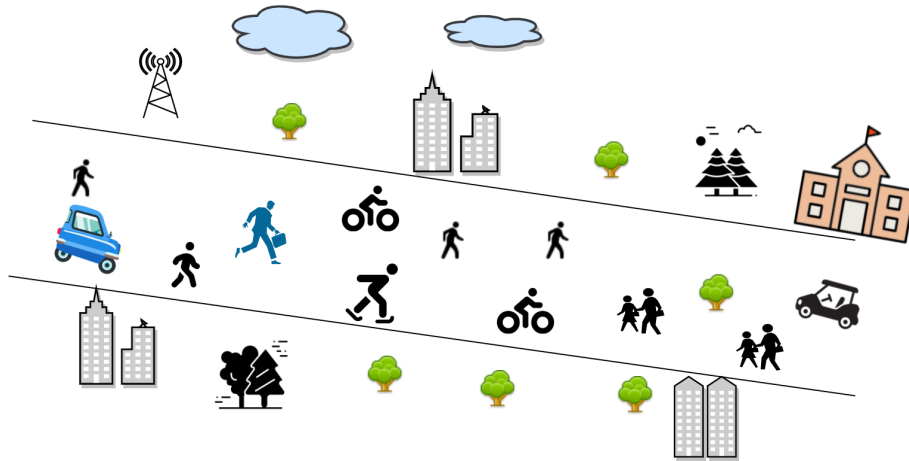


Figure 1.1: A Shared Space concept - Woonerf - where the distinction between various modes of transportation is blurred. There is absence of sidewalks, curbs, lanes. Woonerf is a living street with improved safety for VRUs

showed substantial progress in the automatic capture of human motion and analysis, which is assisting in the understanding pedestrian behaviors [30].

A realistic pedestrian generative and simulation model requires consideration of human behavior and interaction rules. However, a careful investigation of the above mentioned literature reveals that there are two *critical gaps* in the existing pedestrian trajectory modeling and simulation approaches that limit their application to the previously discussed needs. First, current approaches do not effectively consider scenario specific pedestrian walking behavior, the nature of interactions, group interactions, and route optimization. Secondly, there is a lack of a well-defined yet flexible parameterized model that requires minimal training data while remaining transferable amongst broad classes of environments and scenarios. This motivates the research pursued in this dissertation with the following goals.

1.2 Goals and Objectives

The dissertation's goal is to develop a generative pedestrian trajectory planning model incorporating human walking behaviors and interactions, and demonstrate the model's application in predicting ad hoc network topology. The proposed modeling approach developed at the foundation

of receding horizon control generates pedestrian trajectory instances by continuously assessing the traffic environment. Specifically, the dissertation aims to develop a pedestrian trajectory modeling framework named HISS (Human Interactions in Shared Space) that is (a) generative, (b) based on pedestrian behavior and interaction rules, (c) transferable to different locations with same calibrated parameters, and (d) requires minimal data to calibrate the model parameters.

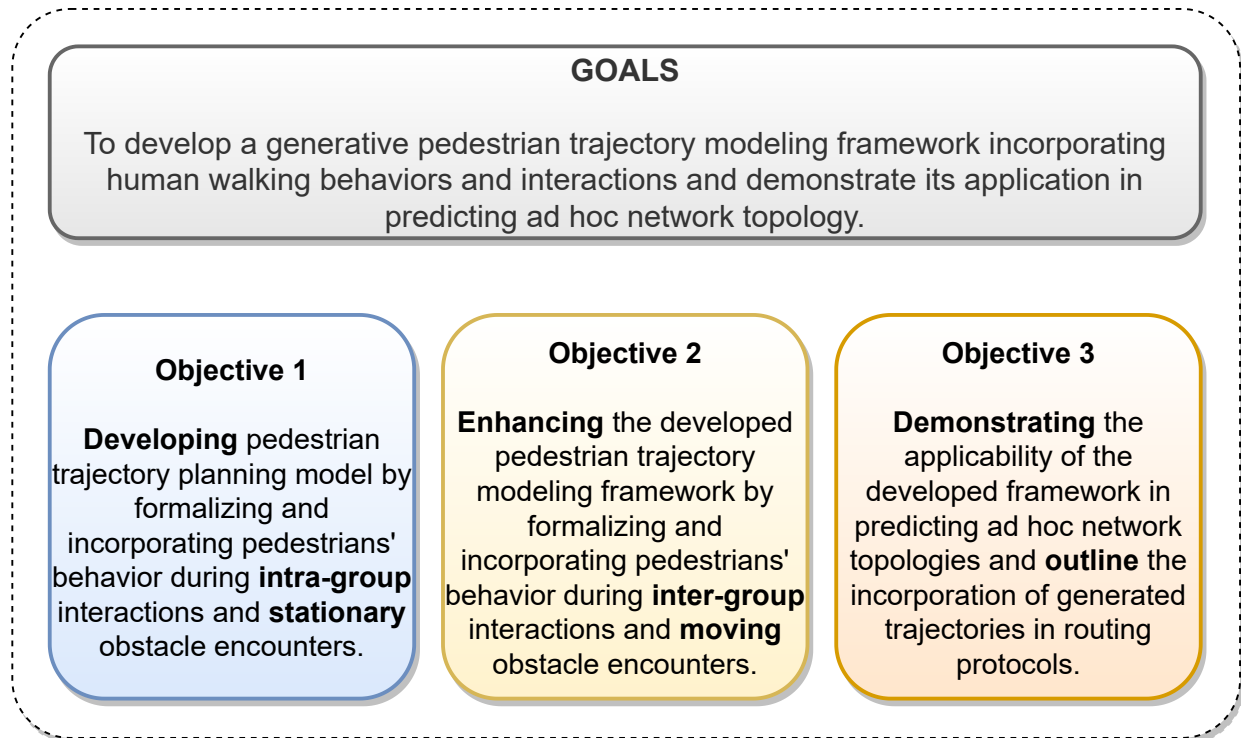


Figure 1.2: Research Goals and Objectives

1.3 Contributions

Trajectory control and modeling based on mixed integer linear programming (MILP) provides fast computational speed, which explains its successful application in robotics motion planning. To the best knowledge of authors, this is the first research effort to utilize MILP embedded within receding horizon control (RHC) loop for pedestrian-centric modeling. Through our research we are bringing together the domain of operations research, urban transportation, and pedestrian behavioral studies. The corresponding contributions are as follows:

- We formalized the pedestrian walking behavior and interaction rules during intra-group interactions, inter-group interactions, stationary obstacle encounters, and moving obstacle interactions.
- We develop a receding horizon optimization-based pedestrian trajectory planning framework to generate time-efficient, dynamically-feasible, and realistic pedestrian trajectories for a given traffic scenario.
- The trajectory planning and execution adapts to the uncertainties in the environment as the model plans the trajectory and the interactions among agents at the current time as well over a next few time-steps (i.e. over the planning horizon).
- We illustrate the applicability of proposed modeling framework in analyzing future ad hoc network topology. We also incorporate the predicted trajectories to leverage pedestrian behavior when developing ad hoc network routing protocols.

1.4 Research Impact

The pedestrian trajectory planning model lies between the two sets of modeling paradigms — the black-box algorithms (such as machine learning), which are hard to interpret and parameterize, and the analytical modeling with a set of parametrized equations. In summary, the proposed model is fully defined and parametrized with pedestrians' behavioral rules, and gait parameters can serve as a basis for exploring pedestrian behavior in different scenarios. The developed model, expanded as a simulation framework, will provide a more realistic demonstration of how pedestrians use traffic facilities and interact with their environment. Given the formulation and ability of the model, it is expected to be utilized by urban planners to test and evaluate various traffic scenarios and designs related to shared spaces with the goal of enabling efficient transportation management supporting active mobility. Moreover, the model's applicability is not limited to road traffic and shared spaces. It can find broader applications such as the emergency evacuation of buildings,

large events, airports, and railway stations. Note that the developed model also supports encounter modeling which is essential in air traffic control to develop and test collision avoidance systems [31].

1.5 Interdisciplinary Aspects

The proposed work in the dissertation addresses key challenges of the in smart urban micro-mobility design. If successful, this research could significantly broaden the understanding of urban shared spaces having various agents (peds, bikes, scooters). The proposed research is of truly interdisciplinary nature as it borrows concepts and methods from transportation engineering, urban planning, human behavior, network engineering, control, and operations research. For instance, to capture the rational decision-making of an agent (human behavior), the research involves observing and analyzing the walking behavior of agents [32], their response to a particular scenario, and their interaction with other elements in shared spaces [33]. Through this analysis, we can develop a realistic mobility model of an agent capable of simulating the movement of the agents in the facility in a precise way (transportation engineering) and subsequently enhance the performance of connectivity protocols for an infrastructure-less and self-configuring MANETs communication (network engineering). We also derive optimal policy for specific performance criteria such as maximizing safety, maximizing throughput, and guaranteeing equitably shared space (operations research). The model will be calibrated from real life video data and test scenarios will be developed for validation (computer vision). The developed reliable MANET will ensure real-time decision making and information dissemination among the shared-space agents.

1.6 Dissertation Outline

The dissertation is divided into seven chapters. Chapter 2 presents a literature review of the existing research in pedestrian modeling and highlights key research gaps. Chapter 3 includes a basic introduction to the mathematical concepts of MILP and RHC, and the pedestrian trajectory clas-

sification based on behavior and interactions. Chapter 3 also overviews the proposed pedestrian trajectory generation methodology. Chapters 4 covers the Intra-group interactions and Chapter 5 covers the Inter-group interactions problem formulation. Chapter 6 discussed the application of the proposed trajectory framework in predicting ad hoc network topology. Finally, the dissertation is summarized along with the proposed modeling unique features, contribution, applications, limitations, and future work in Chapter 7.

CHAPTER 2

LITERATURE REVIEW

There are several important aspects of pedestrian mobility to consider when designing a modeling approach, they include: individual walking behaviors, group behaviors, crowd interactions, interaction with other traffic agents (e.g. cyclists and scooters), and interaction with the environment. Overall, understanding and modeling pedestrian motion requires consideration of both the macro and micro-movement characteristics [34], [35].

The decision-making of a pedestrian is affected by several factors such as physical, mental, psychological, and environmental conditions. It is well established in the literature that having the freedom to execute their movements, pedestrians exhibit the least predictable behavior and do not always follow an expected logical pattern. Therefore, it is not trivial to model pedestrian trajectories. The last two decades of the twentieth century have witnessed significant efforts towards pedestrian motion analysis through pedestrian detection, tracking, and understanding its behavior [27] [36]. The computer vision and pattern recognition techniques, showed substantial progress in the automatic capture of human movement and its analysis, thereby helping in understanding pedestrian behavior [30].

2.1 Evolution of Pedestrian Models

Many pedestrian trajectory simulation models rely on the physics-based and the cellular automata-based modeling approaches [37]. Physics-based modeling approaches treat pedestrians as particles, and their interactions with other elements are estimated by considering different exerted physical forces. The updates to pedestrian trajectories depend on the direction and magnitude of the resulting force. The Social Force Model, developed by Helbing and Molnar in 1995 [38] was the first physics-based modeling approach considered to design a pedestrian mobility model.

The social forces - attractive and repulsive forces - reflected the pedestrian interaction with the environment.

The cellular automata method employs a discrete spatial representation of the environment, whereby the environment is divided into cells of fixed size that can only be occupied by one pedestrian at a time. The pedestrian moves from one cell to another depending on pre-defined transitional rules (primarily dependent on a probability of choosing the target cell). The cellular automata modeling approach was applied by Blue and Adler [39] to build pedestrian simulation models for unidirectional flow, bidirectional flow, and extended the work to four-directional pedestrian flows [25] [40].

Other modeling approaches utilize concepts such as fuzzy logic, gas-kinetic model, control methods, and utility maximization (Hoogendoorn and Bovy's Nomas Model) [41]. The corresponding simulation models provided an excellent platform for performing evacuation studies and understanding large-scale crowd behavior; however, applications requiring a detailed understanding of pedestrian behavior and precise outputs cannot be tested. These limitations were originally associated with the limited availability of pedestrian datasets. At the start of the twenty-first century computer vision, along with pattern recognition techniques, has helped to create databases [20], [42] which support understanding and characterizing human interaction behavior [43], [30], [44]. That said, simulation or recreation of realistic pedestrian walking behavior is not a trivial task, as pedestrian walking behavior depends on the context, spatial configuration, obstacle avoidance, and group interactions [45] [46].

2.2 Agent-based Models

With the increase in computing power, a shift has been seen from aggregate to individual level (microscopic) modeling. It has become more practical in recent times, and the progression is seen since the development of automata approaches [47], [48]. Agent based modeling (ABM) approaches provide a new paradigm for pedestrian simulation. It enables a realistic simulation of

pedestrian behavior by considering agents (pedestrians) as rational entities that (a) are autonomous (can decide their motion independently), (b) are heterogeneous (not all pedestrians are assumed to behave in the same fashion), (c) learn from their environment, and (d) adapt their behavior according to environmental changes [49].

One of the first attempts to apply ABM techniques was the STREETS model [50]. The STREETS model demonstrated that every agent could be represented as having unique behavioral characteristics, like speed, direction, and visual range, allowing for realistic simulations. The research by Helbing in 2012 [17] highlighted the ability of agent-based modeling in handling heterogeneous pedestrian systems, specifically when analyzing different agent types and different pedestrian behaviors, and when performing both microscopic and macroscopic studies of various traffic scenarios. The ABM models were found to be suitable for modeling complex pedestrian behavior and capturing complex real-world pedestrian-pedestrian and pedestrian-traffic interaction scenarios [51], [17], [52]. Application of agent-based modeling (ABM) techniques have been used to develop pedestrian trajectory simulations [53, 17]. Agent-based modeling supports simulation models capable of including pedestrian walking behavior rules while interacting with the environment, thereby resulting in better realizations [54].

However, there are certain limitations to the ABM approach. Since the approach is based on microscopic individual agent modeling dependent upon initial conditions, the results are not reproducible enough i.e., changes in initial conditions lead to different simulation outputs. Moreover, the individual-level details are difficult to quantify and calibrate, often requiring a large number of parameters to be tuned, limiting the range of agent representation and, consequently, the model's utility in the understanding of the real world [55]. Moreover, in ABM, each agent takes the instantaneous information of the traffic social forces, and respond to that at that instant. That is to say that ABM does not incorporate any planning for the next few time-steps, as is expected in the case of an actual human pedestrian. Nonetheless, every model has its own characteristics, advantages, and disadvantages; making them suitable for different applications.

Table 2.1: Major Approaches to Model Pedestrian Walking Behavior and Interactions

Approach	Concept
Physical-based	Pedestrians are modeled as particles and their interactions with other elements are simulated when they are subject to different physical forces. The movement of pedestrians in each model update is dependent on the direction and magnitude of the resultant force.
Cellular automata based	This approach employs discrete spatial representation of the environment. The environment is divided into fixed-size cells that can only be occupied by one object at a certain time instant. The pedestrians move from one cell to another depending on pre-defined transitional rules (mainly dependent on a probability of choosing the target cell).
Agent-based	In this technique, the individuals of interests are represented as agents, which are embedded in an environment. Agents interact with other agents in the environment and with the environment itself through a set of pre-defined decisions and behavioral rules.

Environmental Factors: Other studies have performed detailed pedestrian behavioral studies [56], [57] and estimated pedestrian gait parameters [58]. These studies have considered case scenarios at signalized and non-signalized crosswalks, and at railway stations, along with behavioral changes with group size, age, and gender. Defining the environment and its key contextual factors are required to effectively study and analyze scenarios of interest. An agent’s inherent characteristics and behaviors towards the considered environment has to be carefully embedded in any model to achieve the model objectives [59] [32].

Human Trajectory Prediction: Predicting the future positions of pedestrians, along with trajectory planning, has become increasingly important to studies related to autonomous vehicles, robotics, and advanced surveillance systems. The papers [21] and [60] provides a detailed survey of research works based on human motion planning and prediction. Examples include trajectory forecasting frameworks that predict trajectories based on observed partial trajectories or from observed agents’ states such as position, velocity [61, 62]. There are also recent works based on deep learning-based algorithms [63], [64] for pedestrian trajectory prediction, this includes [65] which presents a detailed analysis of existing deep learning-based human trajectory forecasting models. The aforementioned paper also proposes two new models that effectively consider social

interactions and forecast trajectories. TrajNet++, a large-scale social interaction-centric database, is also a comprehensive resource that will allow researchers to perform further research on human behavior and modeling.

2.3 Summary and Research Gaps

The Social Force Model and cellular automata modeling has been successfully applied to existing pedestrian simulation models, many of which are still being used today in their design and decision-making process. However, a key shortcoming of many existing models is that they lack sufficient consideration of pedestrian interactions, and therefore they are not capable of capturing critical and commonplace behaviors, especially in shared spaces. On the other hand, ABM approaches incorporate behavior and interaction rules. However, ABM is often times overly complicated as it involves numerous parameters that make them difficult to extend to diverse agent-types and environments without significant hand-tuning. Alternatively, models require a considerable amount of data for training and parameter estimation, making machine learning-based algorithms highly data-dependent.

In summary, current approaches often have one or many of the following limitations:

- Location specific and/or requires extensive calibration for proper transferability.
- Make use of non-parametric (machine learning) approaches that are black boxes in nature, relying on large dataset. Meanwhile, parametric approaches (such as ABM) often require large number of parameters, often resulting in a complex, unintuitive model.
- ABM approaches lack the planning, i.e, how agents plan for the trajectory for the next few time steps in the presence of various social interactions.
- Learning-based models require a vast amount of data for training or parameter estimation purposes. This can be challenging when collected pedestrian data for training is limited.

- Current pedestrian-group modeling approaches lack an explicit description of the commonality in walking behavior between group members

CHAPTER 3

PROPOSED FRAMEWORK

3.1 Preliminaries

3.1.1 Pedestrian Interactions

When pedestrians move from one place to another, it is done so intuitively that hardly ever anybody bothers to think about the complexities underlying those movements. Their trajectories are influenced by many observable and unobservable factors such as spatial and temporal aspects, gender and age aspects, individual or group movement, and the presence of other traffic elements. For designing safe and walkable street areas, it becomes essential to understand the unique characteristics of human-human interaction and human-environment interactions.

The proposed research is based on observations of the pedestrians' movement and the literature on pedestrian traffic behavior and interaction rules [66, 67, 57, 18, 60, 56]. Human motion in shared spaces can be classified based on the type of pedestrian-pedestrian and pedestrian-environment interactions. For instance, the movement of an individual pedestrian depends on how the pedestrian observes the surroundings and processes the observed information, e.g., intuitively estimating the distance of the obstacle to adapt their walking. Additionally, when expanded to a group of pedestrians, the pedestrian interactions with the surroundings and their interactions within the group have to be understood. In the following section, we briefly describe these interactions.

3.1.2 Trajectory Categorization

Pedestrian motion is *characterized* by their behavior and social interactions such as human-human and human-environment interactions. Based on the observation of pedestrian trajectories in TrajNet++ data, paper [65] classifies them into three broad categories - linear, static, and non-linear.

To classify each of these broad trajectory categories effectively a pedestrian of interest, *primary pedestrian*, is chosen in a traffic scene. Figure 3.1 shows a classification of pedestrian trajectories, adapted from [65].

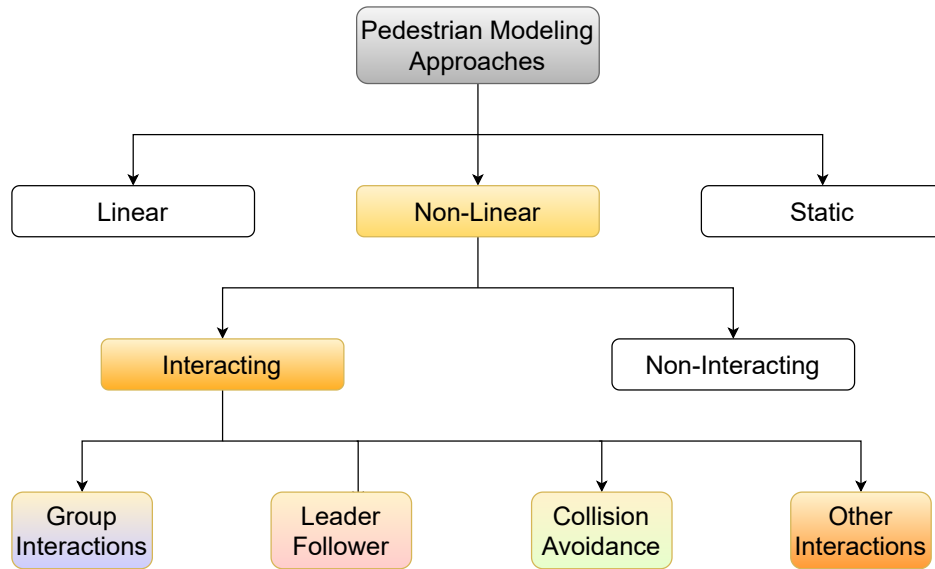


Figure 3.1: Pedestrian Trajectory Categories

A *linear trajectory* occurs when the primary pedestrian (having no interactions) maintains an almost linear movement in the direction of motion. A *static trajectory* where the primary pedestrian exhibits limited movement, eg. the case where the pedestrian is standing and talking with another person. The *non-linear trajectory* is the category with ‘non-linear’ pedestrian trajectories (with or without interactions). The non-linear **interacting trajectory** is the most challenging to model as it involves a variety of behavior and interactions. The trajectories are referred to as *interacting* when the primary pedestrian undergoes social (i.e., human-human) interactions. The non-linear interaction trajectory category can be further classified as follows:

- *Group Interactions trajectory*: When the primary pedestrian maintains a group by keeping a close and comfortable distance with its neighbor [57], [56].
- *Leader Follower trajectory*: When the primary pedestrian follows another walking pedestrian while maintaining a safe following distance.

- *Collision Avoidance trajectory*: When a primary pedestrian avoids a collision with another pedestrian or a group of pedestrians crossing paths.
- *Other Interactions trajectory*: This category includes the trajectories where the primary pedestrian interacts with various active mobility traffic agents such as a cyclist and e-bikes.

The defined pedestrian trajectory categorization is useful in trajectory modeling as it helps to identify the case studies and scenarios critical for successful modeling.

3.1.3 Solution Concepts

Starting with a convex-optimization formulation for the design of the path planning algorithm with group dynamics modeling, the underlying optimization is extended into a mixed-integer linear program (MILP), which, when embedded within receding horizon control, can generate pedestrian trajectories responding to other nearby pedestrians and obstacles.

Mixed-Integer Linear Programming (MILP)

The general form of a *convex optimization* problem is represented as:

$$\left\{ \begin{array}{ll} \text{minimize} & f_0(z) \\ \text{subject to} & g_i(z) \leq 0, \quad i = 1, 2, 3, \dots, m, \\ & h_i(z) = 0, \quad i = 1, 2, 3, \dots, l, \end{array} \right. \quad (3.1)$$

where the vector $z \in \mathbb{R}^n$ contains the decision variables, convex function $f_0 : \mathbb{R}^n \rightarrow \mathbb{R}$ is the objective function (or cost function), while $g_1, g_2, \dots, g_m : \mathbb{R}^n \rightarrow \mathbb{R}$ and $h_1, h_2, \dots, h_l : \mathbb{R}^n \rightarrow \mathbb{R}$ are constraints that define convex feasible spaces on the decision variables. The problem represented in (Equation 3.1) is a mathematical abstraction of the optimization problem of making the best choice of a vector z in \mathbb{R}^n from a set of possible choices, given a set of constraints. Convex

optimization formulations are often considered ideal as there numerous computation and theoretical advantages over other non-linear optimization problems, specifically, there exist libraries and algorithms to solve them in polynomial time, also, there exist tests for optimality [68].

An optimization formulation is called a *Mixed Integer Linear Program* (MILP) if the decision variables are a mix of integers and real values, and the objective function and all the constraints are linear. MILP formulation is NP-complete. Hence, we don't have guarantees that MILPs can be solved in polynomial time like a convex formulation. However, there exists algorithms and commercial solvers that solve it efficiently. As we will see in the next section, assignment and avoidance problems in pedestrian movement lead to non-convex constraint equations. The use of a MILP formulation allows us to overcome the challenges related to nonconvexity and obtain the solution using a standard solver.

Receding Horizon Control (RHC)

The receding horizon control (RHC) (also referred as Model Predictive Control (MPC)) is a feedback control technique using which an optimization problem is solved at each time step t to determine a plan of action over a fixed time horizon and therefore predicts the future states of the system. At the each time step, the planning process is repeated; a new optimization problem is solved with the time horizon shifted one step forward. Using RHC, the optimization problem becomes dynamic and takes into account estimates of future quantities based on available information at each time step [69] [70]. The RHC optimization problem work as follows:

- At time step t , a time interval extending T steps into the future, $t, t + 1, \dots, t + T$ is considered.
- The RHC optimization problem handles the objective function, and system constraints. The problem minimize the estimated objective over the time interval $t, t + 1, \dots, t + T$ subject to the estimated dynamics and constraints, and generates a plan of action for the next T steps.

- The RHC optimization problem’s output at initial time is the input to RHC. At the next time step, process is repeated with updated system state.

3.2 Problem Definition

In this section, the proposed generative pedestrian trajectory modeling framework named HISS, Human Interactions in Shared Space is explained. The pedestrian trajectory planning and execution is developed at the foundation of RHC, incorporating pedestrian behavioral and environment interaction rules. Next, the MILP trajectory optimization embedded within a receding horizon control loop is explained, which serves as the primary component by which pedestrian decision-making is modeled. The next two chapters provide the detailed formulation of decision variables, constraints, and private and common objective functions.

Our simulation framework begins by considering the generalized problem of multiple agents or pedestrians in the set \mathcal{P} , traversing an environment with a set of obstacles \mathcal{O} . When moving about the environment, the pedestrians are further sub-divided into groups of pedestrians or individual pedestrians. That is to say, some of the pedestrians are walking alone, while others might be walking together in groups. Consistent with existing research on pedestrian behaviors, when walking together, a group of pedestrians will naturally self-organize into a moving cluster in which each person maintains a relative separation between themselves and others in their group. As depicted in Figure 3.2a, such a self-organized group of pedestrians can be mathematically modeled as a moving graph structure $\mathcal{G} = (\mathcal{V}, \mathcal{E})$ where each node v_i in the vertex set \mathcal{V} corresponds to the i^{th} pedestrian in the pedestrian set \mathcal{P} . Meanwhile, the edge set \mathcal{E} contains linkages (i, j) between any two pedestrians i and j walking in the same group that seeks to maintain fixed proximity with each other. Accordingly, associated with each group of pedestrians are desired separations, $d_{i,j}^{des} = (d_{i,j}^{\parallel des}, d_{i,j}^{\perp des}) \in \mathbb{R}^2$, consisting the longitudinal and lateral separation, between any two pedestrians i and j , along the group’s direction of travel. A pictorial representation of the induced graph structure and desired separation distance between agents is illustrated in Figure 3.2.

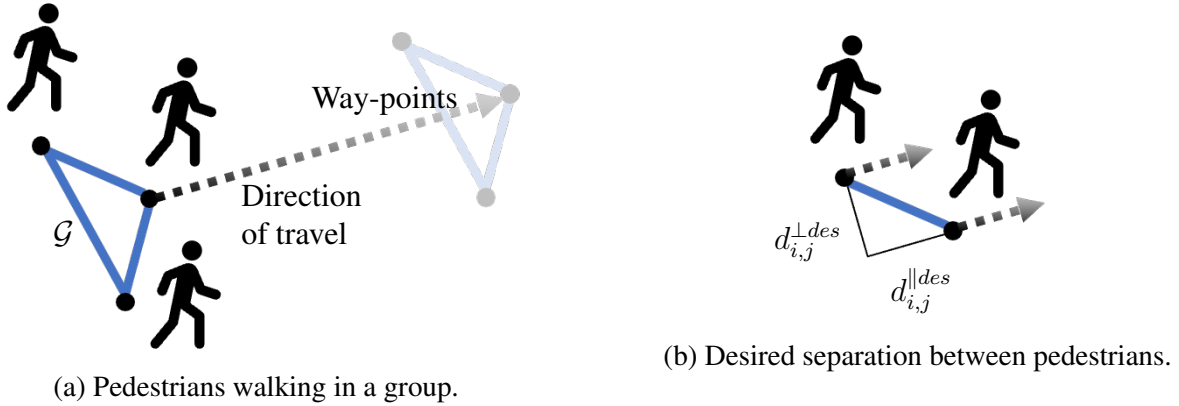


Figure 3.2: Pedestrian groups walk towards a common way-point while maintaining a desired separation from each other.

Within this framework, each pedestrian is associated with a final destination. However, by means of reaching their destination, the pedestrian will move through a series of segments defined by an ordered set of way-points. For the case of pedestrian i , the next desired way-point is given by w_i . When located at position $x_{i,t}$ in a global coordinate frame at time-step t , the direction of travel for the pedestrian is given by the angle $\theta_i = \angle(w_i - x_{i,t})$. When walking together in a group, it is assumed that all pedestrians maintain the same way-point goal. However, the goal is sufficiently far away so that small angle approximations are permissible when modeling the pedestrian dynamics. That is to say, $\|\theta_i - \theta_j\| \leq \epsilon$, where ϵ is small, for all pedestrians i and j walking in the same group.

Consider the lower half of Figure 3.3 that considers a group of pedestrians in the set \mathcal{P} , traversing an environment, with a set of obstacles \mathcal{O} , where each static obstacle o is located at the position coordinates $(p_{o,x}^{Obs}, p_{o,y}^{Obs})$ so that $p_o^{Obs} \in \mathbb{R}^2 \forall o \in \mathcal{O}$. When walking from one way-point to the next, we assume pedestrians will become aware of changes in their environment (e.g., the appearance of obstacles) or adjust their path according to others in their walking group. In this context, we focus our attention on the tasks of trajectory planning and trajectory execution as each pedestrian moves between way-points; that is to say, the broader path planning problem of how pedestrians select way-points to arrive at their final destination is not addressed. Nonetheless, the modeling analogue

of such a dynamic trajectory planning and execution process can be represented using a receding horizon control framework.

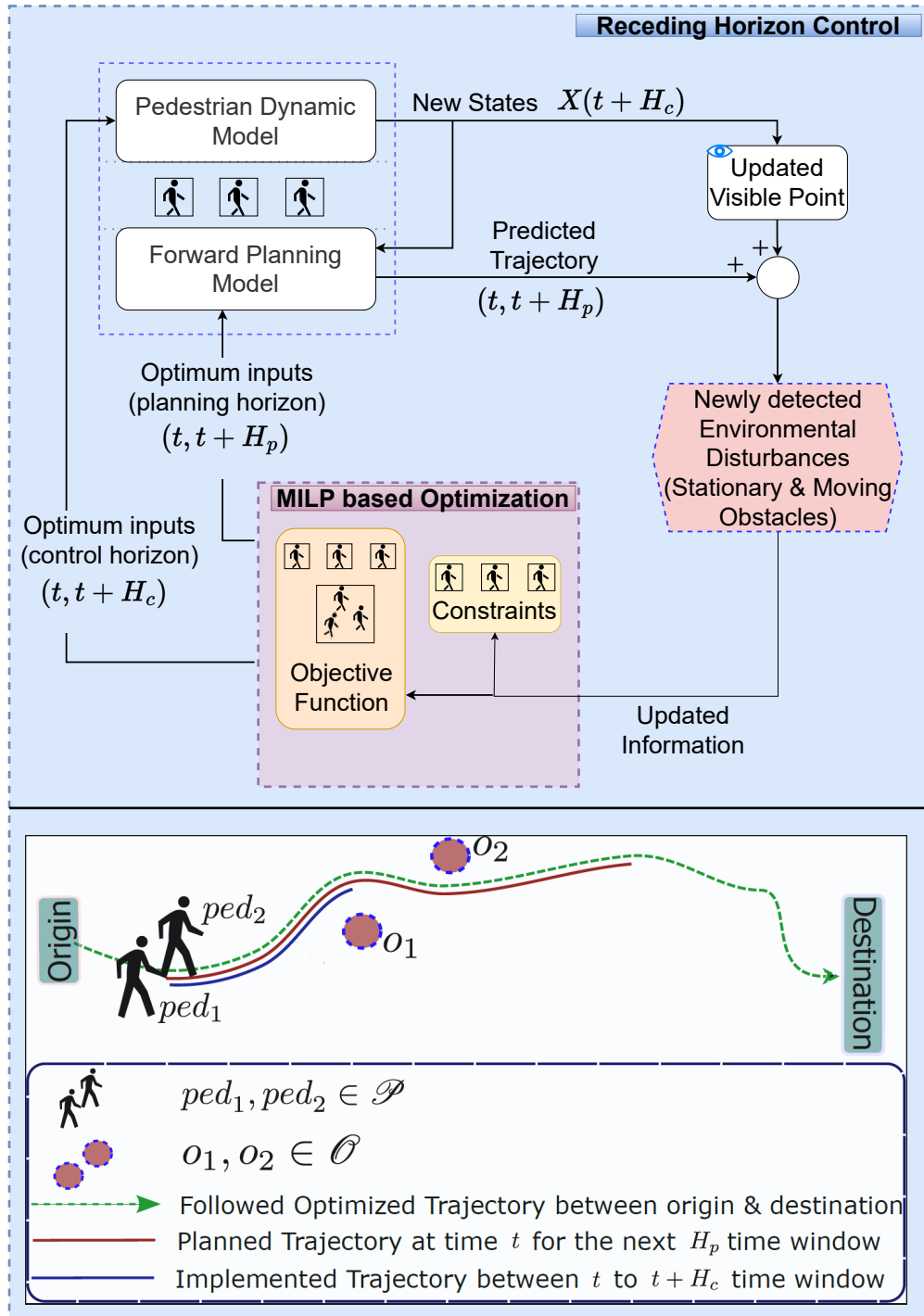


Figure 3.3: Modeling of the trajectory planning and trajectory execution process using a receding horizon control framework.

3.3 Receding Horizon Control based trajectory planning

The receding horizon control framework, as depicted in Figure 3.3, begins with each pedestrian maintaining an awareness of their next desired way-point, the local environment (i.e., the obstacles), and the other pedestrians they are walking with, if any. Based on these factors, the pedestrian will be modeled to generate a path looking H_p seconds into the future, thereby establishing a planning-horizon. The pedestrian will begin to implement their planned path for a fixed control-horizon of H_c seconds, where $H_c \ll H_p$. After H_c seconds, the process of planning ahead for H_p seconds is repeated, followed by executing the resulting plan. This planning and execution process occurs ad infinitum until the pedestrian has cleared the environment; again, at each iteration, the pedestrian updates their estimate of the environment and the location of other pedestrians in their group. As the pedestrian reaches their desired way-point a new way-point is set, and the process begins again. A summary of the relevant parameters describing the receding horizon control framework for modeling pedestrian motion is provided in Table 3.1.

Table 3.1: Relevant parameters describing the pedestrian simulation model.

Symbol	Meaning
\mathcal{P}	Set of pedestrians
\mathcal{O}	Set of obstacles
\mathcal{F}_o	Set of facets associated with obstacle o .
$\mathcal{G} = (\mathcal{V}, \mathcal{E})$	Graph structure defining pedestrian groups.
H_p	Planning horizon [seconds]
H_c	Control horizon [seconds]
$x_{i,t} \in \mathbb{R}^2$	X-Y position of the i^{th} pedestrian at time-step t .
$w_i \in \mathbb{R}^2$	Next way-point of the i^{th} pedestrian.
$\theta_i = \angle(w_i - x_{i,t})$	Direction of travel of i^{th} pedestrian at time-step t .
$d_{i,j}^{des} = (d_{i,j}^{\parallel des}, d_{i,j}^{\perp des}) \in \mathbb{R}^2$	The desired longitudinal and lateral separation between pedestrians i and j along their common direction of travel.

Within this chapter, the goal is to develop and describe the trajectory planning and trajectory execution processes at the foundation of the receding horizon control framework used to model pedestrians. And more specifically, to provide a flexible representation that can be easily adapted

to consider other types of active mobility agents. Here, the planning process is modeled and solved using Mixed-Integer Linear Programming (MILP). As part of the trajectory planning process, the underlying MILP optimization model assumes that each pedestrian maintains an accurate representation of the world (i.e., knows the location of obstacles and their group members); this information is encoded through constraint equations that model pedestrian dynamics and obstacle constraints. As pedestrians walk within a group, we assume they maintain private and common objectives. In this case, private objectives can include or consider: walking speeds, distance to obstacles, and time-to-arrival or distance-from-destination. Common objectives are associated with maintaining the moving graph structure discussed above, which is accomplished by maintaining the desired separation distance between other pedestrians in their group.

3.4 Summary

This chapter begins with the preliminaries on pedestrian interactions and pedestrian trajectory categorization. It also provided a mathematical background of the concepts used in the research, including convex optimization, mixed integer linear programming, and receding horizon control. Further, the chapter provided the details on the proposed framework, including the problem formulation and problem solution using MILP optimization embedded in the receding horizon control loop for pedestrian trajectory planning.

CHAPTER 4

MODELING INTRA-GROUP INTERACTIONS AND STATIONERY OBSTACLE ENCOUNTERS

This chapter provides the details of the model for pedestrians motion considering group interactions within the group and the interaction with stationery objects in the environment such as trees or poles.

4.1 Trajectory Optimization

Within the receding horizon control framework introduced in the previous chapter is the MILP optimization, which serves as the primary component by which pedestrian decision-making is modeled. The MILP optimization seeks to represent the private and common objectives and the dynamic and static constraints associated with pedestrians as they move within their environment. By clearly defining the objective functions (and associated coefficients) along with any constraints, the formulation, when solved, provides an optimal trajectory representative of the goals and objectives of each individual pedestrian. In this sub-section, details of the optimization formulation is provided, beginning with introducing important decision variables, followed by detailing of the constraint equations, and finally, describing the private and common objective functions for the pedestrians.

4.1.1 Decision Variables

For a given instantiation of the trajectory planning and execution cycle, each pedestrian i in the pedestrian set \mathcal{P} is first described according to their current x-y position $x_{i,t_0} \in \mathbb{R}^2$ at time-step t_0 and their desired next way-point, $w_i \in \mathbb{R}^2$. When optimizing the trajectories for H_p seconds over the planning horizon it is necessary to introduce new decision variables representing the planned

position and velocity of each pedestrian. To distinguish between the actual position of the pedestrians, $x_{i,t}$, and the planned position of the pedestrians is denoted, $z_{i,k} \forall k \in \{1, \dots, H_p\}$, representing the position of pedestrian i over H_p seconds when using 1-second increments. We also introduce the decision variables related to the position, velocity, and acceleration of each pedestrian relative to their direction of travel; for clarity, all decision variables described according to the coordinate frame in the direction of travel are indicated by the harpoon accent (e.g. $\vec{z}_{i,k}$). Accordingly, the decision variables for the position, velocity, and acceleration of pedestrian i in the rotated coordinate frame along the direction of travel are given by $\vec{z}_{i,k} = (\vec{z}_{i,k}^{\parallel}, \vec{z}_{i,k}^{\perp})$, $\vec{v}_{i,k} = (\vec{v}_{i,k}^{\parallel}, \vec{v}_{i,k}^{\perp})$ and $\vec{u}_{i,k} = (\vec{u}_{i,k}^{\parallel}, \vec{u}_{i,k}^{\perp})$, all defined over $\mathbb{R}^2 \forall k \in \{0, \dots, H_p - 1\}$; each term inside the vectors corresponds to the longitudinal and lateral values along the nominal direction of travel.

The distinction between the position of pedestrians in a global coordinate frame versus a local coordination frame assists in establishing constraints and objective costs related to the position of pedestrians relative to obstacles and other pedestrians in their group. When constructing optimization constraints associated with obstacle avoidance, it is easiest to describe these obstacle constraints using a common global coordinate frame. Meanwhile, because the desired separation between pedestrians walking in a group is described in a relative frame, using a coordinate system aligned with this relative coordinate frame is preferred. Similarly, velocity and acceleration constraints for each pedestrian are easily described in the local coordinate frame. Translation of the pedestrian position at any time-step between the global and a rotated local coordinate frame is possible using the linear transformation

$$z_{i,k} = R(-\theta_i) \vec{z}_{i,k} \forall k \in \{0, \dots, H_p - 1\} \quad (4.1)$$

where $R(\theta_i)$ is the standard rotation matrix

$$R(\theta_i) = \begin{bmatrix} \cos \theta_i & -\sin \theta_i \\ \sin \theta_i & \cos \theta_i \end{bmatrix}$$

Table 4.1: Relevant decision variables for the pedestrian trajectory planning optimization model.

Symbol	Meaning
$z_{i,k} \in \mathbb{R}^2$	Planned position of pedestrian i at time-step k in global X-Y coordinate frame
$\vec{z}_{i,k} = (\vec{z}_{i,k}^{\parallel}, \vec{z}_{i,k}^{\perp}) \in \mathbb{R}^2$	Planned position of pedestrian i at time-step k in rotated coordinate frame in direction of travel
$\vec{v}_{i,k} = (\vec{v}_{i,k}^{\parallel}, \vec{v}_{i,k}^{\perp}) \in \mathbb{R}^2$	Planned velocity of pedestrian i at time-step k in rotated coordinate frame in direction of travel
$\vec{u}_{i,k} = (\vec{u}_{i,k}^{\parallel}, \vec{u}_{i,k}^{\perp}) \in \mathbb{R}^2$	Planned acceleration of pedestrian i at time-step k in rotated coordinate frame in direction of travel
$b_{o,f,i,k} \in \{0, 1\}$	Binary variable used to indicated that pedestrian i is outside of the boundary of obstacle o , in reference to facet f of the obstacle, at time-step k

parameterized by the direction of travel θ_i .

Based on the descriptions above a complete list of decision-variables is provided in Table 4.1.

4.1.2 Dynamic Constraint Equations

A portion of the constraint equations seek to represent the dynamic constraints describing pedestrian motion. For the i^{th} pedestrian the second-order discrete-time update equation for their position relative to their direction of travel is given by the set of constraints

$$\begin{aligned}\vec{z}_{i,k+1} &= \vec{z}_{i,k} + \vec{v}_{i,k}\Delta T + 1/2\vec{u}_{i,k}\Delta T^2 \\ \vec{v}_{i,k+1} &= \vec{v}_{i,k} + \vec{u}_{i,k}\Delta T\end{aligned}\tag{4.2}$$

and $k \in \{0, \dots, H_p - 1\}$

The discrete-time update equation in (Equation 4.2) assumes a regularly updating process that occurs at a regular time-step of ΔT seconds (e.g. 1 sec, 5 sec), during which in between time-stamps, the acceleration is asserted to be constant.

The motion of each pedestrian can also be constrained according to their minimum and maximum walking velocity, denoted by $\underline{v}_i, \bar{v}_i$, and their minimum and maximum acceleration. Applying the small angle approximation, whereby it is assumed that the lateral velocity of pedestrians is

small compared to their longitudinal velocity, it is sufficient to write

$$\underline{v}_i \leq \overrightarrow{v}_{i,k} \leq \bar{v}_i \quad \forall i \in \mathcal{P}. \quad (4.3)$$

In many cases, pedestrians can be restricted to only walk forward so that $\underline{v}_i > 0$. In the case when the small angle approximation is likely to be violated, it is possible to replace the velocity constraint in (Equation 5.3) with

$$\|\overrightarrow{v}_{i,k}\|_2^2 \leq \bar{v}_i \quad \forall i \in \mathcal{P}. \quad (4.4)$$

which corresponds to a convex quadratic constraint that can be represented in CPLEX, CVX, or other commonly used optimization solvers. The limitation of the constraint in (Equation 4.4) is that non-zero minimum bounds on the magnitude of the velocity (e.g. $\underline{v}_i \leq \|v_{i,k}\|_2 \leq \bar{v}_i$) cannot be enforced without converting the constraint to be non-convex – thereby making it unsolvable in CVX without significant approximations, or expansion and manipulation of the constraint. That said, (Equation 4.4) can be approximated using the ℓ_∞ or ℓ_0 norms, or can be approximated with a convex polygon.

Similar constraints on the acceleration rate of pedestrians is also possible using similar representations. That is to say, it is possible to include the acceleration constraint

$$\|\overrightarrow{u}_{i,k}\|_2^2 \leq \bar{u}_i \quad \forall i \in \mathcal{P}. \quad (4.5)$$

4.1.3 Obstacle Constraint Equations

The potential presence of obstacles within the environment requires pedestrians to plan their trajectories accordingly. In contrast to the pedestrian constraints and cost equations, the obstacle avoidance constraints are inherently non-convex. Essentially, obstacle avoidance generates binary variables and a set of constraints that correspond to moving *left* or *right* around any obstacle rela-

tive to any given side or facet of the obstacle. For a convex obstacle o that can be approximated by a polygon with a set of facets, $\mathcal{F}_o = \{1, \dots, F_o\}$, it is possible to define a set of linear constraints

$$h_{o,f}^T y \leq g_{o,f} \quad \forall f \in \mathcal{F}_o \quad (4.6)$$

representing half-spaces that can be used to define the set of points $y \in \mathbb{R}^2$ that are blocked by the obstacle.

For obstacle avoidance, the planned position of a pedestrian at any point in time, $z_{i,k}$, must be outside of the convex polygon. In relation to a single facet $f \in \mathcal{F}_o$ of the polygon representing obstacle o , the i^{th} pedestrian is outside of the obstacle if their position at time-step k satisfies the constraint

$$g_{o,f} - h_{o,f}^T x_{i,k} \leq 0 \quad (4.7)$$

Accordingly, to avoid obstacle o , (Equation 4.7) must hold true for at least one of the facets f to ensure that the pedestrian is located outside of the obstacle. The representation of such a constraint is written as

$$\left\{ \begin{array}{l} g_{o,1} - h_{o,1}^T x_{i,k} \leq 0 \\ or \\ \vdots \\ or \\ g_{o,f} - h_{o,f}^T x_{i,k} \leq 0 \\ or \\ \vdots \\ or \\ g_{o,F} - h_{o,F}^T x_{i,k} \leq 0. \end{array} \right. \quad (4.8)$$

Implementation of the constraint in (Equation 4.8) can be achieved using Big-M notation within a

MILP solver after introducing binary variables $b_{o,f,i,k} \in \{0, 1\} \forall f \in \mathcal{F}$ and $k \in \{1, \dots, H_p\}$; the binary logical condition $b_{o,f,i,k} = 1$ indicates that pedestrian i is avoiding obstacle o at time-step k relative to facet f . Within a MILP formulation, this is implemented for all pedestrians and all obstacles using the following constraint equations:

$$\begin{aligned}
g_{o,f} - h_{o,f}^T x_{i,k} &\leq M(1 - b_{o,f,i,k}) \quad \forall f \in \mathcal{F}_o, o \in \mathcal{O} \\
& \quad i \in \mathcal{P}, k \in \{1, \dots, H_p\} \\
\sum_{f \in \mathcal{F}_o} b_{o,f,i,k} &\geq 1 \quad \forall o \in \mathcal{O}, i \in \mathcal{P} \\
& \quad k \in \{1, \dots, H_p\}
\end{aligned} \tag{4.9}$$

where M is sufficiently large such that the f^{th} constraint holds when $b_{o,f} = 0$ regardless of the position of the pedestrian. For practical purposes, the value of M can be set based on the dimensions of the environment. Alternatively, when implementing the constraints in (Equation 4.8) in CVX, instead of using Big-M notation, it is suggested that readers make use of indicator constraints.

While not explicitly stated, a buffer distance can be added around each obstacle. If it is assumed that any extra buffer distance, $e_{o,i}$, depends on the specific obstacle o and pedestrian i then each obstacle constraint from (Equation 4.7) is adjusted to

$$g_{o,f} - h_{o,f}^T x_{i,k} \leq - \|h_{o,f}\| e_{o,i}. \tag{4.10}$$

4.1.4 Private and Common Objective Functions

Research suggests that pedestrians pursue personal objectives (e.g., minimization of their individual effort, reaching the desired destination) as well as global objectives shared with other agents (e.g., maintaining desired separations when walking in formation) [66, 71, 72, 73]. Accordingly, we have formulated a generalizable objective function that takes into account all these factors.

Beginning with personal objectives, the objective function can account for the regulation of

walking speeds, as well as running costs and the terminal cost of reaching a desired way-point.

$$\begin{aligned}
& \sum_{k=1}^{H_p} \sum_{i \in \mathcal{P}} (k_i^{acc} \|u_{i,k} - u_i^{des}\| + k_i^{speed} \|v_{i,k} - v_i^{des}\| \\
& \quad + k_i^{run} \|x_{i,k} - w_i\|) \\
& \quad + \sum_{i \in \mathcal{P}} k_i^{term} \|x_{i,H_p} - w_i\|
\end{aligned} \tag{4.11}$$

In the private objective costs above, each norm can be adjusted according to desired modeling (i.e., ℓ_1 , ℓ_2 , or ℓ_∞). Additionally, each weighting can be adjusted to reflect the relative value.

When walking as part of a group, pedestrians can optimize their planned trajectories in order to maintain a desired formation. This is accomplished by penalizing any deviations between the actual and desired separation. This can be accomplished using the following objective equation:

$$\sum_{k=1}^{H_p} \sum_{(i,j) \in \mathcal{E}} k_{i,j}^{sep} \|\vec{z}_{i,k} - \vec{z}_{j,k} - d_{i,j}^{des}\| \tag{4.12}$$

The summation over the edge-set \mathcal{E} in the graph structure \mathcal{G} provides for significant flexibility. For example, it is not necessary to ensure consistency in the desired separation between pedestrians. So for any three pedestrians h , i , and j in the same pedestrian group there is no requirement that $d_{i,j}^{des} + d_{j,h}^{des} = d_{i,h}^{des}$. In fact, it is not even necessary that pedestrians in the same group seek to maintain a desired separation.

In specific cases (e.g. a parent and small child walking together), it may be more appropriate to represent separation distances within constraints instead of within objective costs. For the case in which two pedestrians must remain within a specified range $r_{i,j}$ of each other, the equivalent convex constraint is expressed as

$$\|\vec{z}_{i,k} - \vec{z}_{j,k}\| \leq r_{i,j} \quad \forall k \in \{1, \dots, H_p\} \tag{4.13}$$

Table 4.2: Short-hand markers indicating the ranges over which constraints apply.

Sets	Short-hand notation
$i \in \mathcal{P}, k \in \{1, \dots, H_p\}$	*
$i \in \mathcal{P}, k \in \{0, \dots, H_p - 1\}$	•
$i \in \mathcal{P}, k \in \{0, \dots, H_p\}$	◇
$i \in \mathcal{P}, k \in \{1, \dots, H_p\}, o \in \mathcal{O}, f \in \mathcal{F}_o$	△
$i \in \mathcal{P}, k \in \{1, \dots, H_p\}, o \in \mathcal{O}$	†

4.1.5 Model Summary

A summary of the complete formulation is provided below. Due to space constraints, a short-hand notation listed in Table 4.2 is used to indicate the ranges for which each the constraints hold. For example, all equations that hold true over $i \in \mathcal{P}, k \in \{1, \dots, H_p\}$ are indicted by the * symbol. As written below, all decision variables are assumed to be unrestricted, except for any binary variables. Furthermore, in summary below, we refrain from specifying which norm is used in the objective function and constraints. While in many cases, the ℓ_2 norm is appropriate, representations using the ℓ_1 or ℓ_∞ are permissible as well. Also, as noted in subsection 4.1.2, ℓ_2 norms that restrict walking velocities and accelerations can be approximated through a series of linear convex constraints. The advantage of using an alternative to the ℓ_2 norm is that a broader array of optimization solvers can be used since the problem can be represented using a linear objective function and constraints.

$$\begin{aligned}
\min & \sum_{k=1}^{H_p} \sum_{i \in \mathcal{P}} (k_i^{acc} \|u_{i,k} - u_i^{des}\| \\
& + k_i^{speed} \|v_{i,k} - v_i^{des}\| \\
& + k_i^{pos} \|x_{i,k} - w_i\|) \\
& + \sum_{i \in \mathcal{P}} k_i^{term} \|x_{i,H_p} - w_i\| \\
& + \sum_{k=1}^{H_p} \sum_{(i,j) \in \mathcal{E}} k_{i,j}^{sep} \|\vec{z}_{i,k} - \vec{z}_{j,k} - d_{i,j}^{des}\| \\
s.t. & \vec{z}_{i,k+1} = \vec{z}_{i,k} + \vec{v}_{i,k} \Delta T + 1/2 \vec{u}_{i,k} \Delta T^2 & \bullet \\
& \vec{v}_{i,k+1} = \vec{v}_{i,k} + \vec{u}_{i,k} \Delta T & \bullet \\
& \|\vec{v}_{i,k}\| \leq \bar{v}_i & * \\
& \|\vec{u}_{i,k}\| \leq \bar{u}_i & * \\
& z_{i,k} = R(-\theta_i) \vec{z}_{i,k} & \diamond \\
& g_{o,f} - h_{o,f}^T x_{i,k} \leq M(1 - b_{o,f,i,k}) & \triangle \\
& \sum_{f \in \mathcal{F}_o} b_{o,f,i,k} \geq 1 & \dagger \\
& b_{o,f,i,k} \in \{0, 1\} & \triangle
\end{aligned}$$

4.2 Implementation Details

Implementation of the receding-horizon control framework with the embedded MILP is completed in MATLAB using the CVX optimization library. While the CVX library is primarily targeted at solving convex optimization problems, it has recently gained support for both Mixed-Integer Linear Programs and Mixed-Integer Quadratic Programs. The proposed framework is applicable to a broad range of traffic scenarios. In our research, the three traffic scenarios manifesting a large portion of pedestrians' walking behavior and social interaction rules are identified. The traffic sce-

narios where a group of two agents walks together, a group of three agents walks together, and an agent avoids a stationary obstacle are considered. They are developed as three case studies, discussed in section 4.3 and section 4.4. While experimenting with the case studies, we made a few adjustments - the terminal cost of reaching the desired waypoint is used while the running cost weight $k_i^{pos} = 0$; the factor for speed regulation to have desired speed is made $k_i^{speed} = 0$; the minimization of acceleration is included but the objective to maintain the desired acceleration is not implemented ($u_i^{des} = 0$). Each norm in the private objective cost is adjusted to the ℓ_1 norm. The common objective cost (Equation 4.12) is adjusted to ℓ_1 norm. The velocity and acceleration are constrained to an average minimum and maximum values, each in the lateral and longitudinal direction. They are adjusted as ℓ_∞ norm. The idea is to adjust the weights and the norm in the proposed generalized model as it results in a good Mixed-Integer Linear Programming problem.

Despite being the same here, within the receding-horizon control framework, the actual dynamics of the pedestrians are distinguished from the modeled dynamics contained in the trajectory planning optimization described in section 4.1, see Figure 3.3. Real-world differences emerge due to uncertainty in an environment (e.g., approximate location of obstacles) or perturbations in dynamics (e.g., a pedestrian tripping). Within a simulated environment, we assumed that the pedestrians' knowledge of the environment is perfect; that is to say, pedestrians are aware of the exact position and location of all obstacles and other pedestrians. The benefit of the proposed receding-horizon control modeling of uncertainties, and pedestrian response to the uncertainties can be modeled. Specifically, the capability of distinguishing between dynamics of pedestrians as different from the modeled dynamics of pedestrians contained in the trajectory planning optimization is particularly beneficial when modeling pedestrians with vision limitations, as well as pedestrians and active mobility users that become distracted or lose awareness of their environment.

4.3 Calibration and Validation

The next step to model development is calibrating the model parameters and validating the model outputs. This section will describe the model parameters, the dataset used, calibration process, performance metrics, and validation process of the developed pedestrian trajectory generating algorithm. The validation process compares the generated agent (i.e., pedestrian) trajectories with the ground truth for a traffic scenario. The proposed framework is generalizable to many pedestrian traffic scenarios. However, to show the validity of the proposed model, we have identified three case studies. Three case studies are performed - Case study 1 (Two agents walk together), Case study 2 (Three agents walk together), and Case study 3 (An agent avoids an obstacle).

4.3.1 Key Model Parameters

The key parameters of the developed pedestrian trajectory planning model are as follows:

- Total time-steps to run a simulation (T)
- The desired longitudinal separation between pedestrians i and j ($d_{i,j}^{\parallel des}$)
- The desired lateral separation between pedestrians i and j ($d_{i,j}^{\perp des}$)
- Control Horizon (H_c)
- Planning Horizon (H_p)
- Maximum and Minimum mean velocity
- Maximum and Minimum mean acceleration
- Buffer zone: The gap that the pedestrian tries to keep while passing the stationary obstacle

4.3.2 Data Description

We considered data from the dataset of paper [74] which was collected at the campus of Dalian University of Technology (DUT) in China. The dataset is one of the crowd interaction benchmark datasets. The scenario includes an area of pedestrian crosswalks at an intersection. Figure 4.1 shows the data collection location and Figure 4.2 shows the sample of extracted trajectories. A *DJI Mavic Pro* Drone with a down-facing camera was used as the recording gear. The video resolution was 1920×1080 with an *fps* of 23.98. Pedestrians in the data are mainly college students. The trajectories were extracted from the recorded data using video stabilization, pedestrian tracking, coordinate transformation, and Kalman filtering techniques.



Figure 4.1: Data Collection Location

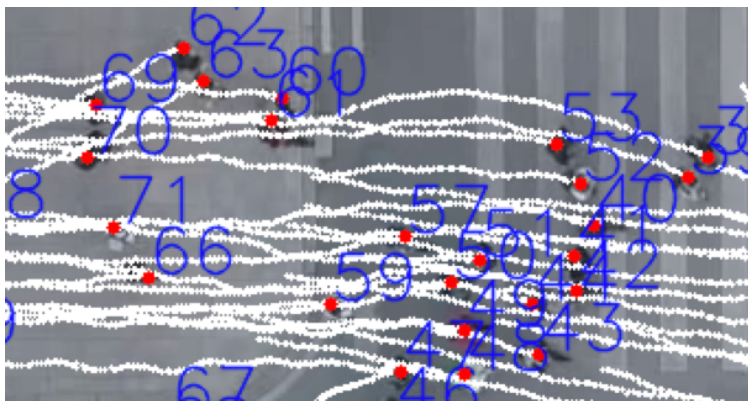


Figure 4.2: Sample Extracted Trajectories

4.3.3 Model Calibration

Methodology

Firstly, we identified traffic scenarios in the dataset where pedestrians are moving as a group of two, as a group of three, and as individual agents avoiding stationary obstacles. For each case study, maximum and minimum velocity, maximum and minimum acceleration, $d_{i,j}^{\perp des}$ and $d_{i,j}^{\parallel des}$ values are extracted, and the average values are calculated. Also, sampling time and pedestrian's initial and final destination values are determined from the dataset.

We have extracted forty samples for two agents group, thirty samples for three agents group, and twenty samples for individuals avoiding the obstacles. Considering the case study of two agents group, we divided the forty collected samples into thirty samples for training the model and ten samples for testing the developed model. We have used the normal distribution method to dynamically calibrate the $d_{i,j}^{\perp des}$ and $d_{i,j}^{\parallel des}$ values. The initial location values of the agent are updated at every control horizon time (H_c) based on receding horizon control.

Calibrated Model Parameters

Table 4.3 shows the calibrated values of parameters for Case Study 1 (two agents walk together). We extracted the $d_{i,j}^{\perp des}$ and $d_{i,j}^{\parallel des}$ values and calculated the average values for all the samples for this case study. The values of $d_{i,j}^{\perp des}$ and $d_{i,j}^{\parallel des}$ aligned well with the normal distribution, further verified by the chi-square test ($h = 0$). The chi-square goodness-of-fit test was done which returns the $h = 0$ value meaning the data comes from a normal distribution. We defined a normal distribution for $d_{i,j}^{\perp des}$ and $d_{i,j}^{\parallel des}$. In the Case Study 1, the planning horizon (H_p) was considered as 2 sec, and control horizon (H_c) was taken as 1 sec. Similarly parameters were computed for Case Study 2 and 3, shown in Table 4.4 and Table 4.5 respectively.

4.3.4 Performance Metrics

To evaluate the results, we use the following performance metrics.

Table 4.3: Model Calibration for Case Study 1

Parameters	Calibrated Values
$d_{i,j}^{\perp des}$	$\mu = 0.52, \sigma = 0.15$
$d_{i,j}^{\parallel des}$	$\mu = 0.097, \sigma = 0.046$
Average minimum velocity	0.97 m/sec
Average maximum velocity	1.70 m/sec
Average minimum acceleration	-0.3 m/sec ²
Average maximum acceleration	0.3 m/sec ²

Table 4.4: Model Calibration for Case Study 2

Parameters	Calibrated Values
$d_{i,j}^{\perp des}$ between agent 1 and agent 2	$\mu = 0.612, \sigma = 0.194$
$d_{i,j}^{\parallel des}$ between agent 1 and agent 2	$\mu = 0.294, \sigma = 0.237$
$d_{i,j}^{\perp des}$ between agent 2 and agent 3	$\mu = 0.241, \sigma = 0.178$
$d_{i,j}^{\parallel des}$ between agent 2 and agent 3	$\mu = 0.719, \sigma = 0.221$
Average minimum velocity	0.97 m/sec
Average maximum velocity	1.48 m/sec
Average minimum acceleration	-0.3 m/sec ²
Average maximum acceleration	0.3 m/sec ²

Table 4.5: Model Calibration for Case Study 3

Parameters	Calibrated Values
Average minimum velocity	0.82 m/sec
Average maximum velocity	1.75 m/sec
Average minimum acceleration	-0.3 m/sec ²
Average maximum acceleration	0.4 m/sec ²
Gap between the agent and obstacle	0.55 m

- MED : Mean Euclidean Distance is the average Euclidean distance between the model predicted coordinates and the actual coordinates of the pedestrian at every instant. Lower is better.
- FDE : Final Displacement Error is the Euclidean distance between the model predicted final destination and the actual final destination at the corresponding time instant.
- $rmse_{d_{i,j}^l}$: It is the root mean square error of the lateral distance between the two agents' actual and the generated trajectories.
- $rmse_{d_{i,j}^l}$: It is the root mean square error of the longitudinal distance between the two agents' actual and the generated trajectories.
- Gait parameters: Analysis of basic gait parameters (step length, step frequency, and walking speed) helps understand a person's walking style. The step length and step frequency are affected by many attributes such as gender, age, group size, commonalities between agents [75] [76]. Step length is defined as the distance from the initial contact point of one foot to the initial contact point of the other foot. Step frequency is measured by the number of steps taken per minute. Following equation shows the relationship between the three determinant gait parameters [77] [78]:

$$\text{walking speed} = \text{step frequency} \times \text{step length.}$$

To further validate our research work, we have compared the gait parameters estimated in the case studies with the ones mentioned in [58].

4.3.5 Validation process

We have performed an extensive validation on a unidirectional pedestrian movement - group movement of two to three pedestrians, interaction with a stationary obstacle. The developed trajectory

planning model is tested on the case studies obtained from the DUT crowd interaction dataset [74]. The case studies are where two agents walk together, three walk together, and an agent avoids a stationary obstacle. The generated trajectories are compared with the actual trajectories of agents for the particular traffic scenarios, and the proposed performance metrics will help to inspect the model performance. The details and results of three case studies are discussed in the following sections.

4.4 Experimental Results

This section provides the experimental results from the chosen case studies. Note that the developed modeling framework is generalizable making it applicable across a broad range of pedestrian scenarios. To demonstrate this, we highlight three case studies that account for a large portion of pedestrian scenarios.

4.4.1 Case Study 1: Two Agents walk together

Description: We consider the scenario where two agents walk together. To perform the calibration and validation, we divided the forty collected samples into thirty samples for training the model and ten samples for testing the developed model. The calibrated values are provided in the Table 4.3. The sample screenshots in Table 4.7 are from actual video data. In the sample screenshots, we can observe that the two agents are walking together, and they always maintain a certain separation between them. This behavior is expected from humans when they walk in a group.

Result: Once the model was calibrated, we performed the validation on the testing data. The trajectories are shown in Table 4.7. The first column shows the screenshots from the real dataset. The second column shows the corresponding model-generated trajectories. These are MATLAB-generated plots showing the generated trajectories and respective real trajectories of the same set of agents. In each graph, the marked lines are real trajectories, and non-marked lines are the corresponding model generated trajectories. For the given scenario's initial and final destination,

the model generates the pedestrian trajectories by evaluating the environment and maintaining the human-human group behavior.


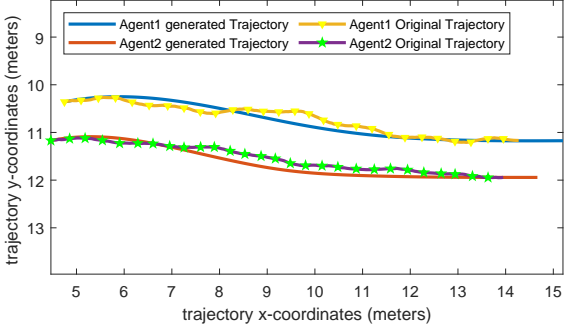
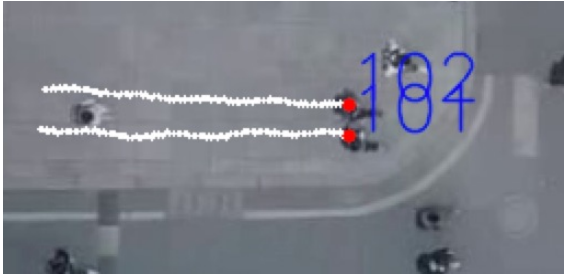
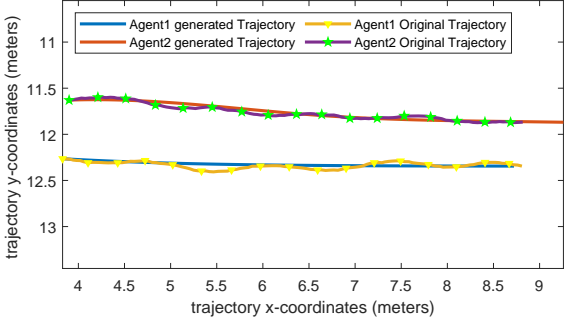
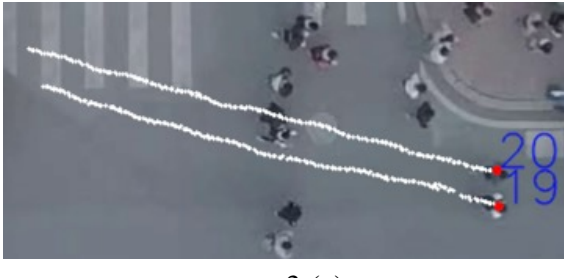
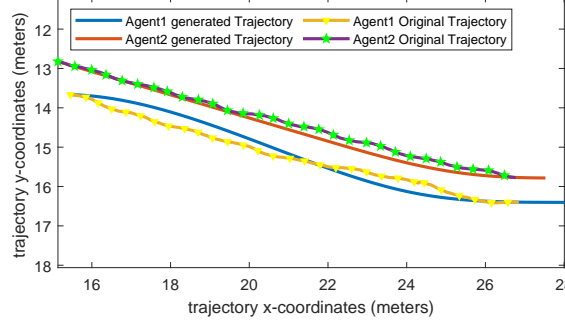
Table 4.6: Case Study 1 Performance metrics average values for DUT dataset

Performance metrics	Average values
MED	0.28
FDE	0.45
$\text{rmse}_{d_{i,j}^\perp}$	0.36
$\text{rmse}_{d_{i,j}^\parallel}$	0.007

The plots in Table 4.7 show the accuracy of the generated trajectories. The lower values of performance metrics validate the good performance of the algorithm. Table 4.6 provides the average values of the performance metrics, MED and FDE. A zero value would indicate that the predicted and actual data are almost identical. However, the value of zero is almost not possible practically; therefore, the closer the average values are to zero, the better fit the data has achieved. The error metrics values are quite low, with $\text{MED} = 0.28$, $\text{FDE} = 0.45$, $\text{rmse}_{d_{i,j}^\perp} = 0.36$, $\text{rmse}_{d_{i,j}^\parallel} = 0.007$. Values confirm what we can visualize from the model generated results in Table 4.7. Table 4.9 illustrates the obtained gait parameters in case study 1. It can be noted that step length remains in the 0.6 to 0.7 meter range. On the other hand, pedestrians increase their step frequency to attain a higher speed to cross the pedestrian crossing in time. The obtained gait parameters are within the range as mentioned in [58]. The step length and step frequency define the walking speed as described in subsection 4.3.4. Those parameters also characterize the person walking style, which changes depending on the scenario, age, gender, and level of group commonalities. For example, the instantaneous value of a gait parameter is influenced by activities such as the walking behavior in a group and obstacle avoidance.

Table 4.8 summarizes the results for the testing dataset. The table shows the average values of root mean square error between the ground truth and the generated trajectory for x-position, y-position, longitudinal velocity of each agent at every instant. The values are near-zero, validating

Table 4.7: Case Study 1 Sample Results

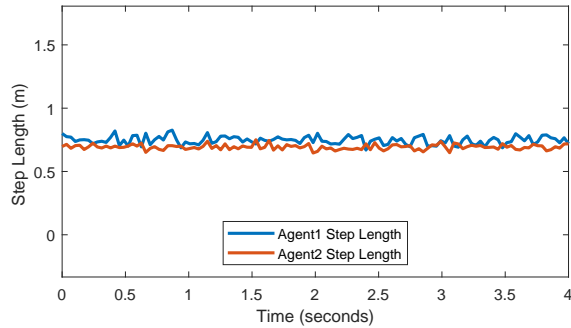
Trajectory Screenshot	Generated Trajectories
	
1 (a)	1 (b)
	
2 (a)	2 (b)
	
3 (a)	3 (b)

the high accuracy of the proposed model.

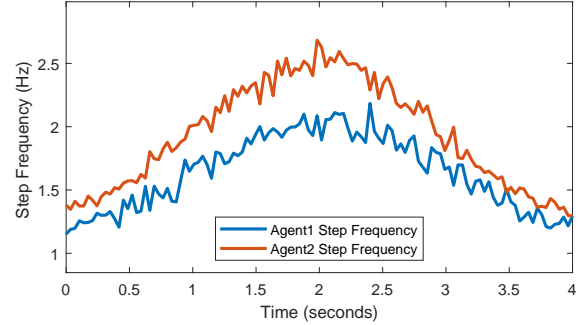
Table 4.8: Table shows detailed performance metric values of Case Study 1. The average value of the Root Mean Square Error (rmse) is between the agents’ generated coordinates and ground truth coordinates.

Agents’ Pair (I and J)	Agent I position		Agent J position		Agent I velocity (rmse_ \vec{v}_i)	Agent J velocity (rmse_ \vec{v}_j)	Lateral separation (rmse_ $d_{i,j}^\perp$)	Longitudinal separation (rmse_ $d_{i,j}^\parallel$)
	X position (rmse_x1)	Y position (rmse_y1)	X position (rmse_x2)	Y position (rmse_y2)				
94 and 95	0.51	0.15	0.45	0.15	0.43	0.45	0.12	0.005
101 and 102	0.07	0.03	0.22	0.02	0.25	0.41	0.52	0.004
22 and 23	0.9	0.61	0.84	0.67	0.41	0.44	0.21	2.88E-05
53 and 54	0.28	0.4	0.47	0.84	0.26	0.33	0.57	3.55E-05
56 and 57	0.39	0.59	0.37	0.67	0.29	0.31	0.09	6.33E-04
2 and 3	0.09	0.09	0.13	0.4	0.34	0.32	0.04	0.015
7 and 8	0.39	0.29	0.18	0.37	0.46	0.33	0.83	0.0065
16 and 17	0.45	0.15	0.06	0.12	0.36	0.3	0.8	0.003
18 and 19	0.07	0.19	0.43	0.12	0.26	0.4	0.6	0.05
30 and 31	0.6	0.3	0.62	0.2	0.32	0.3	0.06	9.41E-06
32 and 33	0.53	0.33	0.43	0.39	0.33	0.31	0.08	7.66E-06

Table 4.9: (a) Step Length (b) Step Frequency of Agents 101 and 102



(a)



(b)

4.4.2 Case Study 2: Three agents walk together

Description: We study the case scenarios where three pedestrian walks in a group, the left column in Table 4.11 shows some sample screenshots from real video data. The model is calibrated, and parameters values are listed in Table 4.4. The sample figures are from the actual data. To perform the calibration and validation of the case study of three agents’ group behavior, we divided the

thirty collected samples into twenty-three samples for training the model and seven samples for testing the developed model.

Result: Once the model was calibrated, we performed the validation on the testing data. The results are shown in Table 4.11. The results show the graphs which compare the actual and predicted trajectories. The left column in the table shows the sample scene from the video dataset, and the right column shows the model generated trajectories and their comparison with the actual trajectories. The plots demonstrate the model’s accuracy and illustrate the group formation, as explained in Figure 3.2a when three agents walk together.

Table 4.10 shows the average euclidean values and root mean square error values for the test samples. The average values indicate good results as almost all values are less than one, with MED = 0.38 and FDE = 0.16. An RMSE value of zero would tell that the predicted and actual data are almost identical. The closer the RMSE values and euclidean distance are to zero, the better the model performance. The lower values of lateral and longitudinal separation ($d_{i,j}^\perp$ and $d_{i,j}^\parallel$) between two agents demonstrate the capability of the model-generated trajectories to emulate the actual trajectories, even when subjects are walking in groups.

Table 4.10: Case Study 2 Performance metrics average values for DUT dataset

Performance metrics	Average values
MED	0.38
FDE	0.16
rmse- $d_{1,2}^\perp$	0.87
rmse- $d_{1,2}^\parallel$	0.005
rmse- $d_{2,3}^\perp$	0.32
rmse- $d_{2,3}^\parallel$	0.002

Table 4.9 shows the walking gait variations in instances of Case Study 2. In general, the step length remains in the 0.6 to 0.75-meter range, the default step length range in group behavior. The measured gait parameters reflect the underlying strategies that govern the behavioral rules. The variation in gait parameters shows how an individual maintains their step length and step

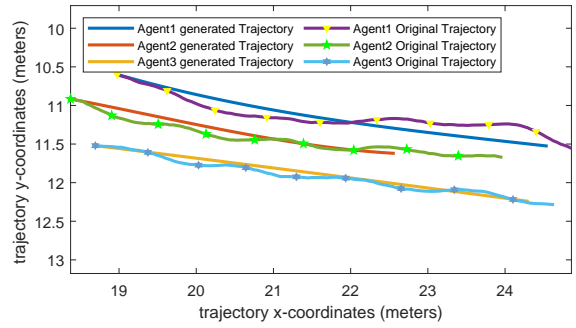
Table 4.11: Case Study 2 Sample Results

Trajectory Screenshot

Generated Trajectories



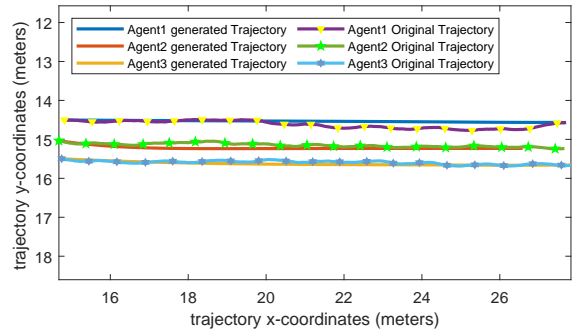
1 (a)



1 (b)



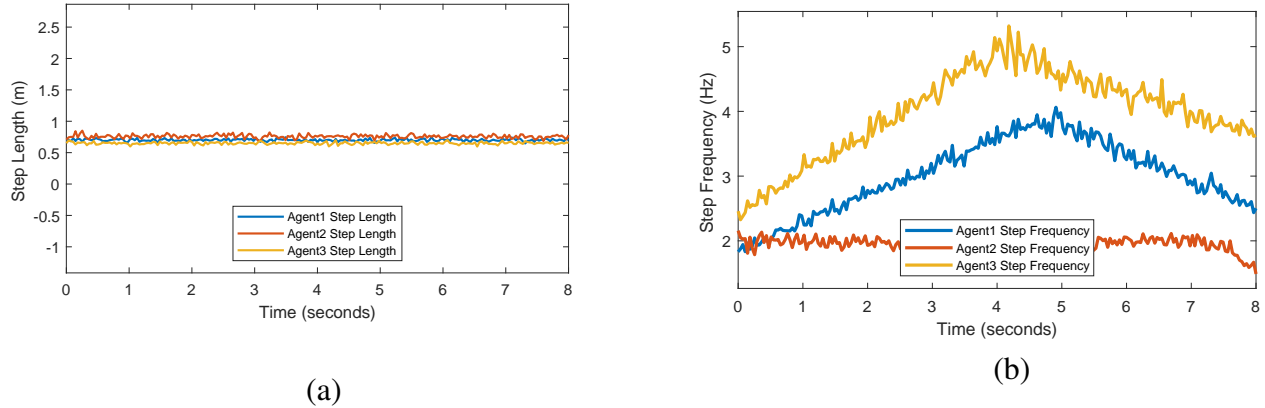
2 (a)



2 (b)

frequency to maintain a group walking behavior. In Table 4.9, we can see that Agent 2 and Agent 3’s step length are almost the same and less than Agent 1, and Agent 2 and Agent 3 have more step frequency, ultimately all three agents in a group maintain similar speed. The results prove humans’ innate ability to adapt their gait parameters to maintain a group movement.

Table 4.12: (a) Step Length (b) Step Frequency of Agents 22, 23, and 24



4.4.3 Case Study 3: An agent avoids an obstacle

Description: The third study demonstrates how individuals avoid stationery obstacles. We study the scenarios where the pedestrian passes the stationery obstacle (in our case, it is a standing car represented as a square obstacle). The average buffer zone that pedestrians keep having a safe pass by the obstacle is calculated using data. The estimated buffer zone is approx 0.55 meters. The model is calibrated, and parameters values are listed in Table 4.5. Twenty case study 3 samples are collected from the dataset, divided the fifteen samples for training the model and five samples for testing the developed model. In the Table 4.14, the left column has the sample screenshots from actual video data. The right column has the corresponding model-generated pedestrian trajectories.

Result: Once the model was calibrated, we validated the testing data. The results are shown in Table 4.14. The table shows the graph which is comparing the actual and predicted trajectories.

The Table 4.13 shows the average Euclidean distance values. The closer the euclidean distance values are to zero, the better fit the data has achieved. The average values indicate good results as

almost all values are under one, with MED = 0.66 and FDE = 0.35.

Table 4.13: Case Study 3 Performance metrics average values for DUT dataset

Performance metrics	Average values
MED	0.66
FDE	0.35

Table 4.14: Case Study 3: Sample Results

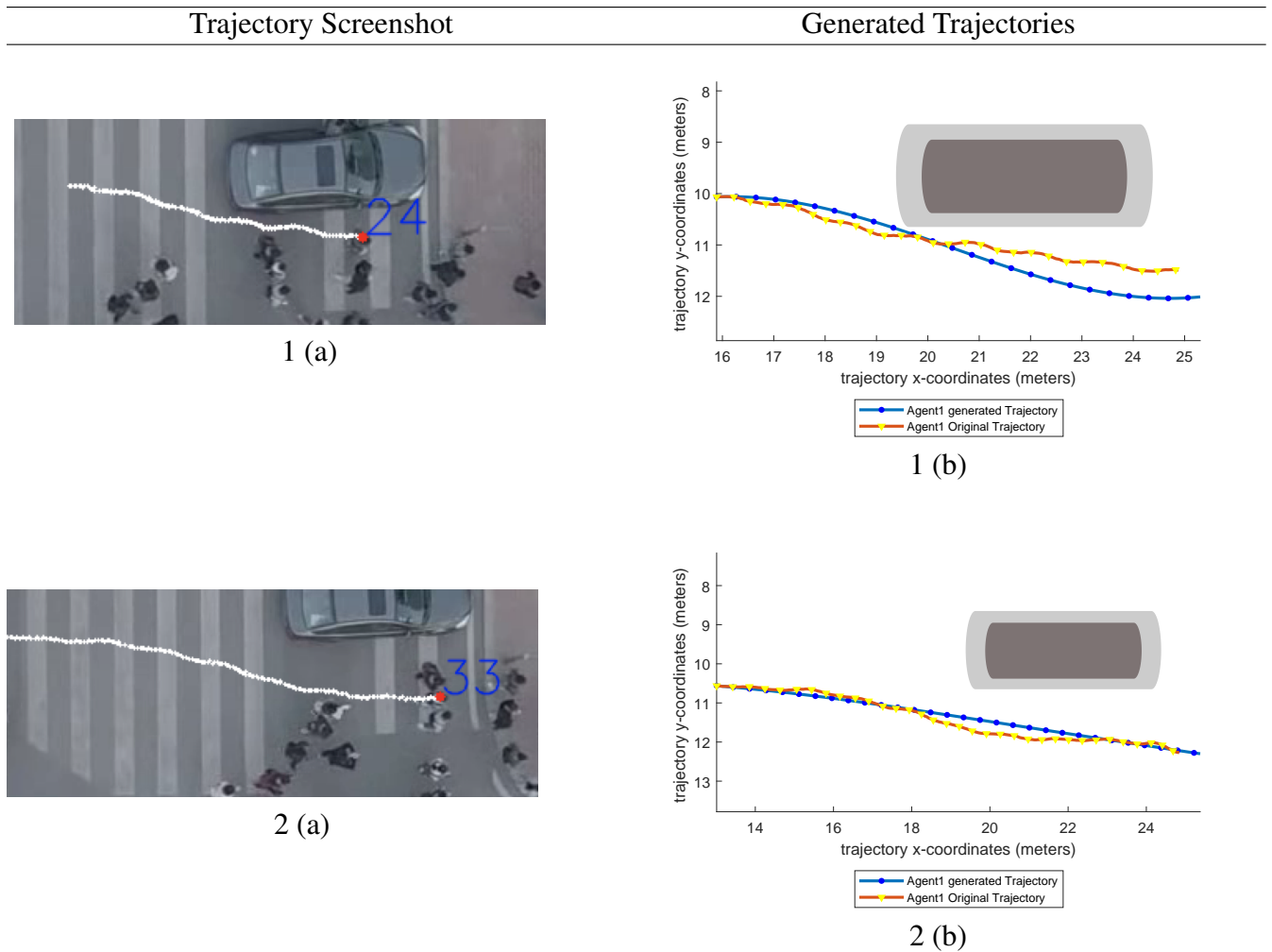
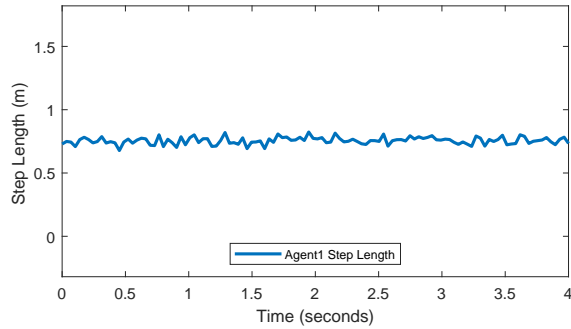


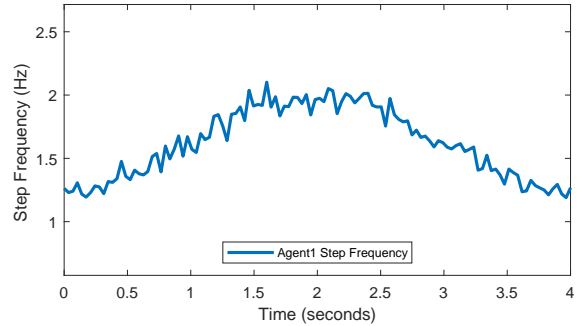
Table 4.15 illustrates the obtained gait parameters in Case study 3. The proposed algorithm plans the trajectories based on RHC, which generates the trajectories for a series of short-horizon

using the current state values for every horizon calculation. Therefore, while avoiding the stationary obstacle, the algorithm considers the buffer zone around the obstacle and generates a trajectory where the agent maintains the walking speed while adjusting the gait parameters. The step length and step frequency results validate that the agent tries to maintain a constant walking speed by adjusting the gait parameters.

Table 4.15: (a) Step Length (b) Step Frequency of an agent avoiding an obstacle



(a)



(b)

4.4.4 Cross-Validation with TrajNet++

TrajNet++ is an interaction-centric trajectory dataset [65]. The data is sampled based on various interaction scenarios. There are leader-follower interactions, group interactions and obstacle avoidance interactions. The TrajNet++ is a current benchmark, and many trajectory forecasting models are using it to validate their efficacy. We have used TrajNet++ to cross-validate our trajectory planning algorithm. The idea is to validate the robustness of the developed algorithm; such the algorithm can be successfully applied to urban traffic scenarios in LA as well as in NYC urban shared space traffic scenarios just by providing the agent’s initial and final destination coordinates.

A group interaction scenario of two agents walking together is Case study 1. The calibrated values are provided in the Table 4.3. We extracted twenty sample trajectories to perform the cross-validation and calculate the performance metrics. Table 4.16 illustrates the result of two agents walking together. The trajectories with markers are the actual trajectories of two pedestrians, and

the non-marker trajectories are model-generated trajectories. The calculated performance metrics are shown below in Table 4.17. The evaluation metrics in the table have values less than one, which demonstrates the good performance of the approach.

Table 4.16: Cross Validation with TrajNet++ (showing Trajectory generation for Case Study 1: Two Agents Walking Together)

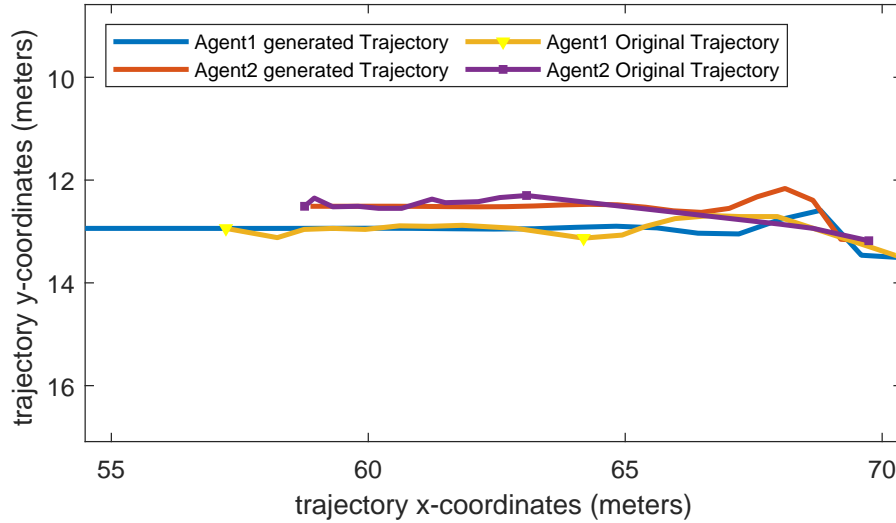


Table 4.17: Case Study 1 Performance metrics average values in TrajNet++ dataset

Performance metrics	Average values
MED	0.32
FDE	0.41
$\text{rmse}_{d_{i,j}^\perp}$	0.40
$\text{rmse}_{d_{i,j}^\parallel}$	0.01

A group interaction scenario of three agents walking together is Case study 2. The calibrated values are provided in Table 4.4. We extracted fifteen sample trajectories to perform the cross-validation and calculate the performance metrics. The calculated performance metrics are shown in Table 4.18. Almost all error metrics values are less than one, except root mean square error in the lateral separation value between two agents, which is close to one. The pedestrian group interaction

is very complex and involves multiple behavioral factors. There are in-group interactions and group-surrounding interactions that affect the trajectories; which justifies the observed results. The algorithm performance for Case study 3, where the pedestrian passes the stationary obstacle (in our case, a standing car represented as a square), is also cross-validated. Refer the Table 4.5 for model calibrated values. We extracted ten sample trajectories to perform the cross-validation and calculate the performance metrics. The performance metrics are shown in Table 4.19. The MED = 0.78 and FDE = 0.45, again reassures the algorithms' performance.

Table 4.18: Case Study 2 Performance metrics average values in TrajNet++ dataset

Performance metrics	Average values
MED	0.39
FDE	0.18
$\text{rmse}_{d_{1,2}}^{\perp}$	1.05
$\text{rmse}_{d_{1,2}}^{\parallel}$	0.01
$\text{rmse}_{d_{2,3}}^{\perp}$	0.9
$\text{rmse}_{d_{2,3}}^{\parallel}$	0.04

Table 4.19: Case Study 3 Performance metrics average values in TrajNet++ dataset

Performance metrics	Average values
MED	0.78
FDE	0.45

4.4.5 Baseline Comparison

In this section, we provide a comparative summary of the performance of our approach with existing machine learning algorithms for trajectory generation. However, it is important to note that a direct comprehensive comparison is not possible given the "black box" nature of the algorithms. Also, the role of the machine learning models is different from the generative approach adopted in our dissertation. Mostly, machine learning models are prediction models. It means that a model

predicts the pedestrians’ spatial coordinates in the near future (let’s say for 4-5 seconds) using some historical observations. The predictive models are also trained on large datasets. The training prepares the model to capture the underlying social norms and generalize the models for the various scenarios. However, this is very challenging as the training data often only contains examples from safe surroundings with very few occurrences of dangerous scenarios. On the other hand, our generative approach is fully defined, parameterized and can be tuned as needed. It does not require prior training and once the model parameters are calibrated, the model is fit to generate trajectories for various scenarios. Table 4.20 compares the MED and FED for state of the art models and for our algorithm in the three case studies using the TrajNet++ dataset. Note that the proposed approach has comparable (or even better) error metrics. However, the comparison table should be interpreted subjectively since, as we stated earlier, the model objectives are not aligned.

Table 4.20: Performance Metrics Comparison chart for Different Pedestrian Trajectory Forecasting Models based on TrajNet++ dataset

Experimental Results for TrajNet++ dataset	Performance Metrics	
	MED	FDE
PecNet [79][80]	0.57	1.18
AIN [81] [80]	0.62	1.24
Social NCE [82] [80]	0.53	1.14
AMENet [83] [80]	0.62	1.30
Proposed Approach - Case Study1	0.32	0.41
Proposed Approach - Case Study2	0.39	0.18
Proposed Approach - Case Study3	0.78	0.45

4.5 Summary

This chapter developed the pedestrian trajectory planning framework considering intra-group interactions and stationary obstacle encounters. The chapter begins by detailing the receding horizon optimization-based trajectory generation framework by describing decision variables, dynamic

constraint equations describing pedestrian motion, obstacle avoidance constraint equations, and private and common objective functions. It also provides the model summary. Furthermore, the chapter detailed three case studies that included model calibration and validation. Cross validation was performed on a different dataset. The simulation run-time for the case study ‘two agents walk together’ is 0.08 sec. The run-time increased to 0.085 sec for the case study with three agents having intra-group interactions.

CHAPTER 5

MODELING INTER-GROUP INTERACTIONS AND MOVING OBSTACLE INTERACTIONS

In the previous chapter, we developed a pedestrian trajectory modeling approach incorporating pedestrian behavior and interaction rules during intra-group interactions and stationary obstacle interactions. The model was generative, could represent a range of interaction scenarios, and required minimal data to calibrate the model parameters. The model was validated for scenarios involving two and three pedestrians walking in a group and their interactions with a stationary obstacle (e.g., a tree). However, a significant shortcoming in it was that it lacked the ability to incorporate the interactions with the pedestrians outside of the group. In other words, it could not maneuver in the presence of moving objects (e.g., other pedestrians, micro-mobility agents). Hence the collision avoidance capabilities of a pedestrian (or group of pedestrians) were lacking during inter-group interactions and moving obstacles interactions. This severely limited the applicability of the model to simulate realistic scenarios. Collision avoidance trajectory generation is crucial for realistic pedestrian modeling. However, including pedestrian behavior and interaction rules involving moving obstacles (such as another pedestrian) is not trivial. The pedestrian has unpredictable, complex walking behavior; the interactions with a moving obstacle are complicated and involve multiple behavioral factors which we discuss next.

5.1 Scenario Selection and Parameter Design

In our previous chapter 4, we analyzed the traffic scenarios of group interactions between two and three pedestrians, and pedestrians avoiding a stationary obstacle. Recall that this dissertation aims to augment the previous model with traffic scenarios involving collision avoidance with other moving pedestrians or a group of pedestrians moving in the pedestrian's *line-of-sight*, or the

field-of-view. Accounting for pedestrian social interactions with other moving obstacles is critical for pedestrians' trajectory planning. The moving objects seen or not seen during trajectory planning depend on pedestrian's visual acuity, central vision field, peripheral vision field, surrounding activities, and many other traffic distractions [84], [85]. This necessitates updating the planned pedestrian's trajectory at regular short intervals.

We will focus on the following pedestrians' moving obstacle (collision avoidance) traffic scenarios that are critical for trajectory generation modeling.

- *Line-of-sight Collision Avoidance (LCA):*

An individual pedestrian (or a group) avoids another moving pedestrian (or a group) coming from the opposite direction. See Figure 5.1a and Figure 5.1b. The line-of-sight (LoS) means that an agent has an unobstructed view along the straight line of an object.

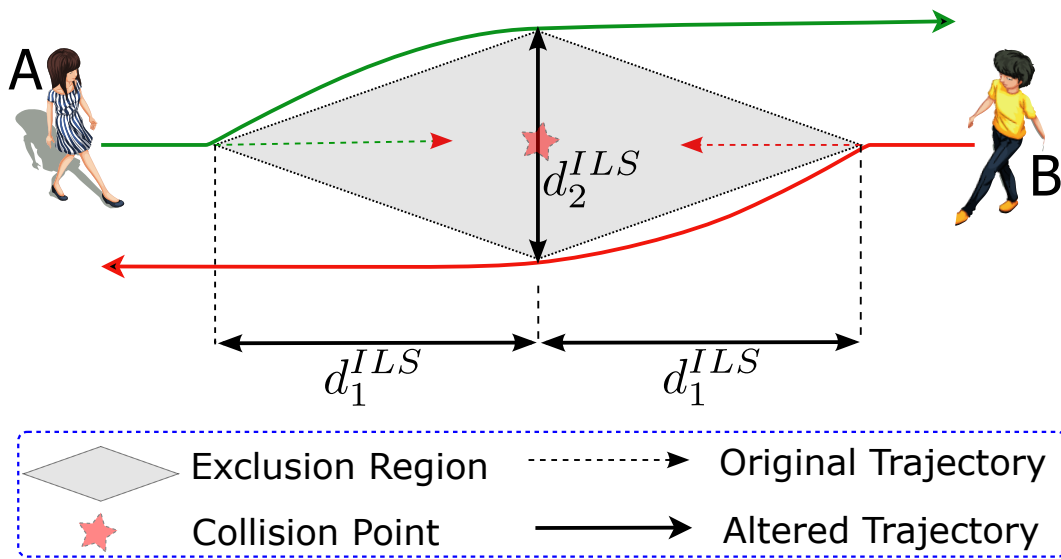
- *Field-of-view Collision Avoidance (FCA):*

A moving pedestrian (or group of pedestrians) lies in the field-of-view (FoV) of the primary pedestrian (or group of pedestrians). See Figure 5.2a and Figure 5.2b.

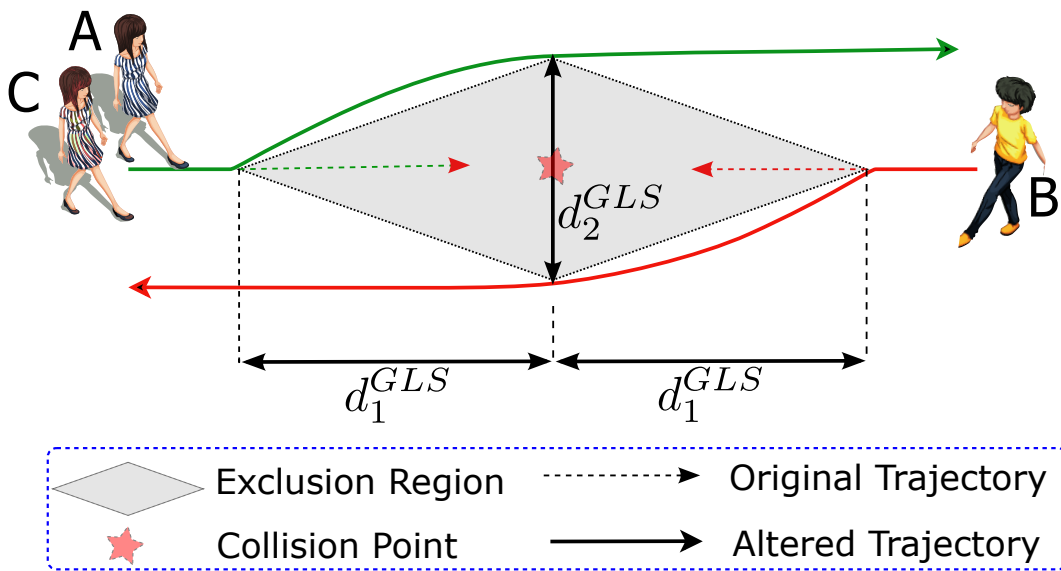
5.1.1 Designed Behavioral Parameters

The pedestrian interactions with a moving obstacle are complicated and involve multiple behavioral factors. Modeling of collision avoidance traffic scenario is crucial for developing pedestrian trajectory generation framework, also its not a trivial task. This necessitates defining new pedestrian's behavioral parameters. We introduce the behavioral parameters by building on the chosen collision avoidance traffic scenarios in the previous section 5.1. These parameters are indicative of characteristic behavior during collision avoidance. The description of the proposed parameters are described below and summarized in Table 5.1.

LCA - Individual and Group Scenarios: In Figure 5.1a (and Figure 5.1b), we observe two pedestrians (or groups) moving straight towards each other; they are in each other's line-of-sight



(a) Line-of-sight collision avoidance between two pedestrians



(b) Line-of-sight collision avoidance between a pedestrian and a group of pedestrians

Figure 5.1: Line-of-sight Traffic Scenarios and Designed Behavioral Parameters

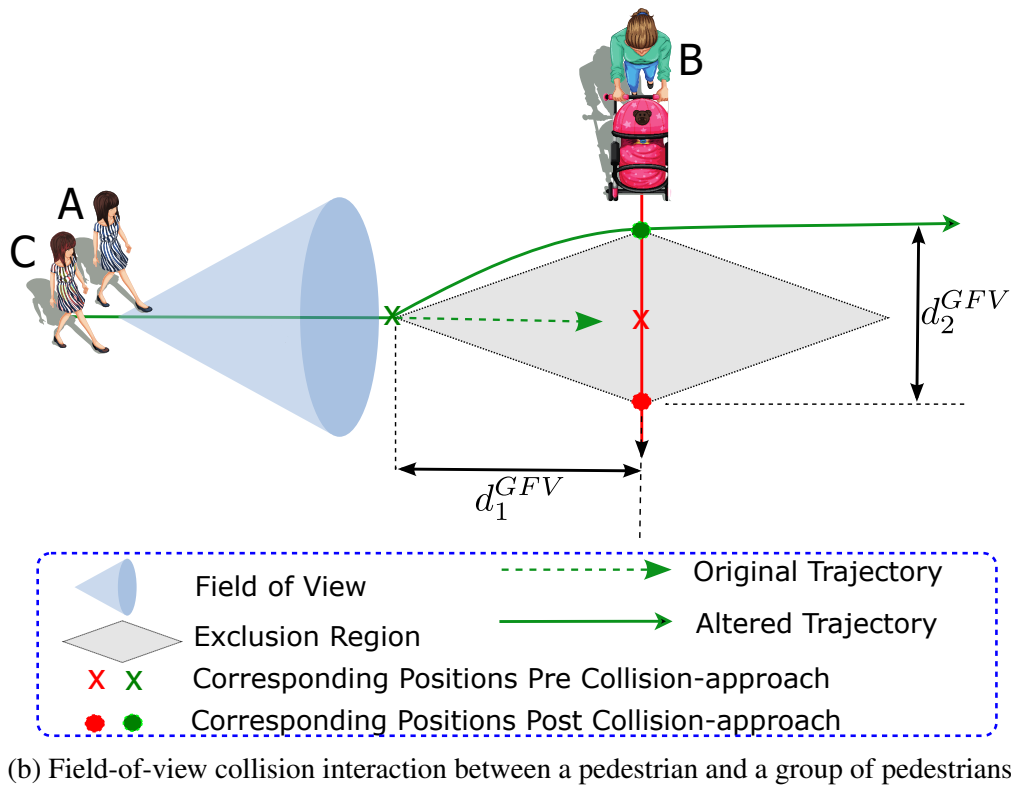
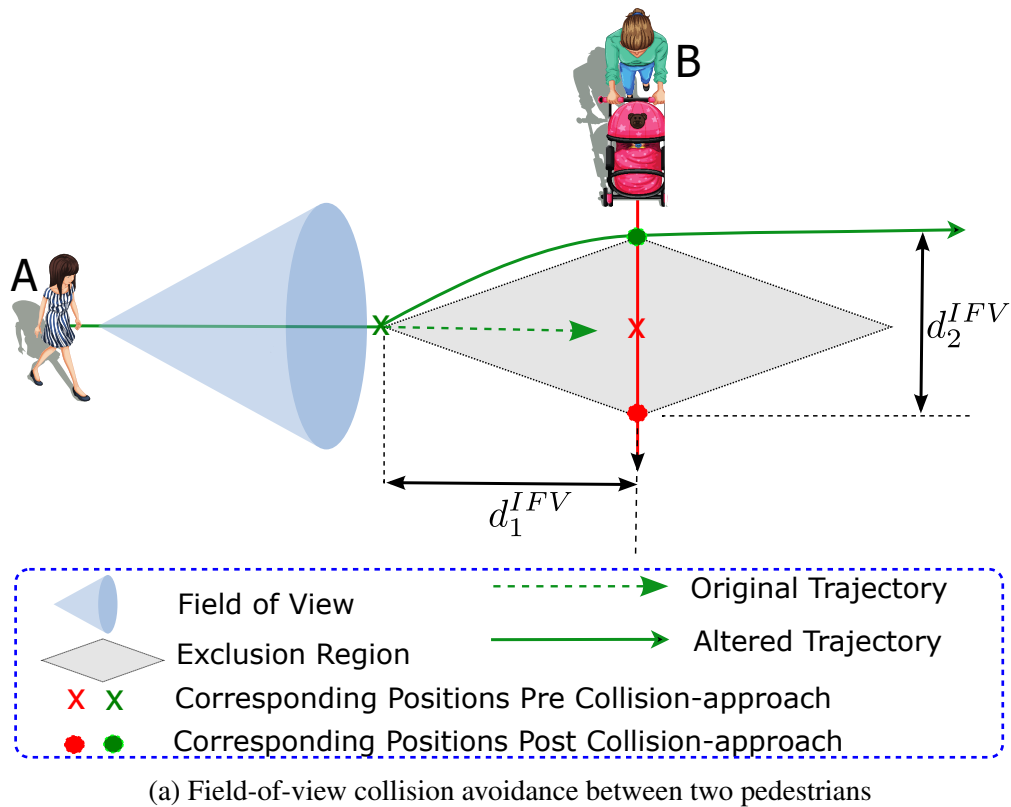


Figure 5.2: Field-of-view Traffic Scenarios and Designed Behavioral Parameters

Table 5.1: Description of Proposed Parameters

Parameter	Description
d_1^{ILS} (& d_1^{GLS})	Euclidean distance between the collision point and the point at which two pedestrians (or groups) start to change their trajectory to avoid the collision and keep a comfortable distance between them.
d_2^{ILS} (& d_2^{GLS})	Euclidean distance between two points at which two pedestrians (or groups) directly moving towards each other come closest and pass each other while maintaining a minimum safe distance required to avoid a collision. In many cases, this Euclidean distance segment will be perpendicular to the direction of their motion. In other words, d_2^{ILS} is the length of the line segment between the two closest points on the individual pedestrian's trajectories. Note that we measure the distance from the trajectory representing their center of mass for the pedestrian group.
d_1^{IFV} (& d_1^{GFV})	Euclidean distance between the pedestrians when the primary pedestrian (or group) (with another pedestrian in its FOV) starts to change its trajectory to avoid the collision and keep a comfortable distance between them.
d_2^{IFV} (& d_2^{GFV})	Euclidean distance between the pedestrians (or groups) when they come closest and pass each other while maintaining a minimum safe distance required to avoid a collision. In other words, d_2^{IFV} is the length of the line segment between the two closest points on the individual pedestrian's trajectories on the post-collision approach. Note that for the group of pedestrians, we measure the distance from the trajectory representing their center of mass.

(LoS). The LoS means that an agent has an unobstructed view along the straight line of an object. In such cases, intuitively, pedestrians' change the direction of motion slightly so that they can avoid a collision. In the figures, d_1^{ILS} (or d_1^{GLS}) represents the distance between the collision point and pedestrian (or group) when the direction of motion starts to change. The d_2^{ILS} (or d_2^{GLS}) distance is the minimum safe distance between two pedestrians (or groups) when they pass each other. In this scenario, both pedestrians (or groups) are responsible for maintaining a safe distance as both can see each other. Note that the exact alteration in their trajectories might differ (one might change their trajectory more than the other). However, for the modeling purpose, we only require d_2^{ILS} and d_2^{GLS} . Note that both d_1^{IFV} and d_2^{IFV} would be greater (or equal to) than the minimum comfortable distance between two pedestrians. Their actual values will depend from case to case ; however, an average of the values observed in a dataset would suffice in the algorithm.

FCA - Individual and Group Scenarios: In Figure 5.2a (and Figure 5.2b), we consider the case(s) where a pedestrian (or group) lies in another pedestrian's (or group's) field-of-view (FoV). In such scenarios, only the pedestrian (or group) who can see the other pedestrian (or group) present in its FoV re-plans its trajectory to avoid the collision. In Figure 5.2a, a pedestrian B (with a stroller) is moving in the FoV of another pedestrian A . If pedestrian A does not change the trajectory (motion direction or speed), then there are high chances of them getting too close to be comfortable or even colliding. The *red* and *green cross* indicate their corresponding positions in the pre-collision (unaltered) approach. Pedestrian A starts altering its trajectory at a distance d_1^{IFV} (the distance between red and green crosses). The altered trajectory of pedestrian A crosses the trajectory of pedestrian B at the *green dot*; in the meantime, pedestrian B has moved to the red dot on its unaltered trajectory. The *red* and *green dots* indicate their corresponding positions in the post-collision (altered) approach. d_2^{IFV} is the distance between the two pedestrians when their trajectories intersect. Note that both d_1^{IFV} and d_2^{IFV} would be greater than the minimum comfortable distance between two pedestrians. Their actual value will depend from case to case; however, an average of the values observed in a dataset would suffice for the algorithm.

5.2 Trajectory Optimization

In this section, firstly, we briefly describe the trajectory planning problem and then specify our research approach to the pedestrian trajectory planning problem. *Trajectory planning problem* are often solved using optimization to generate a collision-free path over time from an initial to a final point in a specified environment. These optimization algorithms generate trajectories when considering a variety of optimality criteria such as minimum time, minimum energy, minimum jerk, or a weighted combination of them. The key ingredients of these algorithms include the designed optimality criteria (objective function), description of state and decision variables, kinematics dynamics of the considered agent, and constraints of the obstacles in the environment. Output is a trajectory expressed as a sequence of values of position, velocity, and acceleration at regular time intervals [86], [87]. Optimization based trajectory planning have been used extensively for robots, UAVs, and aircraft.

We propose a control-based pedestrian trajectory generation framework with multi-criteria optimization that considers minimum energy and pedestrian social interaction rules. Section section 5.1 discussed the pedestrians' interaction complexities and behavioral parameters, which play an integral role in the development of the framework [88], [89]. The HISS (Human Interaction in Shared space) framework is formulated as a MILP embedded within RHC. The modeling framework presented in this chapter considers collision avoidance, along with the unique scenarios emanating from multiple pedestrians sharing the same space. Note that the framework for inter-group interactions is similar to the framework for with-in group interactions (described in the previous chapter). The differences occur in the objective function and constraint equations. Accordingly, the design of RHC embedding, changes in the objective function and constraints are discussed in the following sections. We borrow the same notation set as described in the previous chapter. However, for the sake of completeness and ease of the readers, we provide a complete formulation here.

Table 5.2 provides a summary of the applicable parameters characterizing the receding horizon

control framework for modeling pedestrian movement. Please refer the previous chapter 4 for more details.

Table 5.2: Description of used Parameters.

Symbol	Meaning
\mathcal{P}	Set of pedestrians
\mathcal{O}	Set of obstacles
\mathcal{F}_o	Set of facets associated with obstacle o .
\mathcal{S}_{jk}	Set of facets associated with pedestrian j at time-step k .
$\mathcal{G} = (\mathcal{V}, \mathcal{E})$	Graph structure defining pedestrian groups.
H_p	Planning horizon [seconds]
H_c	Control horizon [seconds]
$x_{i,t} \in \mathbb{R}^2$	X-Y position of the i^{th} pedestrian at time-step t .
$w_i \in \mathbb{R}^2$	Next way-point of the i^{th} pedestrian.
$\theta_i = \angle(w_i - x_{i,t})$	Direction of travel of i^{th} pedestrian at time-step t .
$d_{i,j}^{des} = (d_{i,j}^{\parallel des}, d_{i,j}^{\perp des}) \in \mathbb{R}^2$	The desired longitudinal and lateral separation between pedestrians i and j along their common direction of travel.

Consider the lower part of Figure 3.3 that illustrates a cluster of pedestrians in the set \mathcal{P} . For simplified understanding, we consider two sub-graphs structures $\mathcal{G}_1, \mathcal{G}_2$ in a traffic scene. The sub-graphs are either in line-of-sight or in field-of-view of each other. Within each sub-graphs, pedestrians will maintain their respective private and common objectives. Personal objectives include walking speeds, safe distance to obstacles, collision avoidance, and time-to-arrival or distance-from-destination. Common objectives are to maintain the moving graph structure discussed previously, which is achieved by preserving the preferred spread between pedestrians in the group. The MILP optimization aims to capture the personal and common objectives along with the dynamic and static constraints associated with pedestrians traveling in the surroundings. The formulation, consisting of the objective functions, associated coefficients, and constraints, when solved, generates an optimal trajectory assessing the goals and objectives of each pedestrian (and groups). Next, we describe the formulation, decision variables, constraints, and objective functions.

5.2.1 Decision variables

For a given instantiation of the trajectory planning and execution cycle, each pedestrian i in the pedestrian set \mathcal{P} is foremost characterized according to their current x-y position $x_{i,t_0} \in \mathbb{R}^2$ at time-step t_0 and their preferred next way-point, $w_i \in \mathbb{R}^2$. When optimizing the trajectories for H_p seconds over the planning horizon, it is essential to introduce new decision variables representing each pedestrian's planned position and velocity. To differentiate between the actual position of the pedestrians, $x_{i,t}$, and the planned position of the pedestrians is denoted, $z_{i,k} \forall k \in \{1, \dots, H_p\}$, representing the position of pedestrian i over H_p seconds when using 1-second increments. We also introduce the decision variables related to the position, velocity, and acceleration of each pedestrian relative to their direction of travel. For clarity, all decision variables described according to the coordinate frame in the direction of travel are indicated by the harpoon accent (e.g., $\overrightarrow{z}_{i,k}$). Therefore, the decision variables for the position, velocity, and acceleration of pedestrian i in the rotated coordinate frame along the direction of travel are presented by $\overrightarrow{z}_{i,k} = (\overrightarrow{z}_{i,k}^{\parallel}, \overrightarrow{z}_{i,k}^{\perp})$, $\overrightarrow{v}_{i,k} = (\overrightarrow{v}_{i,k}^{\parallel}, \overrightarrow{v}_{i,k}^{\perp})$ and $\overrightarrow{u}_{i,k} = (\overrightarrow{u}_{i,k}^{\parallel}, \overrightarrow{u}_{i,k}^{\perp})$, all defined over $\mathbb{R}^2 \forall k \in \{0, \dots, H_p - 1\}$; each term inside the vectors corresponds to the longitudinal and lateral values along the nominal direction of travel.

The distinction between the position of pedestrians in a global coordinate frame versus a local coordination frame assists in specifying constraints and objective costs related to the position of pedestrians relative to obstacles, other moving pedestrians, and the pedestrians in their group. When forming optimization constraints associated with obstacle/collision avoidance, it is most straightforward to describe these obstacle constraints using a common global coordinate frame. Meanwhile, because the desired separation between pedestrians walking in a group is described in a relative frame, using a coordinate system aligned with this relative coordinate frame is preferred. Again, velocity and acceleration constraints for every pedestrian are efficiently described in the local coordinate frame. At any time-step, translation of the pedestrian position between the global

Table 5.3: Description of decision variables.

Symbol	Meaning
$z_{i,k} \in \mathbb{R}^2$	Planned position of pedestrian i at time-step k in global frame
$z_{i,k}^x \in \mathbb{R}$	x-coordinate of planned position of pedestrian i at time-step k in global frame
$z_{i,k}^y \in \mathbb{R}$	y-coordinate of planned position of pedestrian i at time-step k in global frame
$\vec{x}_{i,k} = (\vec{x}_{i,k}^{\parallel}, \vec{x}_{i,k}^{\perp}) \in \mathbb{R}^2$	Planned position of pedestrian i at time-step k in local frame
$\vec{v}_{i,k} = (\vec{v}_{i,k}^{\parallel}, \vec{v}_{i,k}^{\perp}) \in \mathbb{R}^2$	Planned velocity of pedestrian i at time-step k in local frame
$\vec{u}_{i,k} = (\vec{u}_{i,k}^{\parallel}, \vec{u}_{i,k}^{\perp}) \in \mathbb{R}^2$	Planned acceleration of pedestrian i at time-step k in local frame
$b_{o,f,i,k} \in \{0, 1\}$	Binary variable indicating that pedestrian i is outside of the boundary of obstacle o , in reference to facet f of the obstacle, at time-step k
$a_{j,s,i,k} \in \{0, 1\}$	Binary variable indicating that pedestrian i is outside of the boundary of the other pedestrian j , in reference to facet s of the pedestrian, at time-step k

and a rotated local coordinate frame is provided by the following linear transformation

$$z_{i,k} = R(-\theta_i) \vec{z}_{i,k} \quad \forall k \in \{0, \dots, H_p - 1\} \quad (5.1)$$

where $R(\theta_i)$ is a rotation matrix

$$R(\theta_i) = \begin{bmatrix} \cos \theta_i & -\sin \theta_i \\ \sin \theta_i & \cos \theta_i \end{bmatrix}$$

parameterized by the direction of travel θ_i .

Table 5.3 provides a list of decision-variables and their descriptions.

5.2.2 Dynamic Constraint

One part of the constraint equations represents the dynamic constraints of pedestrian motion. For the i^{th} pedestrian, the second-order discrete-time update equation for their position relative to their direction of travel is given by the following set of constraints

$$\begin{aligned}\vec{z}_{i,k+1} &= \vec{z}_{i,k} + \vec{v}_{i,k}\Delta T + 1/2\vec{u}_{i,k}\Delta T^2 \\ \vec{v}_{i,k+1} &= \vec{v}_{i,k} + \vec{u}_{i,k}\Delta T \\ \text{and } k &\in \{0, \dots, H_p - 1\}\end{aligned}\tag{5.2}$$

(Equation 5.2) adopts a continuously revising process that occurs at a regular time-step of ΔT seconds, during which the acceleration is assumed to be constant.

The pedestrian motion is also constrained by their minimum and maximum walking velocity ($\underline{v}_i, \bar{v}_i$) and their minimum and maximum acceleration ($\underline{u}_i, \bar{u}_i$). Assuming that the lateral velocity of pedestrians is small compared to their longitudinal velocity (small angle approximation), we can write

$$\underline{v}_i \leq \vec{v}_{i,k}^{\parallel} \leq \bar{v}_i \quad \forall i \in \mathcal{P}.\tag{5.3}$$

If the small angle approximation is probable to be violated, it is possible to substitute the velocity constraint in (Equation 5.3) with

$$\|\vec{v}_{i,k}\|_2^2 \leq \bar{v}_i^2 \quad \forall i \in \mathcal{P}.\tag{5.4}$$

Similarly, the acceleration constraints can be given by

$$\|\vec{u}_{i,k}\|_2^2 \leq \bar{u}_i^2 \quad \forall i \in \mathcal{P}.\tag{5.5}$$

5.2.3 Stationary Obstacle Constraint

The obstacle avoidance constraints are inherently non-convex. This can be overcome by using the MILP approach, where each obstacle avoidance generates binary variables and a set of constraints that correspond to moving *left* or *right* around any obstacle relative to any given side or facet of the obstacle. Consider a convex obstacle o that a polygon can approximate with a set of facets, $\mathcal{F}_o = \{1, \dots, F_o\}$; it is possible to define a set of linear constraints

$$h_{o,f}^T y \leq g_{o,f} \quad \forall f \in \mathcal{F}_o \quad (5.6)$$

that represent half-spaces that can be used to define the set of points $y \in \mathbb{R}^2$ that is blocked by the obstacle.

For obstacle avoidance, the planned position of a pedestrian, $z_{i,k}$, must be outside the convex polygon at each time. The i^{th} pedestrian is outside of the obstacle o (with respect to a single facet $f \in \mathcal{F}_o$), if their position at time-step k satisfies the constraint

$$g_{o,f} - h_{o,f}^T x_{i,k} \leq 0 \quad (5.7)$$

Therefore, to dodge obstacle o , (Equation 5.7) must hold for at least one of the facets f . The

manifestation of such a constraint is composed as

$$\left\{ \begin{array}{l} g_{o,1} - h_{o,1}^T x_{i,k}, \leq 0 \\ or \\ \vdots \\ or \\ g_{o,f} - h_{o,f}^T x_{i,k}, \leq 0 \\ or \\ \vdots \\ or \\ g_{o,F} - h_{o,F}^T x_{i,k}, \leq 0. \end{array} \right. \quad (5.8)$$

Implementation of the constraint in (Equation 5.8) can be achieved using Big-M notation within a MILP solver by introducing binary variables $b_{o,f,i,k} \in \{0, 1\} \forall f \in \mathcal{F}$ and $k \in \{1, \dots, H_p\}$. Here the binary logical condition $b_{o,f,i,k} = 1$ indicates that pedestrian i is evading obstacle o at time-step k relative to facet f . This is implemented for all pedestrians and all obstacles using the following constraint equations:

$$\begin{aligned} g_{o,f} - h_{o,f}^T x_{i,k} &\leq M(1 - b_{o,f,i,k}) \quad \forall f \in \mathcal{F}_o, o \in \mathcal{O} \\ & \quad i \in \mathcal{P}, k \in \{1, \dots, H_p\} \\ \sum_{f \in \mathcal{F}_o} b_{o,f,i,k} &\geq 1 \quad \forall o \in \mathcal{O}, i \in \mathcal{P} \\ & \quad k \in \{1, \dots, H_p\} \end{aligned} \quad (5.9)$$

where M is sufficiently large such that the f^{th} constraint holds when $b_{o,f} = 0$ regardless of the pedestrian's position.

A buffer distance can be added around each obstacle that can work as a buffer of comfort distance. Any extra buffer distance, $e_{o,i}$, depends on the specific obstacle o and pedestrian i ; in this case, each obstacle constraint can be adjusted to

$$g_{o,f} - h_{o,f}^T x_{i,k} \leq - \|h_{o,f}\| e_{o,i}. \quad (5.10)$$

5.2.4 Collision Avoidance Constraint

The potential presence of moving obstacles (e.g., other pedestrians) within the surroundings requires pedestrians to plan their trajectories accordingly. One approach for collision avoidance is similar to stationary obstacle avoidance, using inherently non-convex constraints. The non-convexity challenge can be mitigated by using binary variables and a set of constraints that correspond to moving *left* or *right* around the other pedestrian relative to any given side. In order to avoid collision with other moving pedestrians, the pedestrian tries to maintain certain safety/comfort distances with them in each direction at every time-step. The section 5.1 illustrated how safety/comfort distances would depend from case to case in the chosen case scenarios. However, for the sake of simplicity, we assume that at time-step k , j^{th} pedestrian can be represented by a polygon with a set of facets, $\mathcal{S}_{jk} = \{1, \dots, S_j\}$. For collision avoidance, the planned position of another pedestrian i at any point in time, $z_{i,k}$, must be outside the approximated convex polygon. The i^{th} pedestrian avoids collision with j if their position at time-step k satisfies the constraint

$$g_{j,s} - h_{j,s}^T x_{i,k} \leq 0 \quad (5.11)$$

Note that the collision avoidance is about a single facet $s \in \mathcal{S}_{jk}$ of the polygon representing pedestrian j at time-step k . Accordingly, to avoid the collision, (Equation 5.11) must hold for at

least one of the facets s at every time-step k . The manifestation of such a constraint is given as

$$\left\{ \begin{array}{l} g_{j,1} - h_{j,1}^T x_{i,k}, \leq 0 \\ or \\ \vdots \\ or \\ g_{j,s} - h_{j,s}^T x_{i,k}, \leq 0 \\ or \\ \vdots \\ or \\ g_{j,S} - h_{j,S}^T x_{i,k}, \leq 0. \end{array} \right. \quad (5.12)$$

Implementation of the constraint in (Equation 5.12) can be achieved using Big-M notation within a MILP solver after introducing binary variables $a_{j,s,i,k} \in \{0, 1\} \forall s \in \mathcal{S}$ and $k \in \{1, \dots, H_p\}$. Here the binary logical condition $a_{j,s,i,k} = 1$ indicates that pedestrian i avoids a collision with pedestrian j at time-step k relative to facet s . This can be implemented for all pedestrians using the following constraint equations:

$$\begin{aligned} g_{j,s} - h_{j,s}^T x_{i,k} &\leq L(1 - a_{j,s,i,k}) \quad \forall s \in \mathcal{S}_{jk}, j \in \mathcal{P} \\ & \quad i \in \mathcal{P}, k \in \{1, \dots, H_p\} \\ \sum_{s \in \mathcal{S}_{jk}} a_{j,s,i,k} &\geq 1 \quad \forall j \in \mathcal{P}, i \in \mathcal{P} \\ & \quad k \in \{1, \dots, H_p\} \end{aligned} \quad (5.13)$$

where L is large enough such that the s^{th} constraint holds when $a_{j,s} = 0$ regardless of the pedestrian's position. For practical purposes, the value of L can be set based on the dimensions of the

environment.

5.2.5 Private and Common Objective Functions

Pedestrians seek personal objectives (e.g., minimization of their effort, minimizing travel time) as well as global goals shared with other pedestrians (e.g., maintaining the desired formation) [66, 71, 72, 73]. Therefore, we have formulated a generalizable objective function taking into account all these aspects.

Personal Objectives

The personal or private objective function can account for regulating walking speeds, running costs, and the terminal cost of reaching the desired way-point.

$$\begin{aligned}
 \sum_{k=1}^{H_p} \sum_{i \in \mathcal{P}} & (k_i^{acc} \|u_{i,k} - u_i^{des}\| + k_i^{speed} \|v_{i,k} - v_i^{des}\| \\
 & + k_i^{run} \|x_{i,k} - w_i\|) \\
 & + \sum_{i \in \mathcal{P}} k_i^{term} \|x_{i,H_p} - w_i\|
 \end{aligned} \tag{5.14}$$

In the personal objective costs described above, each norm can be adapted according to chosen modeling (i.e., ℓ_1 , ℓ_2 , or ℓ_∞). Further, the weights can be adjusted to reflect their relative importance.

Common Objectives

Desired Formation: When walking as part of a group, pedestrians can optimize their planned trajectories while maintaining the desired formation. It is achieved by penalizing any divergences between the actual and desired separation. The following objective function can achieve it:

$$\sum_{k=1}^{H_p} \sum_{(i,j) \in \mathcal{E}} k_{i,j}^{sep} \|\vec{z}_{i,k} - \vec{z}_{j,k} - d_{i,j}^{des}\| \tag{5.15}$$

Note that the summation over the edge-set \mathcal{E} in the graph structure \mathcal{G} provides for considerable flexibility. For instance, ensuring consistency in the desired separation between pedestrians is unnecessary. So for any three pedestrians h , i , and j in the same pedestrian group there is no necessity that $d_{i,j}^{des} + d_{j,h}^{des} = d_{i,h}^{des}$. Pedestrians in the same group don't need to seek to maintain the desired separation.

Special Cases: In typical cases (e.g., a parent and child are walking together), it may be more suitable to represent separation distances within constraints instead of within objective costs. When two pedestrians must remain within a specified range $r_{i,j}$ of each other, the comparable convex constraint is expressed as

$$\|\vec{z}_{i,k} - \vec{z}_{j,k}\| \leq r_{i,j} \quad \forall k \in \{1, \dots, H_p\} \quad (5.16)$$

5.2.6 Model Summary

A summary of the entire formulation is mentioned next. Table 5.4 provides a short-hand notation to indicate the ranges for which each of the constraints holds. For instance, all equations that hold true over $i \in \mathcal{P}, k \in \{1, \dots, H_p - 1\}$ are indicted by the \bullet symbol. Note that all decision variables mentioned in summary are considered to be unrestricted, barring any binary variables. Also, to preserve generality, we abstain from specifying which norm is used in the objective function and constraints. While the ℓ_2 norm is suitable in many cases, representations using the ℓ_1 or ℓ_∞ are also acceptable.

$$\begin{aligned}
\min & \sum_{k=1}^{H_p} \sum_{i \in \mathcal{P}} (k_i^{acc} \|u_{i,k} - u_i^{des}\| \\
& + k_i^{speed} \|v_{i,k} - v_i^{des}\| \\
& + k_i^{pos} \|x_{i,k} - w_i\|) \\
& + \sum_{i \in \mathcal{P}} k_i^{term} \|x_{i,H_p} - w_i\| \\
& + \sum_{k=1}^{H_p} \sum_{(i,j) \in \mathcal{E}} k_{i,j}^{sep} \|\vec{z}_{i,k} - \vec{z}_{j,k} - d_{i,j}^{des}\|
\end{aligned}$$

$$\mathbf{s.t.} \quad \vec{z}_{i,k+1} = \vec{z}_{i,k} + \vec{v}_{i,k} \Delta T + 1/2 \vec{u}_{i,k} \Delta T^2 \quad \bullet$$

$$\vec{v}_{i,k+1} = \vec{v}_{i,k} + \vec{u}_{i,k} \Delta T \quad \bullet$$

$$\|\vec{v}_{i,k}\| \leq \bar{v}_i \quad \otimes$$

$$\|\vec{u}_{i,k}\| \leq \bar{u}_i \quad \otimes$$

$$z_{i,k} = R(-\theta_i) \vec{z}_{i,k} \quad \blacklozenge$$

$$g_{o,f} - h_{o,f}^T x_{i,k} \leq M(1 - b_{o,f,i,k}) \quad \blacktriangle$$

$$\sum_{f \in \mathcal{F}_o} b_{o,f,i,k} \geq 1 \quad \dagger$$

$$b_{o,f,i,k} \in \{0, 1\} \quad \blacktriangle$$

$$g_{j,s} - h_{j,s}^T x_{i,k} \leq L(1 - a_{j,s,i,k}) \quad \clubsuit$$

$$\sum_{s \in \mathcal{S}_{j,k}} a_{j,s,i,k} \geq 1 \quad \spadesuit$$

$$a_{j,s,i,k} \in \{0, 1\} \quad \clubsuit$$

Table 5.4: Short-hand markers indicating the ranges over which constraints apply.

Sets	Short-hand notation
$i \in \mathcal{P}, k \in \{1, \dots, H_p\}$	⊗
$i \in \mathcal{P}, k \in \{0, \dots, H_p - 1\}$	•
$i \in \mathcal{P}, k \in \{0, \dots, H_p\}$	♦
$i \in \mathcal{P}, k \in \{1, \dots, H_p\}, o \in \mathcal{O}, f \in \mathcal{F}_o$	▲
$i \in \mathcal{P}, k \in \{1, \dots, H_p\}, o \in \mathcal{O}$	†
$i, j \in \mathcal{P}, k \in \{1, \dots, H_p\}, s \in \mathcal{S}_{jk}$	♣
$i, j \in \mathcal{P}, k \in \{1, \dots, H_p\}$	♠

5.3 Implementation details

MATLAB along with the CVX optimization library was used to implement the receding-horizon framework with the embedded MILP [90].

The proposed generative framework is implemented to show the model performance for non-linear collision avoidance (human-human) traffic scenarios. The model can implement various interacting traffic scenarios. To validate the model performance for social interaction traffic scenarios, we identified the case studies where the agents move towards each other - directly or indirectly (more details in section 5.1). The identified case studies are capable of manifesting the most common moving human-human collision avoidance case scenarios. We have previously defined the safety distances (d_1^{ILS} , d_2^{ILS} , d_1^{IFV} , d_2^{IFV} , etc.) that pedestrian tries to maintain with other moving pedestrian. For simplicity in implementation, we approximate the scenario parameters described in Table Table 5.1 with an exclusion zone as a square with each side of d_c units.

5.4 Data description

The datasets used in this chapter to calibrate the proposed model and validate the efficiency of the model are (a) the DUT dataset [74] and (b) the TrajNet++ dataset [65].

The DUT dataset is one of the crowd interaction benchmark datasets [74] collected at the campus of Dalian University of Technology (DUT) in China. The videos was recorded using the *DJI Mavic Pro* Drone with a down-facing camera. The video resolution was 1920×1080 with an *fps*

of 23.98. Pedestrians in the data are mainly college students. The pedestrian trajectories were extracted from the recorded video data using video stabilization, pedestrian tracking, coordinate transformation, and Kalman filtering techniques. The TrajNet++ is a interaction centric human trajectory forecasting benchmark. It comprises largely of human social interactions traffic scenarios [65].

5.5 Model Parameters and Calibration

Model Parameters: The key parameters used in the model are:

1. Total time-steps for a simulation (T)
2. Desired longitudinal distance between pedestrians i and j ($d_{i,j}^{\parallel des}$)
3. Desired lateral distance between pedestrians i and j ($d_{i,j}^{\perp des}$)
4. Control Horizon (H_c)
5. Planning Horizon (H_p)
6. Maximum and Minimum mean velocity
7. Maximum and Minimum mean acceleration

Calibration: The model key parameters are calibrated by identifying the interacting collision avoidance traffic scenarios in the datasets. The key model parameters (numbered 2 to 7 in section 5.5) are taken from our research work [91]. The d_c is calibrated based on traffic scenarios observations. The pedestrian maintain a behavioral safe distance in order to avoid collision. The sampling time T depends on the considered traffic scenario. We extracted fifty samples from the dataset, thirty-five samples are used for training the model and fifteen samples used for testing the developed model. The $d_{i,j}^{\perp des}$ and $d_{i,j}^{\parallel des}$ values are dynamically calibrated using the normal distribution method. The calibrated parameters are shown in Table 5.5.

Table 5.5: Calibrated Model Parameters

Parameters	Calibrated Values
$d_{i,j}^{\perp des}$	$\mu = 0.52, \sigma = 0.15$
$d_{i,j}^{\parallel des}$	$\mu = 0.097, \sigma = 0.046$
Average minimum velocity	0.97 m/sec
Average maximum velocity	1.70 m/sec
Average minimum acceleration	-0.3 m/sec ²
Average maximum acceleration	0.3 m/sec ²

5.6 Performance Metrics

We use the following performance metrics.

- MED : Mean Euclidean Distance is the average Euclidean distance between the model predicted coordinates and the actual coordinates of the pedestrian at every instant. Lower is better.
- FDE : Final Displacement Error is the Euclidean distance between the model predicted final destination and the actual final destination at the corresponding time instant.

5.7 Experimental Results

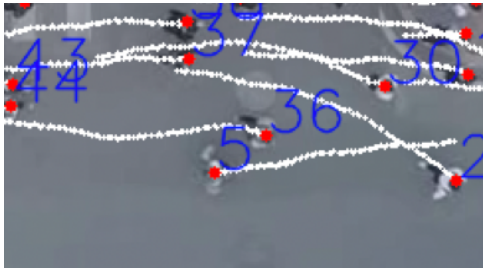
To validate the model, we identify the case studies, as listed in section 5.1, from the datasets. The calibrated model is provided with required input states and then the model generates pedestrian trajectories for the traffic scenario. The chosen case studies are where pedestrian are moving towards each other directly (considered as line-of-sight collision avoidance) or indirectly (considered as field-of-view collision avoidance).

Simulation Results and Discussion: The experimental results demonstrates the capability and efficiency of the proposed human trajectory planning framework. Figure 5.3, Figure 5.4 and Figure 5.5 demonstrates the trajectory generation results. We have taken fifty samples of each chosen

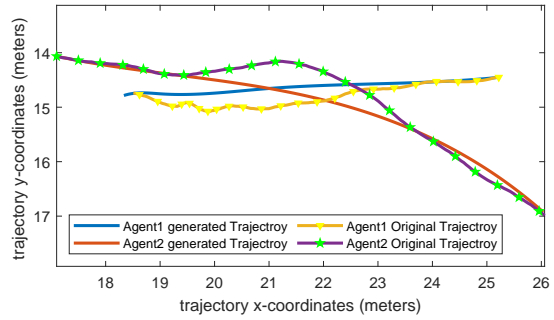
case study. The samples are divided into the ratio of seventy and thirty for calibration and validation, respectively. The calibrated values for all case studies are in Table 5.5. The calibrated values are used depending on the case study, if it has the group of people walking together, and avoiding the collision with an individual or another group, $d_{i,j}^{\perp des}$ and $d_{i,j}^{\parallel des}$ values are also used in the model implementation. The average velocity and acceleration values in the calibration table work equally well for all the case studies.

Figure 5.3a shows the screenshot from DUT dataset in which pedestrians number 5 and 36 are in each other's line-of-sight; the two pedestrian adjusted their trajectories to avoid the collision. Figure 5.3b shows the model generated trajectory for the same set of pedestrians. The solid color lines are the real trajectories of pedestrians' 5 and 36, and the dashed lines are model generated trajectories. Due to the utilization of behavioral and social interaction rules the model is successfully generating trajectories which are similar to real trajectories for the given scenarios. Similar explanation for the other shown case studies results. Figure 5.6 and Figure 5.7 are showing the values of the MED and FDE for the respective case studies samples performed for model validation. Table 5.6 shows the chosen case studies performance metrics - mean euclidean distance (MED) and final displacement error (FDE) values. The performance metrics have low values which supports the model efficiency in generating realistic trajectories for a given scenarios. The FDE values are close to one, the reason is firstly, the performance metrics values are the average values of thirty test samples, and also we are using the average values of velocity which can differ from sample to sample, and therefore for some sample it might be some difference in reaching the final position. It is observed that MED values are near zero for the case studies, which implies that generated trajectories are close to realistic trajectories. The simulation run-time for inter-group interactions and moving obstacle avoidance is approximately 0.1 seconds.

Baseline Comparison: The comparison with existing trajectory generation frameworks is presented in this section. The proposed framework lies between the two sets of modeling paradigms — the black-box algorithms (such as machine learning), which are hard to interpret and parame-

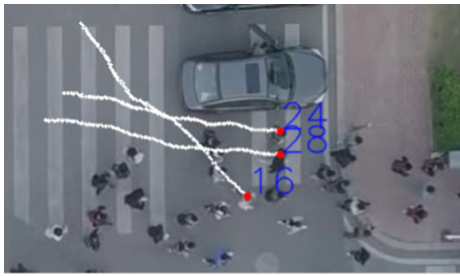


(a) Screenshot of Agent 5 and Agent 36 avoiding line-of-sight collision

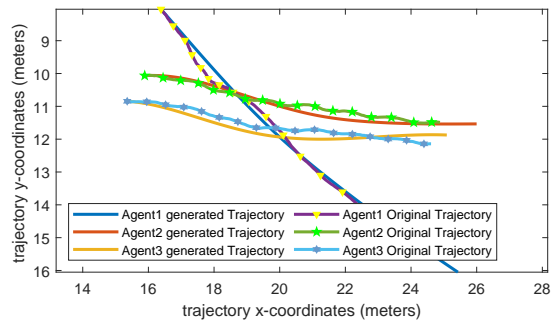


(b) Agent 5 and Agent 36's Actual trajectory and Model generated trajectories

Figure 5.3: Line-of-sight Collision Avoidance - Individual



(a) Screenshot of Agent 16 avoiding collision with the group of two pedestrians 24 and 28

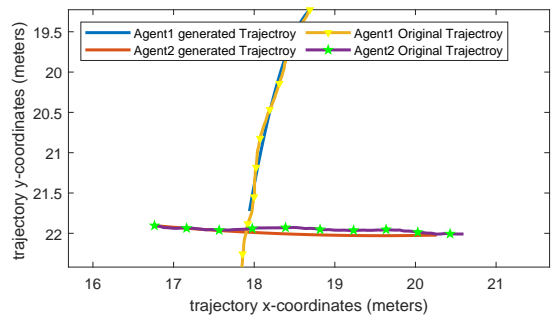


(b) Agent 16, Agent 24 and Agent 28 - Actual trajectory and Model generated trajectories

Figure 5.4: Field-of-view Collision Avoidance - Group



(a) Screenshot from DUT dataset showing Agent 9 and Agent 10 avoiding collision



(b) Actual and Model generated trajectories of Agent 9 and Agent 10

Figure 5.5: Field-of-View Collision Avoidance - Individual

Table 5.6: Performance Metrics Table for Simulated Traffic scenarios on DUT dataset and TrajNet++ dataset

Experimental Results for DUT dataset	Performance Metrics	
	MED	FDE
Line-of-sight Collision Avoidance - Individual	0.54	1.13
Field-of-view Collision Avoidance - Group	0.63	1.21
Field-of-View Collision Avoidance- Individual	0.53	0.98

Experimental Results for TrajNet++ dataset	Performance Metrics	
	MED	FDE
Line-of-sight Collision Avoidance - Individual	0.66	1.10
Field-of-View Collision Avoidance- Individual	0.55	1.05

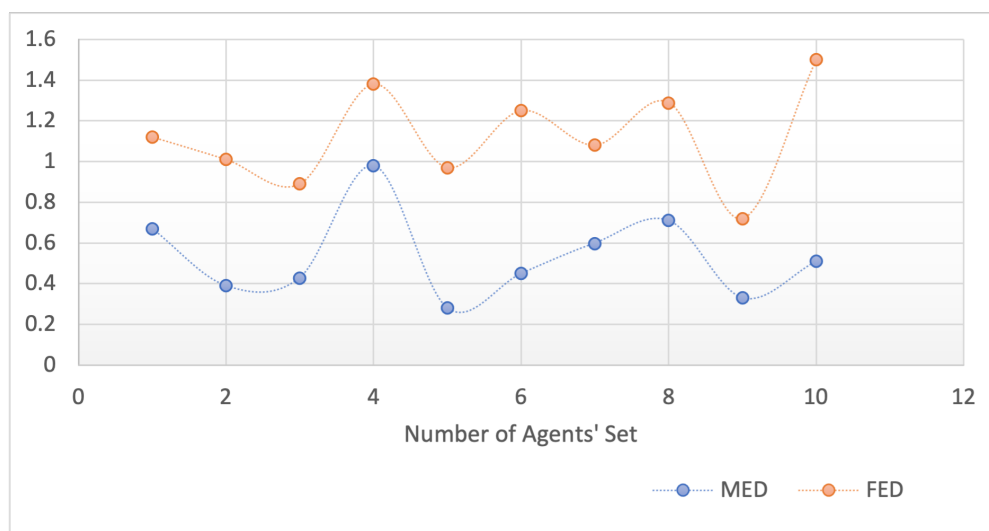


Figure 5.6: Performance Metrics Average Values of Case Study 'Line-of-sight Collision Avoidance-Individual'

terize, and the analytical modeling with a set of parameterized equations. There are some well-known traditional models such as Social Force and Cellular Automata models, these models are non-black-box and are parameterized; however, such models' code availability is an issue and even the used datasets are not openly available. Moreover, these models are not designed for pedestrians group behaviors. The comparison with the black box algorithm (such as machine learning

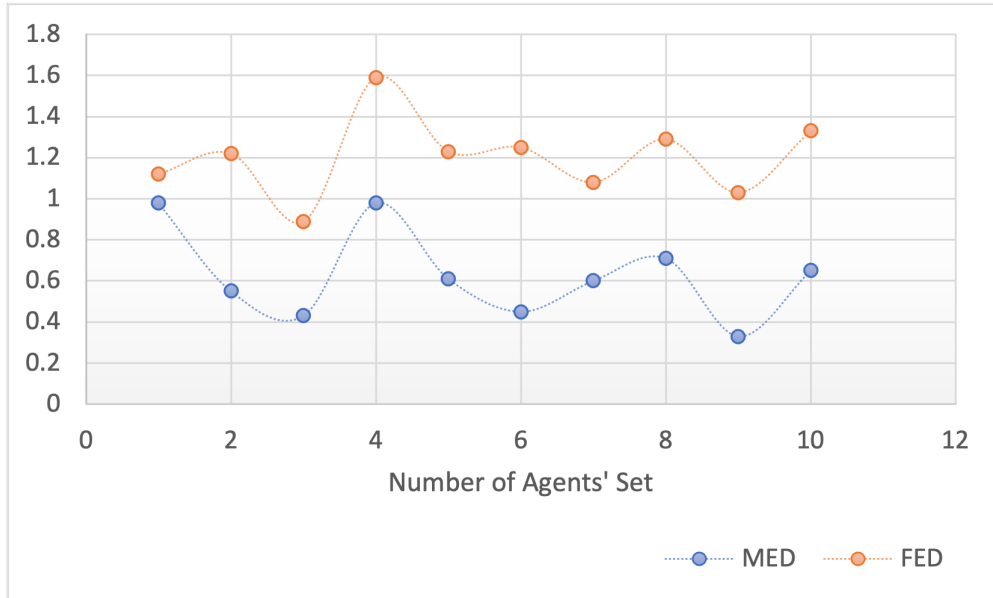


Figure 5.7: Performance Metrics Average Values of Case Study ‘Field-of-view Collision Avoidance-Group’

algorithms) for trajectory generation, ideally, are also not suitable to be considered baselines for comparison with the proposed model. The black-box models are mainly predictive models which predict trajectories for near future using the past observations. The proposed pedestrian trajectory planning framework is fully defined and parameterized with pedestrians’ behavioral and interaction rules. The cost function and constraints for a given scenario are not only observable, but can also be easily modified to reflect different scenarios of pedestrian movements and interactions.

5.8 Summary

This chapter enhanced the developed pedestrian trajectory planning framework by incorporating inter-group interactions and logic for avoiding moving obstacles. The chapter formalized the inter-group pedestrian interactions by describing decision variables, dynamic constraint equations, obstacle/moving avoidance constraint equations, and private and common objective functions. Furthermore, the chapter detailed case studies that included model calibration and validation.

CHAPTER 6

APPLICATIONS IN NETWORKED COORDINATION

Ad-hoc communication networks, namely MANETs (mobile ad-hoc networks) and VANETs (vehicular ad-hoc networks), will play a significant role in maintaining safety and achieving efficient traffic flow. In the urban traffic scenario, MANETs will form among non-motorized traffic agents such as pedestrians, cyclists, and micromobility agents. Therefore these agents' participation in network formation will be crucial for traffic mobility and safety. With the advent of 5G wireless evolution, an ad hoc mobile network is becoming both flexible and powerful, extending internet services to non-infrastructure areas. Therefore their role in the next-generation transportation systems consisting of connected, autonomous, urban, and shared space traffic scenarios, can be immensely significant. As described in the previous chapters, pedestrian walking behavior is dynamic; they have their own decision-making process; therefore, the walking behavior can sometimes be very unpredictable. For shared space scenarios, we require efficient ad-hoc routing protocols that maintain a stable and connected network despite the randomness in pedestrian mobility patterns. Incorporating actual pedestrian walking behavior knowledge can improve the design of ad-hoc network protocols. This chapter demonstrates how mobility predictions can be utilized for analyzing and predicting networks, which can aid in the efficient design of routing protocols. We illustrate the applicability using a couple of case studies.

6.1 Background and Motivation

MANETs are mobile ad-hoc networks where every node is mobile and capable of communicating with each other without any fixed infrastructure. The vision of mobile ad hoc networking is to support robust and efficient operation in mobile wireless networks by incorporating routing functionality into mobile nodes. It extends connectivity into autonomous, mobile, and wireless domains,

such as establishing communications for emergencies, disasters, safety, and rescue operations or other scenarios requiring rapidly-deployable communications.

Many aspects make communication in MANETs different from conventional network communication. These include - transmission in the wireless medium and nodes are mobile. Therefore, they have dynamically changing network topology, the nodes' energy constraints, the link and node capabilities variations due to adjustments in transmission and reception parameters, and other factors [92]. Communication in ad-hoc networking is a multi-layer process as in a conventional network [93]. The *physical layer* is responsible for maintaining link connection and adapting to rapid changes in link characteristics as the wireless medium is significantly less reliable. The *medium access control layer* is responsible for reliably transporting data over shared wireless links, where there are occurrences of the hidden terminal and exposed terminal, by providing fair access and minimizing collisions. The *network layer* is responsible for forming routes between source and receiver and keeping an updated forwarding table. The *transport layer* is responsible for handling transmission delay and packet loss statistics. Finally, the *application layer* handles the frequent disconnection and re-connection and tries to adjust to application transmission loss.

6.2 Challenges Due To Node Mobility

The network layer is responsible for transmitting data packets from the sender to the receiver. It has two main functions - firstly, a routing algorithm determines the routing path from sender to receiver. Second, forwarding the packet is a router's local action, i.e., a router receives the packet at its input link interface and then transfers the packet to one of its appropriate output link interfaces. Determining the routing path and keeping the forwarding table up to date is a critical process and involves an interplay between the route determination and maintaining the forwarding table at each router participating in the determined path between sender and receiver. As a routing algorithm determines the path between the sender and receiver, it makes it possible for routers to build and maintain forwarding (routing) tables. The routing algorithm determines the header and

output link values of the router's forwarding table. With the help of the updated routing table, the routers successfully forward the data toward the path leading to the destination.

The nodes in the MANET may move at any time or even continuously; routing protocols must learn new routes quickly to maintain connectivity. Moreover, since sources of wireless interference and wireless transmission propagation conditions may change frequently, the routing protocol must also be able to react to these changes. One challenge in MANET is minimizing path disconnections to have reliable communication. If the network layer's routing protocol successfully elects and maintains a more stable and sustainable path between nodes, then the path disconnections can be minimized [94]. Another approach is to build a route based on link stability [95].

6.3 Node Mobility Considerations in The Literature

Mobility prediction is a tool to deal with the problems emerging from the mobile nature of MANETs. It can help increase the stability of MANETs by predicting future network topology changes. Knowing the future topology of a network helps the routing algorithms determine the stable nodes, and routing algorithms select the most stable routes between two nodes. The benefits of prediction mobility in MANET can be understood from the following simple scenario. Figure 6.1 illustrates a scenario where source node S wants to transfer the information to destination node D . Now, visualizing the network formation at 3 sec, node D will be out of the transmission range of node B , and the established route $SABD$ will fail. Now, with accurate mobility prediction and the routing protocol keeping an account of nodes' predicted position for the next few time steps, a new route discovery or increasing transmission range can be performed quickly without causing much delay and loss in transmission.

Routing protocols select the best path (or route) between two nodes to relay the packet [94]. Establishing a stable path requires evaluation of the links that constitute that path. The classical routing protocols are based on the paths search strategy, which includes three classes: reactive protocols, proactive protocols, and hybrid protocols.

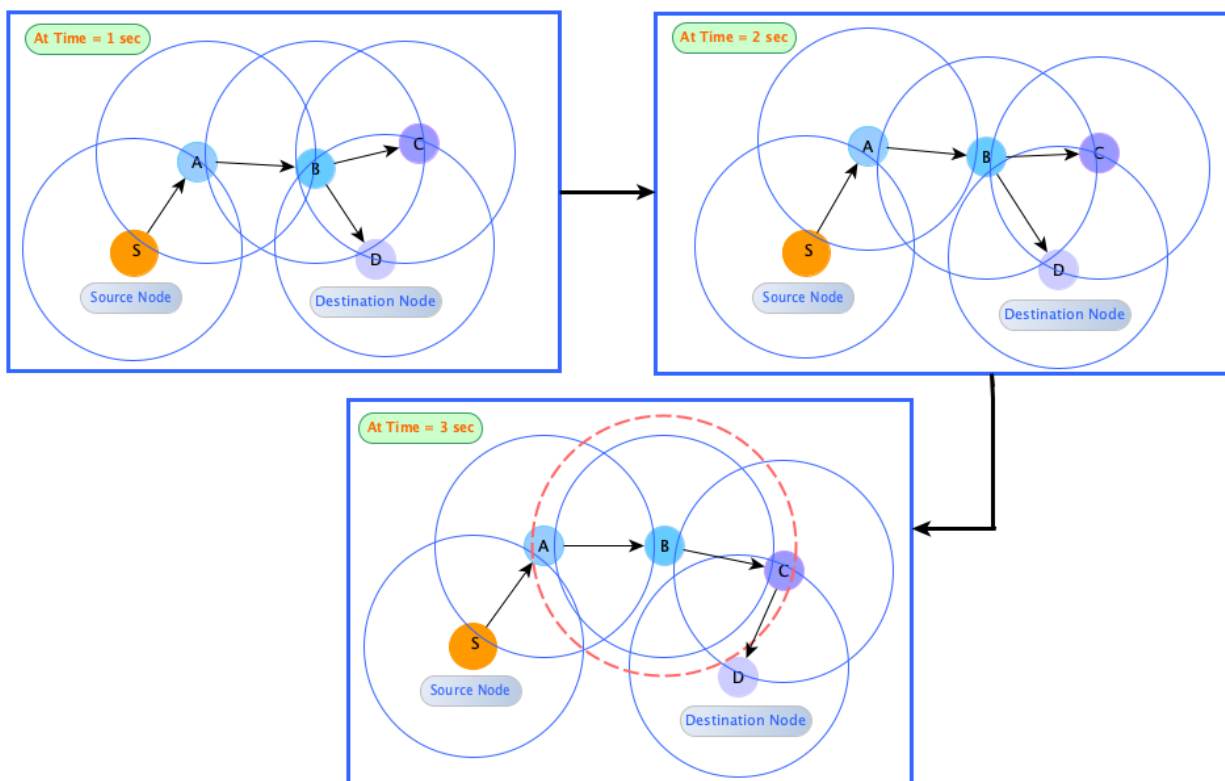


Figure 6.1: Benefits of mobility prediction in MANET routing.

The *link stability* signifies the remaining lifetime of a network link. It can be expressed in terms of distance, probability, or other metrics such as expiration time [95]. The stability metric affects the quality of service (QoS) metrics such as the end-to-end delay, packet loss, and bandwidth. The protocols that consider the mobility of nodes can be classified into (a) protocols based on the parameters of nodes' mobility and (b) protocols based on probabilistic methods. The protocols based on the parameters of nodes' mobility use known knowledge of nodes' mobility (e.g., their coordinates, their directions of movement, or their speeds) in calculating the link/route stability. The literature has analyzed the distance-based link stability by using localization systems, or the signal-power ratio of messages exchanged between the nodes [96] [97] [98]. On the other hand, the protocols based on probabilistic methods calculate the probability that the mobile nodes remain a neighbor of another node [99] [100] [94] [101].

Several researchers have explored enhancements in routing protocols using mobility prediction [102], [103], [104]. E.g., [105] proposed a neural network-based method for mobility prediction in MANET. [102] presented enhancements to unicast and multicast routing protocols using mobility prediction. It utilized GPS location to estimate the expiration time of the link between two adjacent nodes. Based on the prediction, routes were reconstructed before they could expire. Similarly, [103] considered a MANET in the urban environment where the node movements are highly restricted by roadways, i.e., the following movement rules must be obeyed: a vehicle or person can only move along roads, turn or stay at intersections. In addition, the driving speed of a vehicle on a specific road segment cannot exceed its prescribed speed limit. This information was used to arrive at the predicted trajectories of the nodes. Thus, it is well established that having accurate predictions can lead to the following benefits:

- the route reconstruction can be performed proactively on time.
- elimination of control packets transmission that were needed to reconstruct the route and thus reduce overhead.
- makes the routing protocol robust to node mobility by reducing connection interruptions.

Research Gaps: Mobility prediction, in general, is the problem of estimating the trajectory of future positions of the nodes in mobile networks. In the current state of the art, mobility prediction is usually performed by determining the current speed and moving direction of the nodes using hardware like a GPS. Moreover, the random way-point mobility model has dominated mobility incorporation into MANET. While this model may provide valuable insights, it needs to be more realistic and will likely not give reasonable performance estimates of pedestrian MANETs. With the increased understanding of human walking behavior and improved prediction models using machine learning, today, we have much better algorithms to predict future pedestrian trajectories with high accuracy. However, to the author’s best knowledge, the current approaches need to take into account the recent advancements in pedestrian modeling approaches and incorporate them into the routing protocols effectively.

6.4 Mobility Prediction Formulation and Incorporation

This section will provide an outline of how pedestrian trajectory prediction can be incorporated in reactive (on-demand) and subsequently in proactive (table-based) routing protocols.

6.4.1 Formulation for Reactive Protocols

Reactive protocols set up the route between the sender and destination on demand. That means the sender does not have a ready-made route to the destination. Once the sender needs to send a message, it floods the entire network with a route request (*RREQ*) packet. Once the path is established, the destination sends back the path as a route reply packet (*RREP*). The commonly used reactive protocols are AODV (ad hoc On-Demand Distance Vector Routing) and DSR (dynamic source routing).

Example: Figure 6.2 illustrates a minimal example. Node *A* is the source node that needs to send a packet to the destination *F*. To discover the route, *A* floods the network with *RREQ* packets. Nodes *B*, *C*, *D*, and *E* receive *RREQ* and forward it further in the network. We assume

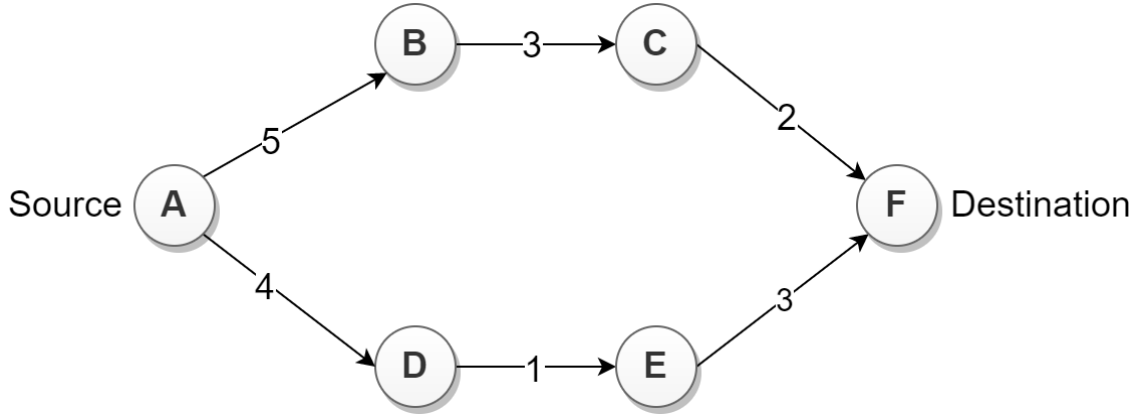


Figure 6.2: Mobility Prediction in Reactive protocols

that each node is aware of its future location and can periodically record its location. We propose that the nodes append the *RREQ* with their predicted trajectory. E.g., When *B* receives the message from *A*, it has the information on the future trajectory of node *A*. Now using its own and *A*'s trajectory prediction, *B* **computes** the predicted link expiration time ($PLET_{AB}$) between *A* and *B*.

When *B* forwards the *RREQ*, it appends the *RREQ* with both the $PLET_{AB}$ and its future trajectory so that the next node *C* can compute the $PLET_{BC}$. For illustration, sample $PLET$ values are mentioned on the edges of the graph. Thus the destination node *F* receives the two *RREQ*. The first one from the path $A - B - C - F$ has the $PLET$ values as $5 - 3 - 2$, and the second one from $A - D - E - F$ has the $PLET$ values as $4 - 1 - 3$. Predicted Path expiration time ($PPET$) is the minimum of all values of the $PLET$ for that path. Thus path $A - B - C - F$ has a $PPET$ of 2 and $A - D - E - F$ has a $PPET$ of 1. Thus path $A - B - C - F$ is more stable.

Formalization: Let us now formalize the approach described in the earlier example. Consider the generalized problem of multiple agents or pedestrians in the set \mathcal{P} , traversing an environment. Such pedestrians can be mathematically modeled as a moving graph structure $\mathcal{G} = (\mathcal{V}, \mathcal{E})$ where each node v_i in the vertex set \mathcal{V} corresponds to the i^{th} pedestrian in the pedestrian set \mathcal{P} . Meanwhile, the edge set \mathcal{E} contains predicted link expiration time $PLET_{i,j}$ between any two pedestrians

i and j . Note that the edges could also represent a combination of parameters such as $PLET_{i,j}$, transmission cost, the link delay, and the number of hops. We assume that the edges denote the $PLET_{i,j}$ for simplicity.

Within this framework, each pedestrian is associated with a final destination. However, by means of reaching their destination, the pedestrian will move through a series of segments defined by an ordered set of way-points. For pedestrian i , the next desired way-point is given by w_i . When located at position $x_{i,t}$ in a global coordinate frame at time-step t , the direction of travel for the pedestrian is given by the angle $\theta_i = \angle(w_i - x_{i,t})$. When walking together in a group, it is assumed that all pedestrians maintain the same way-point goal. However, the goal is sufficiently far away so that small angle approximations are permissible when modeling the pedestrian dynamics. That is to say, $\|\theta_i - \theta_j\| \leq \epsilon$, where ϵ is small, for all pedestrians i and j walking in the same group.

The $PLET$ computation between two nodes i and j at time step k is given by Algorithm 1.

Algorithm 1 Computation of PLET for Reactive protocol

```

1:  $PLET_{i,j}(k)$  = link expiration time between Node  $i$  and Node  $j$  at time  $k$ 
2:  $R$  = transmission range of a node
3:  $D_{ij}(k)$  = predicted graph closeness matrix at time  $k$ 
4:  $T$  = Total time of pedestrian motion
5:  $m$  = prediction window, determined by the prediction method
6:  $Tr_i(k)$  = predicted trajectory matrix of Agent  $i$  from time  $k$  to  $k + m$  steps
7: Initialization:  $PLET_{ij} \leftarrow 0 \ \forall i, j \in \mathcal{P}$ 
8: for  $k = 1:T$  do
9:   Initializing  $Tr_i(k) \leftarrow x_{i[k,k+m]}$ 
10:  Compute  $D_{ij}(k) \leftarrow \|Tr_i(k) - Tr_j(k)\|_2 \ \forall i, j \in \mathcal{P}, i \neq j$ 
11:  for  $t = k:1:k+m$  do
12:    if  $D_{ij}(k) < R \ \forall i, j \in \mathcal{P}, i \neq j$  then
13:       $PLET_{i,j}(k) \leftarrow PLET_{i,j}(k) + 1$ 
14:    end if
15:  end for
16: end for

```

6.4.2 Formulation for Proactive Protocols

Proactive routing protocols, also known as table-driven, require that each node maintains a *table* having information on the topology of the entire network. This table gets updated at regular intervals and shared among the nodes. Commonly used proactive protocols are Distance Vector Routing (DVR), Destination Sequence Distance Vector (DSDV), and Optimal Link State Routing (OLSR). Among these, OLSR is a pure link state protocol based on the Dijkstra algorithm, whereas DVR and DSDV are based on the Bellman-Ford routing mechanism.

A formulation for mobility incorporation in proactive protocols builds on the reactive one described earlier and uses the same notation. Now let's define the Predicted Route Expiration Time (*PRET*), which is the minimum of the set of *LET*'s for the route between two nodes. Assume that $\ell_1, \ell_2, \dots, \ell_p$ be the links of any route \mathfrak{R} between nodes *A* and *E*. Then $PRET_{AE}$ is given as

$$PRET_{AE} = \min_{1 \leq \ell \leq p-1} PLET_{ij}, \quad \forall i, j \in \mathcal{P}, \quad i \neq j \quad (6.1)$$

The *PRET* computation between two nodes *A* and *E* at time step *k* is given by Algorithm 1. Notice that Algorithm 1 and Algorithm 2 provide the pseudo-codes to incorporate mobility predictions into the link and route expiration times.

Once we have computed the *PRET* metric for a source-destination pair, we are ready to provide an illustrative example of how distance vector-based protocols can incorporate mobility prediction through the Figure 6.3. To utilize the mobility prediction, we propose to insert *PRET* in every route table update. Each node in the network broadcasts its routing table at frequent intervals. When node *A* receives a route table from its neighbor *B*, it updates its route table for the destination *E* if a better *PRET* is provided. As an example, Figure 6.3.a shows the initial routing table of node *A* at time *t*. Based on the predicted network topology at time $t+k$, node *B* updates its routing table and broadcasts to its neighbors. Figure 6.3.b shows that node *A* receives the routing

Algorithm 2 Computation of PLET for Proactive protocol

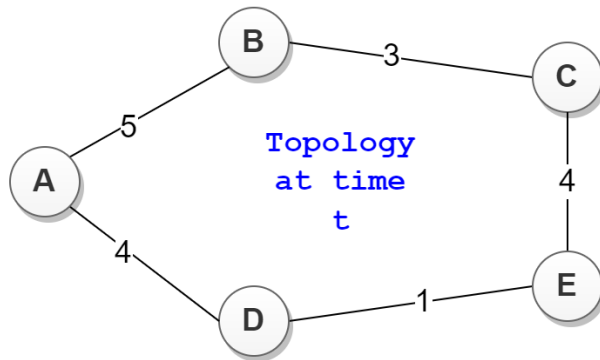
```
1:  $PLET_{i,j}(k)$  = link expiration time between Node  $i$  and Node  $j$  at time  $k$ 
2:  $D_{ij}(k)$  = predicted graph closeness matrix at time  $k$ 
3:  $T$  = Total time of pedestrian motion
4:  $m$  = prediction window, determined by the prediction method
5:  $Tr_i(k)$  = predicted trajectory matrix of Agent  $i$  from time  $k$  to  $k + m$  steps
6:  $PRET_{AE}$  = route expiration time between Node  $A$  and Node  $E$ 
7: Initialization:  $PLET_{ij} \leftarrow 0 \quad \forall i, j \in \mathcal{P}$ 
8: for  $k = 1:T$  do
9:   Initializing  $Tr_i(k) \leftarrow x_{i[k,k+m]}$ 
10:  Compute  $D_{ij}(k) \leftarrow \|Tr_i(k) - Tr_j(k)\|_2, \quad \forall i, j \in \mathcal{P}, i \neq j$ 
11:  for  $t = k:1:k+m$  do
12:    if  $D_{ij}(k) < R, \quad \forall i, j \in \mathcal{P}, i \neq j$  then
13:       $PLET_{i,j}(k) \leftarrow PLET_{i,j}(k) + 1$ 
14:    end if
15:  end for
16:   $PRET_{AE} \leftarrow \min_{1 \leq \ell \leq p-1} PLET_{i,i+1}$ 
17: end for
```

table from node B . Figure 6.3.c shows that node A updates its routing table based on the table received from node B .

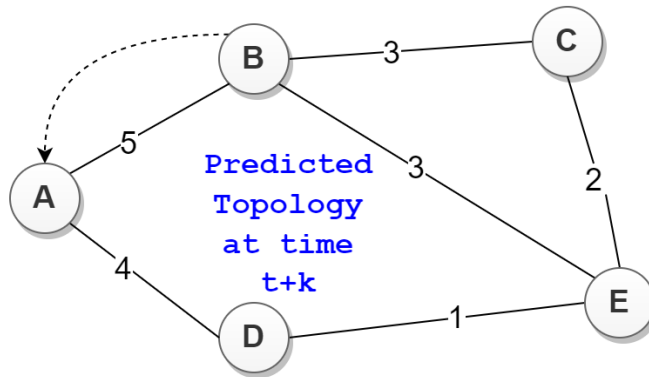
6.5 Case Studies

To demonstrate the computations of $PLET$ and $PRET$ using the proposed Algorithm 1 and Algorithm 2, we perform a case study using the dataset collected at the campus of Dalian University of Technology (DUT) in China [74]. The dataset is one of the crowd interaction benchmark datasets. The scenario includes an area of pedestrian crosswalks at an intersection. Figure 6.4 shows the data collection location and Figure 6.5 shows the sample of extracted trajectories. A *DJI Mavic Pro* Drone with a down-facing camera was used as the recording gear. The video resolution was 1920×1080 with an *fps* of 23.98. Pedestrians in the data are mainly college students. The trajectories were extracted from the recorded data using video stabilization, pedestrian tracking, coordinate transformation, and Kalman filtering techniques.

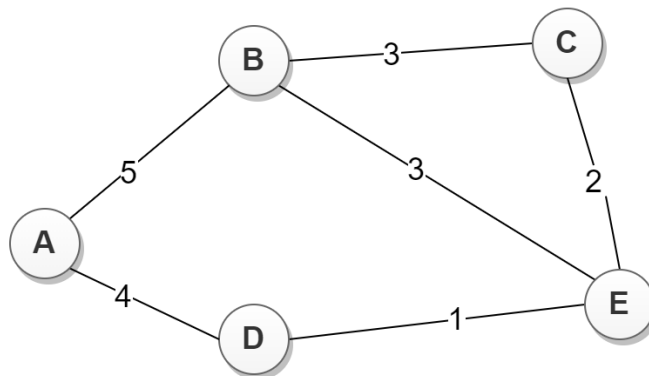
Original Route Table for A		
Destination	Next Hop	Predicted RET
A	N/A	N/A
B	B	5
C	B	3
D	D	4
E	D	1



B shares its Routing Table with A		
Destination	Next Hop	Predicted RET
A	A	5
B	N/A	N/A
C	C	3
D	A	4
E	E	3



Updated Route Table for A		
Destination	Next Hop	Predicted RET
A	N/A	N/A
B	B	5
C	B	3
D	D	4
E	B	3



Update occurring here

Figure 6.3: Mobility Prediction in Proactive protocols



Figure 6.4: Data Collection Location

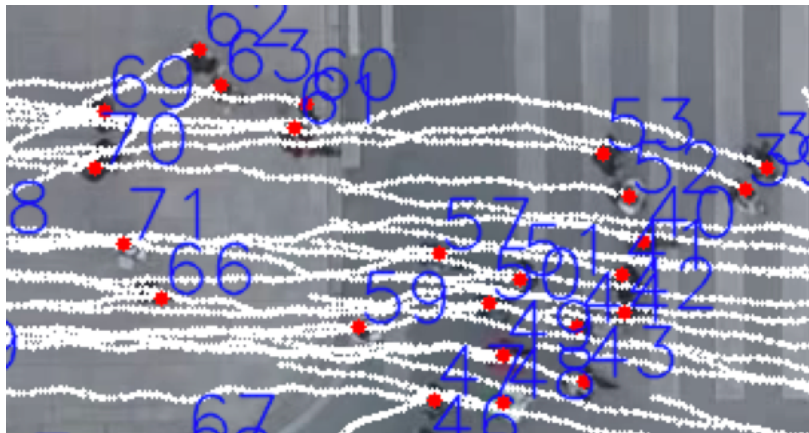


Figure 6.5: Sample Extracted Trajectories

6.5.1 Case Study 1



Figure 6.6: Traffic scenario with four pedestrians

Case study 1 considers a scenario involving four agents as shown in Figure 6.6, and studies the time evolution of *PLET* between each node pair for two values of transmission range. We use Algorithm 1 to compute the *PLET* in the following fashion. We utilize the predicted (planned) trajectory during the planning window of the receding horizon control (RHC) at time step k . While this is not a predicted trajectory in the true sense, however, it serves our purpose well to demonstrate the applicability of the proposed approaches. Also note that similar to the predicted case, the actual trajectories followed by the pedestrians are not necessarily the same as the planned trajectories, as only a portion is executed in the control window. This also serves as an approach that can be used while simulating an ad hoc network for a facility where there is no pedestrian motion data available; i.e., generated trajectories in the planning and control horizon can be used for evaluating mobility-aware routing protocols.

The case study aims to analyze the time evolution of predicted link expiration times (PLET) for each node pair as the nodes move. To this end, we assume the following parameters: prediction window $m = 10$, and transmission range $R = 1\text{m}$ and $R = 2\text{m}$ (we perform two separate analyses with two different values of R). To study the predicted link expiration times between various agents and the evolution of network topology, we compute PLETs for each node pair at time step $k = 1, k = 10, k = 20, k = 30, k = 40, k = 50$. Figure 6.7 illustrates the evolution of network

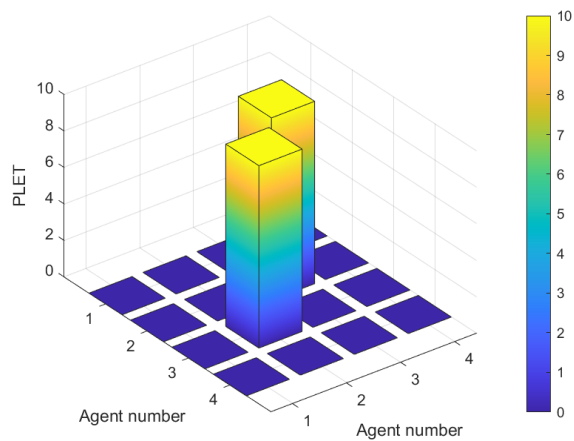
topology assuming transmission range of $R = 1\text{m}$ and Figure 6.8 illustrates the network topology using $R = 2\text{m}$. Notice that for $R = 2\text{m}$ more node pairs have non-zero PLETs (as it was expected).

6.5.2 Case Study 2

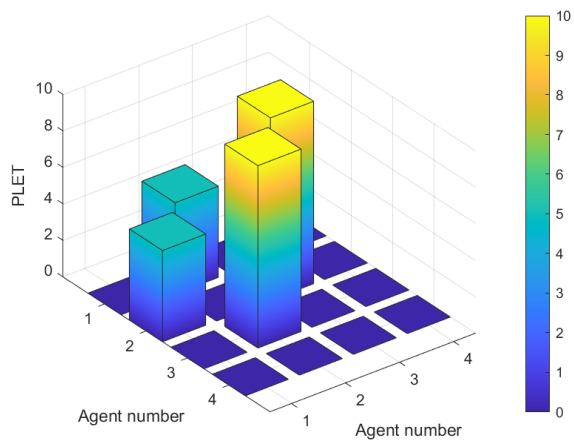
Case study 2 aims to study the predicted network connectedness as a function of the transmission range of nodes. To this end, we study the PLET for various values of transmission range R , analyze the network connectivity for the corresponding values of R , and perform the sensitivity analysis by plotting the average *PLET* in the network against the transmission range. In this case study, we consider a scenario involving six agents as shown in Figure 6.9.

First, we use Algorithm 1 to compute the *PLET* as described in the previous case study. To understand the network topology evolution under varying transmission ranges, the case study considers the prediction window $m = 10$, and at time step $k = 10\text{s}$, with each node's transmission range varied as $R = 2\text{m}$, $R = 5\text{m}$, $R = 10\text{m}$ and $R = 15\text{m}$. Figure 6.10 illustrates the details of the predicted link expiration times (PLETs) between various node pairs. As expected, the PLETs between node pairs increase with an increase in the node transmission range. Using the computed *PLET*s between each node pair, we create a graph structure with *PLET* values as its edges. Figure 6.11 illustrates the resulting network graph structure for different values of transmission range. Network graph in Figure 6.11.a implies that at $k = 10\text{s}$, the link between nodes 1 and 3, and between nodes 4 and 5 have predicted expiration time of 10s . All other node pairs have no links. As we increase the transmission range in Figure 6.11.b and Figure 6.11.c, we observe that more node pairs get connectivity with increased link expiration time. And finally, for $R = 15\text{m}$, the graph is fully connected with one hop, i.e., all the node pairs have direct connectivity. Also note that PLET for all node pairs is 10s , which is the maximum PLET based on the chosen prediction window.

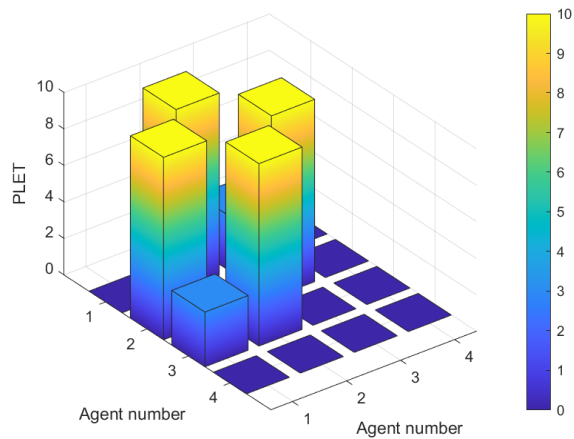
Furthermore, the case study performs the sensitivity analysis by analyzing the average value of *PLET* per node pair against the transmission range R . There is a tradeoff between transmis-



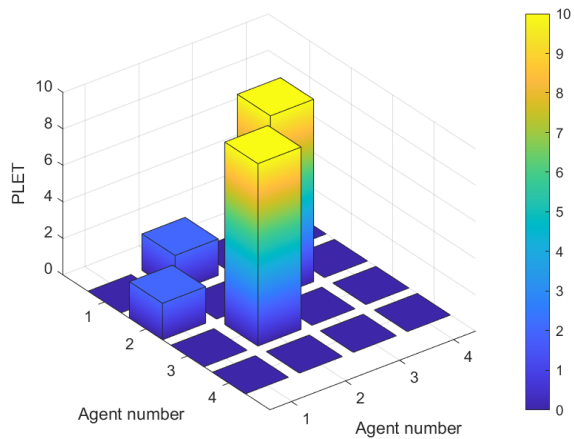
(a) PLET at $k = 1$



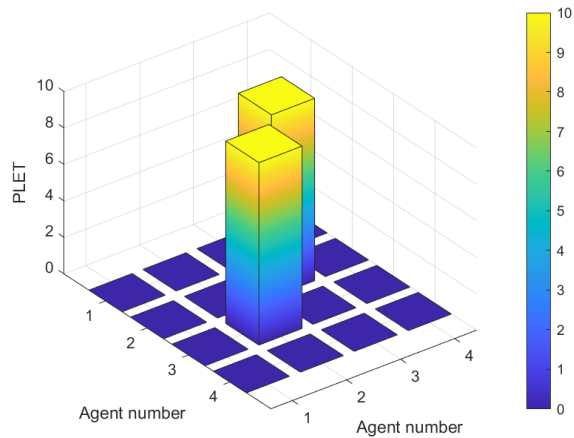
(b) PLET at $k = 10$



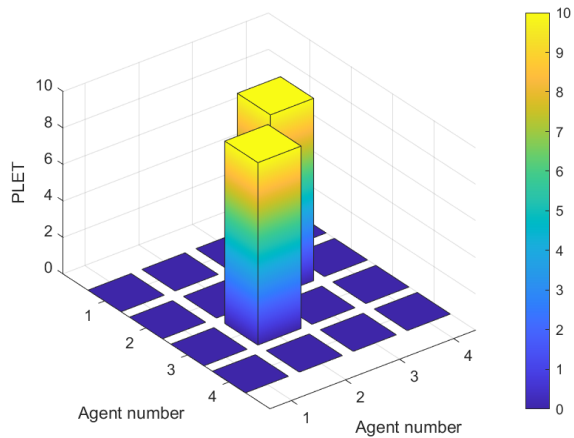
(c) PLET at $k = 20$



(d) PLET at $k = 30$

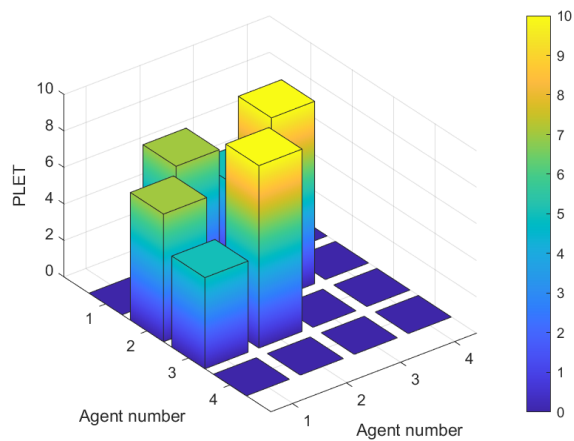


(e) PLET at $k = 40$

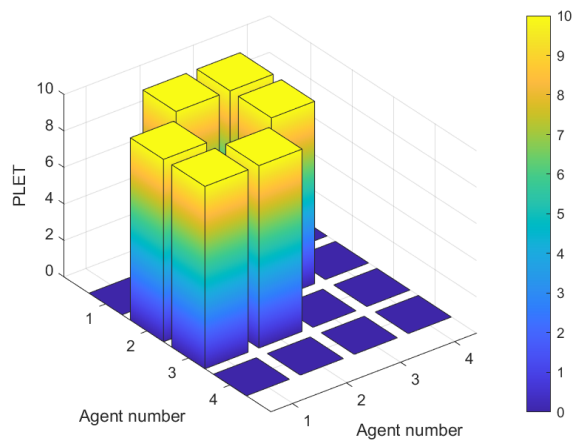


(f) PLET at $k = 50$

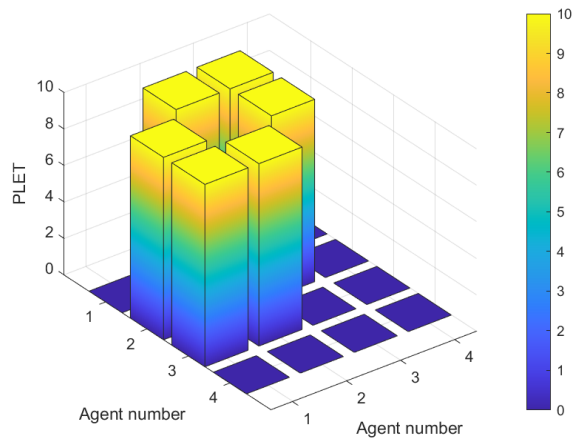
Figure 6.7: Evolution of PLET for $R = 1m$



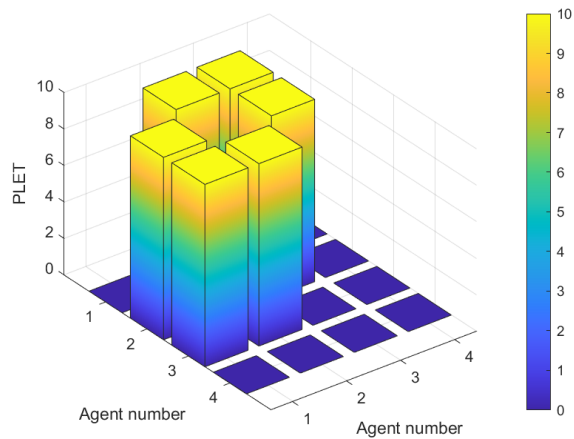
(a) PLET at $k = 1$



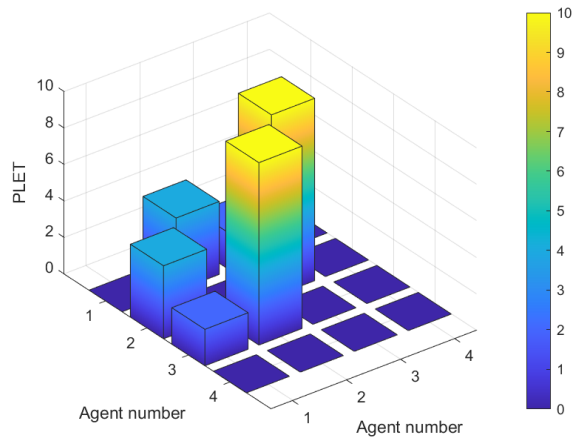
(b) PLET at $k = 10$



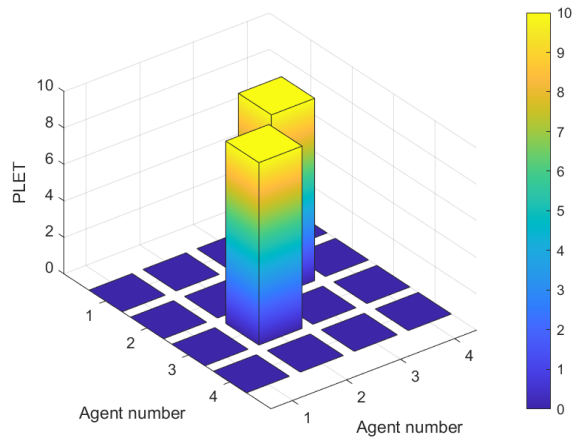
(c) PLET at $k = 20$



(d) PLET at $k = 30$



(e) PLET at $k = 40$



(f) PLET at $k = 50$

Figure 6.8: Evolution of PLET for $R = 2m$

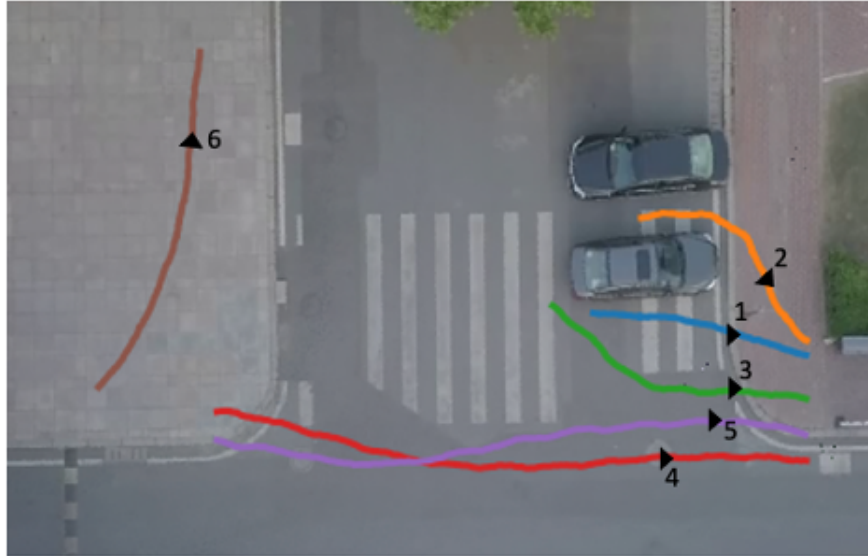
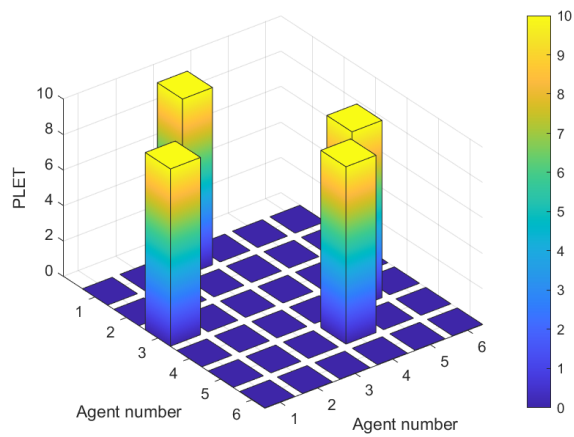


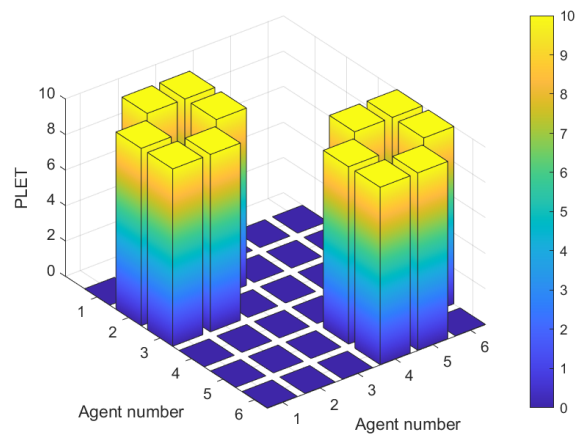
Figure 6.9: Traffic scenario with six pedestrians

sion range and power consumption. For better connectivity, it is essential to have an increased transmission range for each node; however, it comes at the cost of increased power consumption. Transmitting power is proportional to the square of the transmitting range. Thus it is essential to conserve power by judiciously adapting the transmission range of the nodes based on the connectivity requirements and network topology.

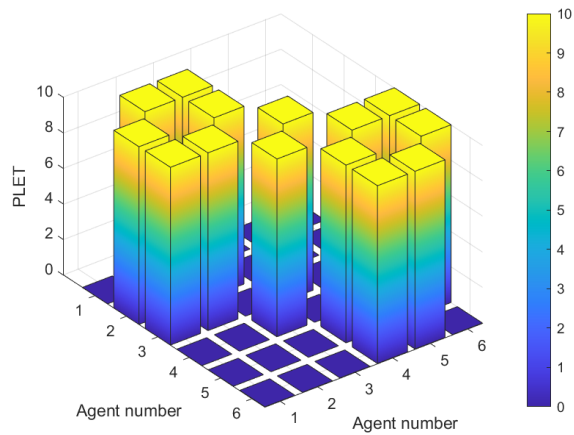
Figure 6.12 shows the average PLET vs. the transmission range. As expected, the average PLET of a network is increasing with increasing R . Note that using the plot of average PLET vs. transmission range it is difficult to determine the predicted connectedness of the network. E.g., the plot gives no idea that Figure 6.11c is a connected graph with an average PLET of 4.6s at $R = 10m$. In other words, although, average PLET does not provide an exact idea of what node pairs are mutually connected, it still gives an overall idea of the graph connectivity. E.g., an average PLET of 10s would mean that all the nodes are one hop connected.



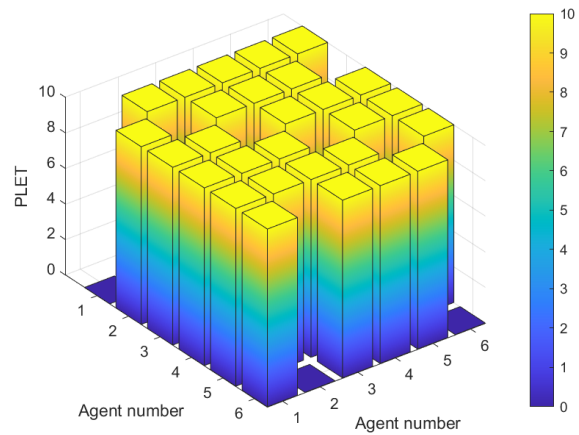
(a) PLET at $R = 2m$



(b) PLET at $R = 5m$

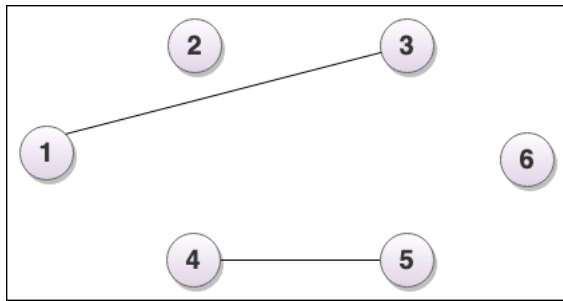


(c) PLET at $R = 10m$

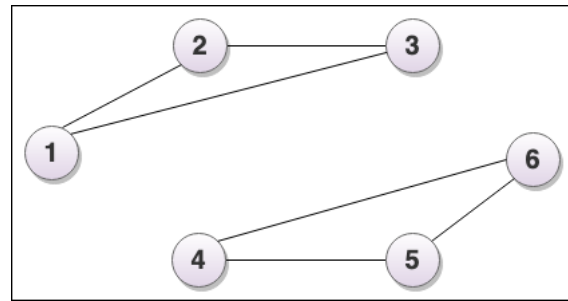


(d) PLET at $R = 15m$

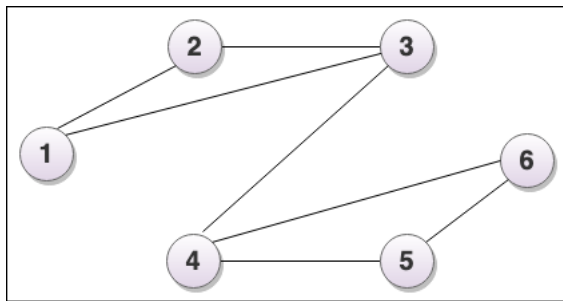
Figure 6.10: PLET against transmitting range R at $k = 10s$



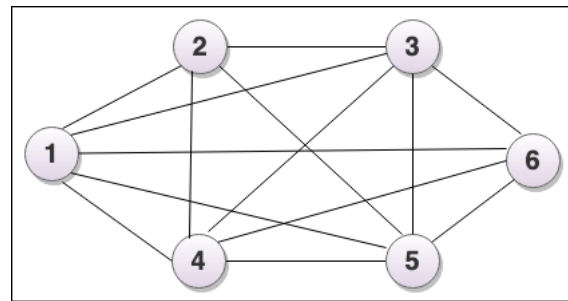
(a) PLET at $R = 2m$



(b) PLET at $R = 5m$



(c) PLET at $R = 10m$



(d) PLET at $R = 15m$

Figure 6.11: Network Graph Structure with varying values of transmitting range R at $k = 10s$. For the case study 2, the PLET value between each two nodes is calculated $10s$ for the prediction window $m = 10s$.

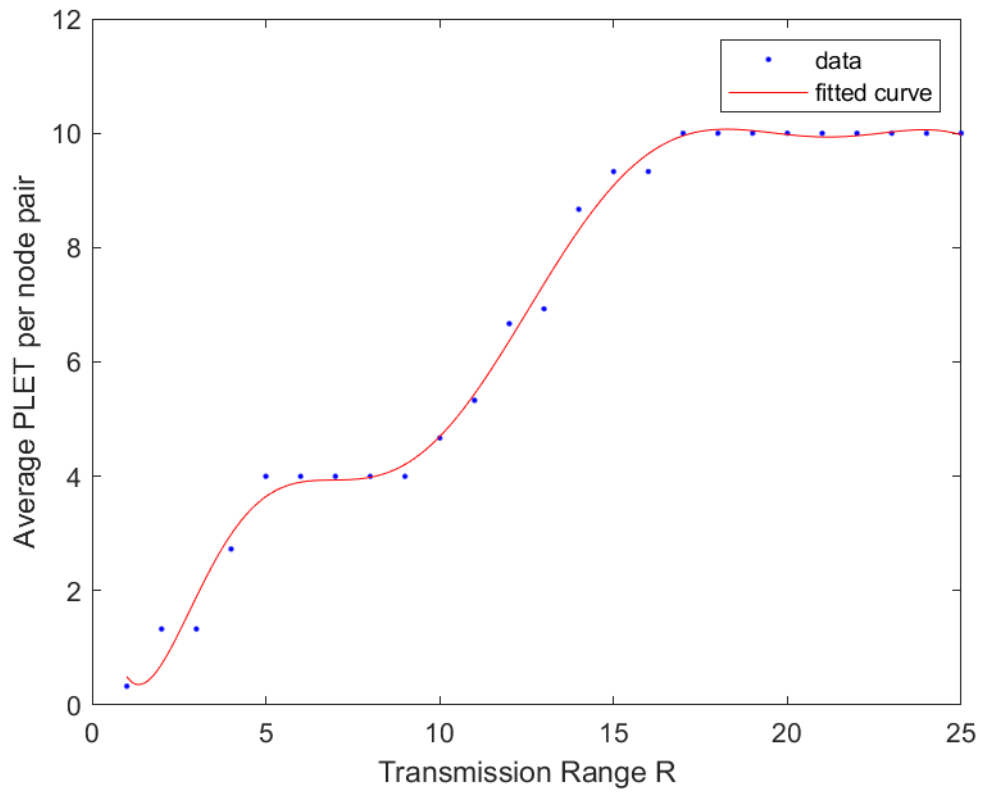


Figure 6.12: Average PLET vs. Transmission Range at $k=10s$

6.6 Summary

This chapter demonstrated the application of developed trajectory planning framework to understand the evolution of ad hoc network structure. The chapter provided a broad outline of incorporating the predicted pedestrian trajectories in the reactive and proactive protocols by defining two key metrics - *PLET* and *PRET*, and subsequently proposing two algorithms. Furthermore, it detailed two case studies. The first case study analyzed the time evolution of the *PLET* for each node pair as the nodes moved. The second case study analyzed the predicted network connectedness as a function of the transmission range and performed a sensitivity analysis.

CHAPTER 7

CONCLUSION

7.1 Summary of Work

This dissertation proposed a novel methodology to generate pedestrian trajectories while interacting with other pedestrians and stationary obstacles (infrastructure obstacles or other types of road users). The model can generate pedestrian trajectories for traffic scenarios based on the road users' behavior and interaction rules. The research was further extended to incorporate collision avoidance with moving obstacles - one of the significant behavioral studies and composes most pedestrian traffic scenarios. The methodology utilized mixed-integer linear programming embedded in the receding horizon control framework for trajectory generation. Validation was performed on two publicly available real datasets. The evaluation metrics, mean euclidean distance, and final displacement error yielded near-zero values, demonstrating the promising performance of the proposed generative trajectory planning model. The obtained gait parameters are also consistent with the previous studies on how pedestrians adjust their gait in different scenarios. The trajectory output and the lower values of the performance metric values validate the effectiveness of the proposed trajectory planning algorithm. Cross-validation with TrajNet++ was also performed to validate the algorithm's robustness. Finally, the applicability of the developed framework is established by predicting ad hoc network topologies and outline the incorporation of generated trajectories in routing protocol.

7.2 Unique Features

The proposed approach is flexible to adapt to the need of various traffic scenarios. The model is formalized for a variety of pedestrian walking behavioral traits during intra-group interactions, inter-

group interactions, stationery obstacle avoidance and moving obstacle avoidance interactions. The generative pedestrian trajectory model can simulate a broad range of pedestrian traffic scenarios. A case-specific pedestrian behavior can be directly incorporated into the cost function or constraints to customize the proposed model further. One can perform parameter tuning to test the behavior and trajectory generation in various traffic scenarios. One can also input the commonality attribute to permit the distinction of a pedestrian group. The proposed algorithm lies between the two sets of modeling paradigms — the black-box algorithms (such as machine learning), which are hard to interpret and parameterize, and the analytical modeling with a set of parametrized equations.

Unique features of the proposed pedestrian trajectory planning framework are as follows:

- The incorporation of Receding Horizon Control makes use of ongoing optimization that mimics a pedestrian's path planning and execution.
- The problem is cast as a MILP to address the complexities of non-convex optimization.
- When considering pedestrian trajectories within obstacle-free environments, the problem formulation is convex, and hence, global optimality of solutions is guaranteed.
- The benefit of the receding-horizon control framework is the capability of modeling traffic uncertainties and pedestrian response to the uncertainties.
- The framework is fully defined and parameterized with pedestrians' behavioral and interaction rules. The cost function and constraints for a given scenario are not only observable, but can also be easily modified to reflect different scenarios of pedestrian movements and interactions.
- The framework generates pedestrian trajectories for intra-group interaction, inter-group interactions, stationery obstacle interaction, and moving obstacle interaction, covering most pedestrian interaction traffic scenarios.

- The framework utilizes relatively a few parameters that can be computed even with limited data availability or drawn from distributions to create randomly generated scenarios.
- The framework is robust and generalizable - meaning that the calibrated parameters can be transferred to other traffic scenarios.
- The framework leverages pedestrian walking behavior to ensure robust topology formation for ad hoc network communication.

7.3 Application as a Simulation Tool

The developed pedestrian trajectory planning model, expanded as a simulation framework, will provide a more realistic demonstration of how pedestrians use traffic facilities and interact with their environment. The traffic simulation tool results will help propose traffic rules to optimize the traffic flows and infrastructure and plan ideas suitable for shared spaces. Moreover, the model's applicability is not limited to road traffic and shared spaces. It can find broader applications such as the emergency evacuation of buildings, large events, airports, and railway stations. Note that the developed model also supports encounter modeling which is essential in air traffic control to develop and test collision avoidance systems.

7.4 Limitations and Future Work

The HISS - a pedestrian trajectory planning framework is formulated as a MILP embedded within RHC. While planning their trajectory to the final destination, a pedestrian will advance via a series of segments characterized by an ordered set of way points before arriving at their final destination. In receding horizon control framework, a pedestrian is maintaining an awareness of their subsequent chosen way-point, the other pedestrians they are walking with (if any), and the local surroundings (i.e., the obstructions and other pedestrians not in their group). In this context, we focus our attention on the tasks of trajectory planning and execution as each pedestrian moves

between way-points; that is to say, the broader path planning problem of how pedestrians select way-points to arrive at their final destination is not addressed. Also, in case of a large number of interacting pedestrians, the adopted MILP approach can lead to computational complexity.

In future work, we will expand the research to include the more complex social interaction traffic scenarios and varying degrees of density. The developed model will be extended to consider pedestrian behavioral and social interaction rules while interacting with varying uncertainties in the traffic environment. It will be useful if we incorporate pedestrian dynamics by considering attributes like age, gender, and distractions that impact the walking gait characteristics. We plan to expand the work to model other VRUs like cyclists and scooter users.

REFERENCES

- [1] UNDESA, “68% of the world population projected to live in urban areas by 2050,” *United Nations Department of Economic and Social Affairs*, 2018.
- [2] A. Gill, “Changing cities and minds for active mobility,” 2018.
- [3] Y. Sun, H. Song, A. J. Jara, and R. Bie, “Internet of things and big data analytics for smart and connected communities,” *IEEE access*, vol. 4, pp. 766–773, 2016.
- [4] “Safety of Vulnerable Road Users,” *Directorate for science, technology and industry, programme of cooperation in the field of research on road transport and intermodal linkages*, 1998, [Online; accessed 30-November-2021].
- [5] “Comparing Demographic Trends in Vulnerable Road User Fatalities and the U.S. Population, 1980–2019,” *NHTSA Traffic Safety Facts Research Note*, 2021, [Online; accessed 2-December-2021].
- [6] “Overview of Motor Vehicle Crashes in 2019,” *NHTSA Traffic Safety Facts Research Note*, 2020, [Online; accessed 26-January-2022].
- [7] B. Hamilton-Baillie, “Shared space: Reconciling people, places and traffic,” *Built environment*, vol. 34, no. 2, pp. 161–181, 2008.
- [8] E. Jaffe, “6 Places Where Cars, Bikes, and Pedestrians All Share the Road As Equals,” *Bloomberg CityLab*, 2021, [Online; accessed 3-December-2021].
- [9] B. C. Tefft, L. S. Arnold, and W. J. Horrey, “Examining the Increase in Pedestrian Fatalities in the United States, 2009-2018 (Research Brief),” *2021 AAA Foundation for Traffic Safety*, 2021, [Online; accessed 22-November-2021].
- [10] “Pedestrian Traffic Fatalities by State: 2019 Preliminary Data,” *GHSA annual spotlight report*, 2020, [Online; accessed 22-November-2021].
- [11] C. Gloor, P. Stucki, and K. Nagel, “Hybrid techniques for pedestrian simulations,” in *International Conference on Cellular Automata*, Springer, 2004, pp. 581–590.
- [12] T. Kretz, “Pedestrian traffic: Simulation and experiments,” Ph.D. dissertation, Duisburg, Essen, Univ., Diss., 2007, 2007.

- [13] T. Robin, G. Antonini, M. Bierlaire, and J. Cruz, “Specification, estimation and validation of a pedestrian walking behavior model,” *Transportation Research Part B: Methodological*, vol. 43, no. 1, pp. 36–56, 2009.
- [14] M. Chraïbi, U. Kemloh, A. Schadschneider, and A. Seyfried, “Force-based models of pedestrian dynamics,” *Networks & Heterogeneous Media*, vol. 6, no. 3, p. 425, 2011.
- [15] G. Waizman, S. Shoval, and I. Benenson, “Micro-simulation model for assessing the risk of vehicle–pedestrian road accidents,” *Journal of Intelligent Transportation Systems*, vol. 19, no. 1, pp. 63–77, 2015.
- [16] L. Crociani, G. Vizzari, D. Yanagisawa, K. Nishinari, and S. Bandini, “Route choice in pedestrian simulation: Design and evaluation of a model based on empirical observations,” *Intelligenza Artificiale*, vol. 10, no. 2, pp. 163–182, 2016.
- [17] D. Helbing, *Social self-organization: Agent-based simulations and experiments to study emergent social behavior*. Springer, 2012.
- [18] M. Seitz, G. Köster, and A. Pfaffinger, “Pedestrian group behavior in a cellular automaton,” in *Pedestrian and Evacuation Dynamics 2012*, Springer, 2014, pp. 807–814.
- [19] A. Schadschneider, “Cellular automaton approach to pedestrian dynamics-theory,” *arXiv preprint cond-mat/0112117*, 2001.
- [20] H. Kuehne, H. Jhuang, E. Garrote, T. Poggio, and T. Serre, “Hmdb: A large video database for human motion recognition,” in *2011 International conference on computer vision*, IEEE, 2011, pp. 2556–2563.
- [21] A. Rudenko, L. Palmieri, M. Herman, K. M. Kitani, D. M. Gavrila, and K. O. Arras, “Human motion trajectory prediction: A survey,” *The International Journal of Robotics Research*, vol. 39, no. 8, pp. 895–935, 2020.
- [22] S. P. Hoogendoorn and P. H. Bovy, “Normative pedestrian behaviour theory and modelling,” in *Transportation and traffic theory in the 21st century*, Emerald Group Publishing Limited, 2002.
- [23] Y. Guo, G. Xu, and S. Tsuji, “Understanding human motion patterns,” in *Proceedings of the 12th IAPR International Conference on Pattern Recognition, Vol. 3-Conference C: Signal Processing (Cat. No. 94CH3440-5)*, IEEE, vol. 2, 1994, pp. 325–329.
- [24] S. Hoogendoorn and P. H. Bovy, “Gas-kinetic modeling and simulation of pedestrian flows,” *Transportation Research Record*, vol. 1710, no. 1, pp. 28–36, 2000.

- [25] V. J. Blue and J. L. Adler, “Cellular automata microsimulation for modeling bi-directional pedestrian walkways,” *Transportation Research Part B: Methodological*, vol. 35, no. 3, pp. 293–312, 2001.
- [26] J. K. Aggarwal and Q. Cai, “Human motion analysis: A review,” *Computer vision and image understanding*, vol. 73, no. 3, pp. 428–440, 1999.
- [27] L. Wang, W. Hu, and T. Tan, “Recent developments in human motion analysis,” *Pattern recognition*, vol. 36, no. 3, pp. 585–601, 2003.
- [28] D. Metaxas and S. Zhang, “A review of motion analysis methods for human nonverbal communication computing,” *Image and Vision Computing*, vol. 31, no. 6-7, pp. 421–433, 2013.
- [29] H. Barbosa *et al.*, “Human mobility: Models and applications,” *Physics Reports*, vol. 734, pp. 1–74, 2018.
- [30] T. B. Moeslund, A. Hilton, and V. Krüger, “A survey of advances in vision-based human motion capture and analysis,” *Computer vision and image understanding*, vol. 104, no. 2-3, pp. 90–126, 2006.
- [31] A. Weinert, S. Campbell, A. Vela, D. Schuldt, and J. Kurucar, “Well-clear recommendation for small unmanned aircraft systems based on unmitigated collision risk,” *Journal of air transportation*, vol. 26, no. 3, pp. 113–122, 2018.
- [32] M. Hussein, “Development of an agent based simulation model for pedestrian interactions,” Ph.D. dissertation, University of British Columbia, 2016.
- [33] P. M. Torrens, “Moving agent pedestrians through space and time,” *Annals of the Association of American Geographers*, vol. 102, no. 1, pp. 35–66, 2012.
- [34] C. G. Keller and D. M. Gavrilu, “Will the pedestrian cross? a study on pedestrian path prediction,” *IEEE Transactions on Intelligent Transportation Systems*, vol. 15, no. 2, pp. 494–506, 2013.
- [35] T. Gandhi and M. M. Trivedi, “Pedestrian protection systems: Issues, survey, and challenges,” *IEEE Transactions on intelligent Transportation systems*, vol. 8, no. 3, pp. 413–430, 2007.
- [36] G. Solmaz and D. Turgut, “A survey of human mobility models,” *IEEE Access*, vol. 7, pp. 125 711–125 731, 2019.

- [37] S. P. Hoogendoorn, “Microscopic pedestrian wayfinding and dynamics modeling,” *Pedestrian and evacuation dynamics*, 2001.
- [38] D. Helbing and P. Molnar, “Social force model for pedestrian dynamics,” *Physical review E*, vol. 51, no. 5, p. 4282, 1995.
- [39] V. J. Blue and J. L. Adler, “Emergent fundamental pedestrian flows from cellular automata microsimulation,” *Transportation Research Record*, vol. 1644, no. 1, pp. 29–36, 1998.
- [40] J. Dijkstra, J. Jessurun, H. J. Timmermans, *et al.*, “A multi-agent cellular automata model of pedestrian movement,” *Pedestrian and evacuation dynamics*, vol. 173, pp. 173–180, 2001.
- [41] S. P. Hoogendoorn and P. H. Bovy, “Pedestrian route-choice and activity scheduling theory and models,” *Transportation Research Part B: Methodological*, vol. 38, no. 2, pp. 169–190, 2004.
- [42] E. Keogh, T. Palpanas, V. B. Zordan, D. Gunopulos, and M. Cardle, “Indexing large human-motion databases,” in *Proceedings of the Thirtieth international conference on Very large data bases-Volume 30*, 2004, pp. 780–791.
- [43] R. Blake and M. Shiffrar, “Perception of human motion,” *Annu. Rev. Psychol.*, vol. 58, pp. 47–73, 2007.
- [44] R. Poppe, “Vision-based human motion analysis: An overview,” *Computer vision and image understanding*, vol. 108, no. 1-2, pp. 4–18, 2007.
- [45] S. Zhou *et al.*, “Crowd modeling and simulation technologies,” *ACM Transactions on Modeling and Computer Simulation (TOMACS)*, vol. 20, no. 4, pp. 1–35, 2010.
- [46] D. C. Duives, W. Daamen, and S. P. Hoogendoorn, “State-of-the-art crowd motion simulation models,” *Transportation research part C: emerging technologies*, vol. 37, pp. 193–209, 2013.
- [47] S. Wolfram *et al.*, *A new kind of science*. Wolfram media Champaign, 2002, vol. 5.
- [48] D. C. Parker, S. M. Manson, M. A. Janssen, M. J. Hoffmann, and P. Deadman, “Multi-agent systems for the simulation of land-use and land-cover change: A review,” *Annals of the association of American Geographers*, vol. 93, no. 2, pp. 314–337, 2003.
- [49] C. J. Castle and A. T. Crooks, “Principles and concepts of agent-based modelling for developing geospatial simulations,” 2006.

- [50] T. Schelhorn, D. O’Sullivan, M. Haklay, and M. Thurstain-Goodwin, “Streets: An agent-based pedestrian model,” 1999.
- [51] N. Cetin, K. Nagel, B. Raney, and A. Voellmy, “Large-scale multi-agent transportation simulations,” *Computer Physics Communications*, vol. 147, no. 1-2, pp. 559–564, 2002.
- [52] M. Hussein and T. Sayed, “A bi-directional agent-based pedestrian microscopic model,” *Transportmetrica A: Transport Science*, vol. 13, no. 4, pp. 326–355, 2017.
- [53] N. R. Jennings, “On agent-based software engineering,” *Artificial intelligence*, vol. 117, no. 2, pp. 277–296, 2000.
- [54] P. Wegner, “Why interaction is more powerful than algorithms,” *Communications of the ACM*, vol. 40, no. 5, pp. 80–91, 1997.
- [55] A. Crooks, C. Castle, and M. Batty, “Key challenges in agent-based modelling for geospatial simulation,” *Computers, Environment and Urban Systems*, vol. 32, no. 6, pp. 417–430, 2008.
- [56] M. H. Zaki and T. Sayed, “Automated analysis of pedestrian group behavior in urban settings,” *IEEE Transactions on Intelligent Transportation Systems*, vol. 19, no. 6, pp. 1880–1889, 2018.
- [57] ———, “Automated classification of road-user movement trajectories,” *Transportation Research Part C*, vol. 33, pp. 50–73, 2013.
- [58] H. Hediye, T. Sayed, M. H. Zaki, and G. Mori, “Pedestrian gait analysis using automated computer vision techniques,” *Transportmetrica A: Transport Science*, vol. 10, no. 3, pp. 214–232, 2014.
- [59] A. Getchell, “Agent-based modeling,” *Physics*, vol. 22, no. 6, pp. 757–767, 2008.
- [60] D. Ridel, E. Rehder, M. Lauer, C. Stiller, and D. Wolf, “A literature review on the prediction of pedestrian behavior in urban scenarios,” in *2018 21st International Conference on Intelligent Transportation Systems (ITSC)*, IEEE, 2018, pp. 3105–3112.
- [61] J. Li, F. Yang, M. Tomizuka, and C. Choi, “Evolvegraph: Multi-agent trajectory prediction with dynamic relational reasoning,” *arXiv preprint arXiv:2003.13924*, 2020.
- [62] H. Zhao *et al.*, “Tnt: Target-driven trajectory prediction,” *arXiv preprint arXiv:2008.08294*, 2020.

- [63] H. Xue, D. Q. Huynh, and M. Reynolds, “Ss-lstm: A hierarchical lstm model for pedestrian trajectory prediction,” in *2018 IEEE Winter Conference on Applications of Computer Vision (WACV)*, IEEE, 2018, pp. 1186–1194.
- [64] P. Zhang, W. Ouyang, P. Zhang, J. Xue, and N. Zheng, “Sr-lstm: State refinement for lstm towards pedestrian trajectory prediction,” in *Proceedings of the IEEE/CVF Conference on Computer Vision and Pattern Recognition*, 2019, pp. 12 085–12 094.
- [65] P. Kothari, S. Kreiss, and A. Alahi, “Human trajectory forecasting in crowds: A deep learning perspective,” *IEEE Transactions on Intelligent Transportation Systems*, 2021.
- [66] M. Moussaid, N. Perozo, S. Garnier, D. Helbing, and G. Theraulaz, “The walking behaviour of pedestrian social groups and its impact on crowd dynamics,” *PloS one*, vol. 5, no. 4, e10047, 2010.
- [67] M. Moussaid, D. Helbing, and G. Theraulaz, “How simple rules determine pedestrian behavior and crowd disasters,” *Proceedings of the National Academy of Sciences*, vol. 108, no. 17, pp. 6884–6888, 2011.
- [68] S. Boyd, S. P. Boyd, and L. Vandenberghe, *Convex optimization*. Cambridge university press, 2004.
- [69] D. Q. Mayne, J. B. Rawlings, C. V. Rao, and P. O. Scokaert, “Constrained model predictive control: Stability and optimality,” *Automatica*, vol. 36, no. 6, pp. 789–814, 2000.
- [70] J. Mattingley, Y. Wang, and S. Boyd, “Code generation for receding horizon control,” in *2010 IEEE International Symposium on Computer-Aided Control System Design*, IEEE, 2010, pp. 985–992.
- [71] W. Ge, R. T. Collins, and R. B. Ruback, “Vision-based analysis of small groups in pedestrian crowds,” *IEEE transactions on pattern analysis and machine intelligence*, vol. 34, no. 5, pp. 1003–1016, 2012.
- [72] W. Daamen and S. P. Hoogendoorn, “Experimental research of pedestrian walking behavior,” *Transportation research record*, vol. 1828, no. 1, pp. 20–30, 2003.
- [73] J. Drury, C. Cocking, and S. Reicher, “Everyone for themselves? a comparative study of crowd solidarity among emergency survivors,” *British Journal of Social Psychology*, vol. 48, no. 3, pp. 487–506, 2009.
- [74] D. Yang, L. Li, K. Redmill, and Ü. Özgüner, “Top-view trajectories: A pedestrian dataset of vehicle-crowd interaction from controlled experiments and crowded campus,” in *2019 IEEE Intelligent Vehicles Symposium (IV)*, IEEE, 2019, pp. 899–904.

- [75] C. Wan, L. Wang, and V. V. Phoha, “A survey on gait recognition,” *ACM Computing Surveys (CSUR)*, vol. 51, no. 5, pp. 1–35, 2018.
- [76] T. Öberg, A. Karsznia, and K. Öberg, “Basic gait parameters: Reference data for normal subjects, 10-79 years of age,” *Journal of rehabilitation research and development*, vol. 30, pp. 210–210, 1993.
- [77] R. B. Dale, “21 - clinical gait assessment,” in *Physical Rehabilitation of the Injured Athlete (Fourth Edition)*, J. R. Andrews, G. L. Harrelson, and K. E. Wilk, Eds., Fourth Edition, Philadelphia: W.B. Saunders, 2012, pp. 464–479, ISBN: 978-1-4377-2411-0.
- [78] M. Matte, “Does Stride Length Affect the Speed You Walk?,” 2018, [Online; accessed 26-April-2022].
- [79] K. Mangalam *et al.*, “It is not the journey but the destination: Endpoint conditioned trajectory prediction,” in *European Conference on Computer Vision*, Springer, 2020, pp. 759–776.
- [80] R. Rozenberg, J. Gesnouin, and F. Moutarde, “Asymmetrical bi-rnn for pedestrian trajectory encoding,” *arXiv preprint arXiv:2106.04419*, 2021.
- [81] Y. Zhu, D. Ren, M. Fan, D. Qian, X. Li, and H. Xia, “Robust trajectory forecasting for multiple intelligent agents in dynamic scene,” *arXiv preprint arXiv:2005.13133*, 2020.
- [82] Y. Liu, Q. Yan, and A. Alahi, “Social nce: Contrastive learning of socially-aware motion representations,” in *Proceedings of the IEEE/CVF International Conference on Computer Vision*, 2021, pp. 15 118–15 129.
- [83] H. Cheng, W. Liao, M. Y. Yang, B. Rosenhahn, and M. Sester, “Amenet: Attentive maps encoder network for trajectory prediction,” *ISPRS Journal of Photogrammetry and Remote Sensing*, vol. 172, pp. 253–266, 2021.
- [84] “Human vision during the walking process-copyright nelson & associates, bryan, texas,” [Online; accessed 18-March-2022].
- [85] A. H. Gloriani and A. C. Schütz, “Humans trust central vision more than peripheral vision even in the dark,” *Current Biology*, vol. 29, no. 7, pp. 1206–1210, 2019.
- [86] A. Gasparetto, P. Boscariol, A. Lanzutti, and R. Vidoni, “Path planning and trajectory planning algorithms: A general overview,” *Motion and operation planning of robotic systems*, pp. 3–27, 2015.

- [87] ———, “Trajectory planning in robotics,” *Mathematics in Computer Science*, vol. 6, no. 3, pp. 269–279, 2012.
- [88] D. Verscheure, B. Demeulenaere, J. Swevers, J. De Schutter, and M. Diehl, “Time-energy optimal path tracking for robots: A numerically efficient optimization approach,” in *2008 10th IEEE International Workshop on Advanced Motion Control*, IEEE, 2008, pp. 727–732.
- [89] H. Xu, J. Zhuang, Z. Zhu, *et al.*, “Global time-energy optimal planning of robot trajectories,” in *2009 International Conference on Mechatronics and Automation*, IEEE, 2009, pp. 4034–4039.
- [90] C. Research, *CVX: Matlab Software for Disciplined Convex Programming*, <http://cvxr.com/cvx/>, [Online; accessed 10-July-2020], 2020.
- [91] S. Gupta, M. H. Zaki, and A. Vela, “Generative modeling of pedestrian behavior: A receding horizon optimization-based trajectory planning approach,” *IEEE Access*, vol. 10, pp. 81 624–81 641, 2022.
- [92] I. Chlamtac, M. Conti, and J. J.-N. Liu, “Mobile ad hoc networking: Imperatives and challenges,” *Ad hoc networks*, vol. 1, no. 1, pp. 13–64, 2003.
- [93] R. Ramanathan and J. Redi, “A brief overview of ad hoc networks: Challenges and directions,” *IEEE communications Magazine*, vol. 40, no. 5, pp. 20–22, 2002.
- [94] A. Moussaoui, F. Semchedine, and A. Boukerram, “A link-state qos routing protocol based on link stability for mobile ad hoc networks,” *Journal of Network and Computer Applications*, vol. 39, pp. 117–125, 2014.
- [95] A. Moussaoui and A. Boukeream, “A survey of routing protocols based on link-stability in mobile ad hoc networks,” *Journal of Network and Computer Applications*, vol. 47, pp. 1–10, 2015.
- [96] W. Zhu, M. Song, and S. Olariu, “Integrating stability estimation into quality of service routing in mobile ad-hoc networks,” in *2006 14th IEEE International Workshop on Quality of Service*, IEEE, 2006, pp. 122–129.
- [97] A. Triviño-Cabrera, I. Nieves-Pérez, E. Casilari, and F. J. González-Cañete, “Ad hoc routing based on the stability of routes,” in *Proceedings of the 4th ACM international workshop on Mobility management and wireless access*, 2006, pp. 100–103.
- [98] S.-Y. Wang, J.-Y. Liu, C.-C. Huang, M.-Y. Kao, and Y.-H. Li, “Signal strength-based routing protocol for mobile ad hoc networks,” in *19th International Conference on Ad-*

vanced Information Networking and Applications (AINA'05) Volume 1 (AINA papers), IEEE, vol. 2, 2005, pp. 17–20.

- [99] Q. Song, Z. Ning, S. Wang, and A. Jamalipour, “Link stability estimation based on link connectivity changes in mobile ad-hoc networks,” *Journal of Network and Computer Applications*, vol. 35, no. 6, pp. 2051–2058, 2012.
- [100] W. Liu and W. Kim, “A stability-considered density-adaptive routing protocol in manets,” *Journal of Systems Architecture*, vol. 59, no. 9, pp. 767–775, 2013.
- [101] T. Clausen *et al.*, “Optimized link state routing protocol (olsr),” 2003.
- [102] W. Su, S.-J. Lee, and M. Gerla, “Mobility prediction and routing in ad hoc wireless networks,” *International journal of network management*, vol. 11, no. 1, pp. 3–30, 2001.
- [103] J. Tang, G. Xue, and W. Zhang, “Reliable routing in mobile ad hoc networks based on mobility prediction,” in *2004 IEEE International Conference on Mobile Ad-hoc and Sensor Systems (IEEE Cat. No. 04EX975)*, IEEE, 2004, pp. 466–474.
- [104] T. Hossmann, “Mobility prediction in manets,” *Zurich: ETH*, 2006.
- [105] H. Kaaniche and F. Kamoun, “Mobility prediction in wireless ad hoc networks using neural networks,” *arXiv preprint arXiv:1004.4610*, 2010.